Assessment of three mitigation techniques for permafrost protection

Roads and airfields in the Arctic

Jørgensen, Anders Stuhr; Villumsen, Arne; Doré, Guy

Publication date:
2009

Document Version
Publisher's PDF, also known as Version of record

Assessment of three mitigation techniques for permafrost protection

PhD Thesis

Department of Civil Engineering

Roads and airfields in the Arctic

2009

Anders Stuhr Jørgensen
DTU Civil Engineering-Report R-202 (UK)
ISBN: 9788778772794
ISSN: 1601-2917
May 2009

DTU Civil Engineering
Department of Civil Engineering

Assessment of three mitigation techniques for permafrost protection

Roads and airfields in the Arctic

Anders Stuhr Jørgensen

PhD thesis

Arctic Technology Centre
Department of Civil Engineering
Technical University of Denmark

Report R-202
ISBN: 9788778772794
ISSN: 1601-2917

May 2009

Assessment of three mitigation techniques for permafrost protection

Roads and airfields in the Arctic

Printed by ? ? ? ?

Arctic Technology Centre
Department of Civil Engineering
Technical University of Denmark

Report R-202
ISBN: 9788778772794
ISSN: 1601-2917
May 2009

Preface

This thesis is submitted for the degree of Philosophiae Doctor. The work has been prepared at the Arctic Technology Centre, Department of Civil Engineering, Technical University of Denmark, and financed by the Commission for Scientific Research in Greenland (Kalaallit Nunaani ilisimatuutut misissuinernut kommissioni / Kommissionen for Videnskabelige Undersøgelser i Grønland). The project was carried out in the period from November 2005 until January 2009 with Professor Arne Villumsen, Technical University of Denmark, and Professor Guy Doré, Université Laval, as supervisors. I would like to thank both of them for guidance and support throughout the project. I would also like to thank my colleague, Assistant Professor Thomas Ingeman-Nielsen, for his assistance and help.

Field work has been carried out at Kangerlussuaq Airport, western Greenland, and Tasiujaq Airport, northwestern Canada. The field work in Kangerlussuaq Airport was financially supported by the Commission for Scientific Research in Greenland (Kalaallit Nunaani ilisimatuutut misissuinernut kommissioni / Kommissionen for Videnskabelige Undersøgelser i Grønland) and with practical support from the Greenlandic Airport Department (Mittarfeqarfiit) and the former Municipality of Sisimiut (Sisimiut Kommunianut, from January 2009 a part of the new Qeqqata Kommunianut). In Tasiujaq Airport the field work was carried out together with the Department of Civil Engineering at l'Université Laval and in cooperation with the Québec Ministry of Transportation.

During the project period I spent three months at l'Université Laval in the Department of Civil Engineering. I would like to thank Professor Guy Doré for making the stay possible, making their facilities available and letting me take an active part in their research projects in Nunavik, the northern part of the Québec region.

Kongens Lyngby, May 2009

Anders Stuhr Jørgensen

Department of Civil Engineering
Technical University of Denmark

Preface

Department of Civil Engineering
Technical University of Denmark

List of papers

This thesis is based on laboratory studies and field work. Parts of the results have, during the PhD-project, been presented at conferences and published in scientific journals. A total number of eight papers have been composed. To summarize the work carried out during the PhD-project five papers have been included in the thesis.

The following papers are included in the thesis (sorted by date):

[A] Jørgensen, A. S., Andreasen, F., 2007. Mapping of permafrost surface using ground-penetrating radar at Kangerlussuaq Airport, western Greenland. Cold Regions Science and Technology, Vol. 48, pp. 64-72. Elsevier B.V., Amsterdam, The Netherlands.

[B] Jørgensen, A. S., Doré, G., Voyer, É., Chataigner, Y., Gosselin, L., 2008. Assessment of the effectiveness of two heat removal techniques for permafrost protection. Cold Regions Science and Technology, Vol. 53, pp. 179-192. Elsevier B.V., Amsterdam, The Netherlands.

[C] Jørgensen, A. S., Ingeman-Nielsen, T., 2008. The impact of light-colored pavements on active layer dynamics revealed by Ground-Penetrating Radar monitoring. Proceedings, 9th International Conference on Permafrost, pp. 865-868. Institute of Northern Engineering, University of Alaska Fairbanks, Fairbanks, Alaska, USA.

[D] Jørgensen, A. S., 2008. Thermal modeling of variations in the depth of the frost table caused by increasing temperatures in Kangerlussuaq Airport, western Greenland. 7 p. To be submitted.

[E] Jørgensen, A. S., Doré, G., 2009. Experimentation of several mitigation methods in Tasiujaq Airport to minimize the effects caused by the melting of permafrost. Abstract accepted to the 14th Conference on Cold Regions Engineering. The paper is currently under revision.

Related papers which have not been included in the thesis:

[F] Jørgensen, A. S., Ingeman-Nielsen, T., Brock, N., 2007. Annual variations of frost table in Kangerlussuaq Airport, western Greenland. Proceedings, International Conference on Arctic Roads, pp. 79-83. The Arctic Technology Centre, Department of Civil Engineering, Technical University of Denmark, Denmark.

[G] Jørgensen, A. S., 2007. Consequences of increased active layer thickness under airport embankments build on continuous permafrost. 6 p. To be submitted.

[H] Jørgensen, A. S., Doré, G., 2007. Use of reflective surfaces on roadway embankment. Proceedings, 8th International Symposium on Cold Region Development, 7 p. (CD-ROM). Finnish Association of Civil Engineers RIL, Helsinki, Finland.

Abstract

The presence of permafrost is an important aspect in civil engineering in arctic regions. The construction of engineering structures, such as road and airfield embankments, will change the thermal regime of the ground, and may lead to permafrost degradation under or adjacent to such structures. This problem, has in the last decades, been amplified by the climate warming, which has been most evident in the arctic regions.

The construction of a road embankment usually results in an increased mean annual surface temperature, which will increase the thawing of permafrost and expose the road embankment to thaw settlements. To avoid or at least minimize the damages caused by thaw settlements, different mitigation techniques have been developed. This thesis concerns laboratory tests and field studies of three mitigation techniques: air convection embankment, heat drain and reflective surfaces. The main objective has been to study the three aforementioned techniques and evaluate their potential for minimizing the problems with thaw settlements in permafrost areas.

The air convection embankment and heat drain techniques have been tested for the implementation in the shoulders of road and airfield embankments. Both methods will allow cold air to penetrate the embankment from the bottom, while warm air is dissipated at the top. The results from the test-site at Tasiujaq Airport (Nunavik, Québec, Canada) showed that both techniques will cause a decrease in the mean annual temperature at the sub-grade level, which will minimize permafrost degradation underneath the embankments.

Ground Penetrating-Radar (GPR) has been used to study the effectiveness of the use of reflective surfaces on the depth of the frost table throughout a complete thaw-freeze season in Kangerlussuaq Airport (Greenland). The results showed that the use of a reflective surface (white paint) will reduce the thickness of the active layer and avoid permafrost degradation underneath the embankment. This should promote the interest in the development and use of light-colored asphalt pavement materials.

Abstract

Department of Civil Engineering
Technical University of Denmark

Resumé

Tilstedeværelsen og udbredelsen af permafrost er et vigtigt aspekt, som bør nøje overvejes i forbindelse med anlægsarbejder i arktiske egne. Opførelsen af et anlægsprojekt, som f.eks. veje og lufthavnsområder, vil ændre jordens termiske forhold, hvilket kan føre til optøning af den underliggende og/eller omkringliggende permafrost. Dette problem er i de seneste årtier blevet forstærket af den globale opvarmning, hvilket har medført betydelige klimaændringer i de arktiske egne.

Opførelsen af en vejkasse vil ofte føre til en stigning i den årlige gennemsnits overfladetemperatur, hvilket vil resultere i en øget optøning af den underliggende permafrost og øge risikoen for sætningsskader i vejkassen. For at minimere mængden af sætningsskader er en række af forebyggende metoder blevet udviklet. Denne afhandling omhandler laboratorieundersøgelser og feltundersøgelser af tre metoder: konvektionskøling (air convection embankment), varme udtræk (heat drain) og reflekterende overflader (reflektive surfaces). Hovedformålet har været at undersøge de tre ovennævnte metoder, for at vurdere deres potentiale til at minimere problemerne med sætningsskader i vejkasser i områder med permafrost.

To af de forebyggende teknikker, konvektionskøling (air convection embankment) og varme udtrækning (heat drain), er blevet testet for en mulig implementering i skulderkonstruktionen af vejkasser og lufthavnskonstruktioner. Begge metoder vil gøre det muligt for kold luft at trænge ind i bunden af konstruktionerne, mens varm luft vil blive presset ud i toppen. Resultaterne fra teststrækningen i Tasiujaq Lufthavn (Nunavik, Québec, Canada) har vist, at begge metoder reducerer den årlige gennemsnitstemperatur i bunden af landingsbanens skulder, hvilket vil minimere eller måske helt forhindre optøning af den underliggende permafrost.

Georadarmetoden (GPR) er blevet anvendt til at undersøge effektiviteten af en reflekterende overflade og dennes indvirkning på dybden til frostspejlet gennem en hel tø-frys periode i Kangerlussuaq Lufthavn (Grønland). Resultaterne har vist, at brugen af en reflekterende overflade (i dette tilfælde hvid maling) vil reducere tykkelsen af aktivlaget og dermed

forebygge optøning af permafrost under konstruktionen. Dette bør fremme interessen for udvikling og øget anvendelse af lysere belægningsmaterialer.

Contents

Chapter 1: Introduction

1.1 Problems

A large portion of the Arctic is underlain by permafrost. Permafrost is defined as soil or rock having temperatures below 0˚C over at least two consecutive winters and the intervening summer (Andersland and Ladanyi, 1994).

The presence of permafrost is an important aspect to consider in civil engineering in arctic regions (Johnston, 1981). The construction of engineering structures, such as road and airfield embankments, changes the thermal regime of the ground, and may lead to permafrost degradation under or adjacent to such structures. This problem is now amplified by climate warming, which is most evident in the Arctic, where the average air temperature has risen at almost twice the rate of the rest of the world in the past few decades (Arctic Climate Impact Assessment, 2004).

The construction of a road embankment changes the ground-surface energy balance, which is a complex function of seasonal snow cover, vegetation, solar and long wave radiation, surface, moisture content and atmospheric air temperature (Lunardini, 1981). All these factors contribute to produce the mean annual surface temperature, which may differ substantially from the mean annual air temperature. The construction of a road embankment usually results in an increased mean annual surface temperature, which will increase the thawing of permafrost (Goering, 1996). More specifically the side-slopes of a road embankment are exposed to thaw settlements (Esch, 1978; Esch, 1983), inducing longitudinal cracks along the embankment edge and shoulder rotation caused by snow cover acting as insulation layer during winter (Figure 1.1). The longitudinal cracks and shoulder rotation will allow water penetration into the structure of the embankment, reducing bearing capacity of the embankment materials and induce problems with frost heave. Reduced road stability will affect the riding quality, cause safety hazards and increase maintenance costs.

The number of stability problems has increased during the last decades (Beaulac and Doré, 2006-A; Instanes and Mjureke, 2005) and is expected to continue to increase with the rising

temperatures (Intergovernmental Panel on Climate Change, 2001). Therefore, the need for new knowledge and ways to secure the stability of road embankments and other infrastructures in the Arctic are of extreme importance. To avoid or at least minimize the damages caused by thaw settlements, different mitigation techniques have been developed: reflective surfaces, air convection embankment, geosynthetic reinforcement, thermosyphons, berms, air ducts, insulation materials and lightweight fill materials (Esch, 1996; Beaulac et al., 2004).

1.2 The goal of the work

This thesis concerns laboratory testing and field studies of three mitigation techniques: air convection embankment, heat drain and reflective surfaces. The laboratory testing, of the air convection embankment and the heat drain techniques, was carried out at l'Université Laval during fall 2006 and winter 2007 together with master student Érika Voyer. The results from these tests have also been included in Érika Voyer's master thesis (Voyer, 2008).

The main objective of the PhD-project has been to study the three above-mentioned mitigation techniques and evaluate their potential to avoid or at least minimize the damages caused by thaw settlements under arctic road and airfield embankments. The field investigations have been carried out in Tasiujaq Airport (Nunavik, Québec, Canada) and Kangerlussuaq Airport (Greenland).

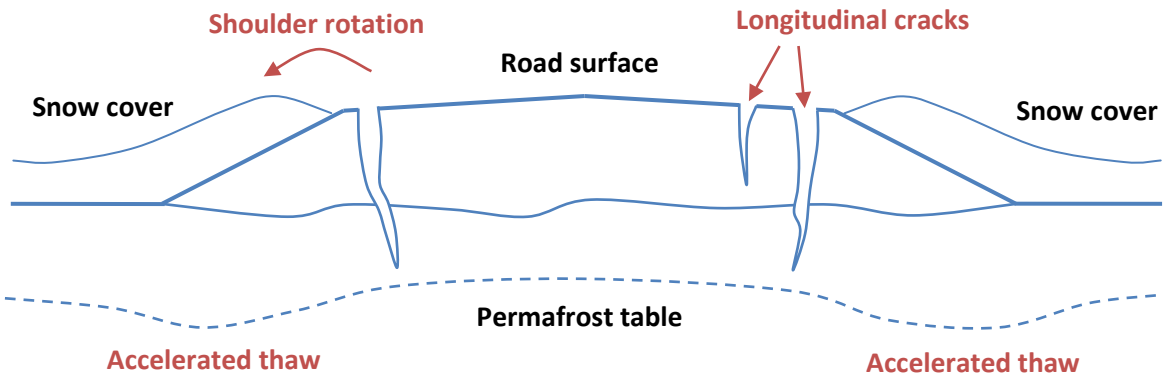

Figure 1.1 Shoulder rotation and development of longitudinal cracks along the edge of a road surface caused by the accelerated thaw of the underlying permafrost (based on Goering and Saboundjian, 2004)

1.3 Thesis structure

The thesis provides a summary of the work, which has been carried out during the PhD-project. The main focus has been on the three studied mitigation techniques, while the theory of the applied methods (e.g. ground-penetrating radar) has not been included in the thesis.

Chapter 1 contains the background, objectives and thesis structure.

Chapter 2 includes a description of the three investigated mitigation techniques, as well as the results from the laboratory tests and the field work.

Chapter 3 contains a discussion of the results and what additional research recommended. Finally the main conclusions are presented in chapter 4 and references are listed in chapter 5.

Appendices A to E contain the five papers included in the thesis. Paper A and B have been published in the international peer reviewed journal Cold Regions Science and Technology. Paper C has been published in the peer reviewed proceedings for the 9th International Conference on Permafrost and presented at the conference in the summer 2008 in Fairbanks, Alaska, USA. Paper D is intended to be submitted to a conference in the nearest future, while paper E is under revision (abstract is accepted) for publication in the peer reviewed proceedings for the 14th Conference on Cold Regions Engineering, which will be held summer 2009 in Duluth, Minnesota, USA.

Paper A, C and D concerns the field work carried out in connection with the use of reflective surfaces, while paper B and E deals with the laboratory studies and field work of the air convection embankment and heat drain techniques.

Chapter 2: Mitigation techniques

2.1 Introduction

This chapter includes a description of the investigated mitigation techniques and the main results from the laboratory tests and field investigations. The laboratory tests were carried out at l'Université Laval (Québec, Canada), while the field investigations were carried out on locations in western Greenland and northeastern Canada.

2.2 Site descriptions

Field investigations have been carried out in Kangerlussuaq Airport, western Greenland, and Tasiujaq Airport, Nunavik, Québec, Canada (Figure 2.1). In Kangerlussuaq Airport, the annual variations of the frost table have been studied underneath a normal dark asphalt surface and a more reflective surface, during the thaw-freeze periods in 2005-2008 (Appendices A, C and D). In the end of the summer 2007, a test-site, including three different mitigation techniques and a reference section, was established in Tasiujaq Airport (Doré et al., 2007). Since the completion of the construction, the annual variations of the thermal regime of the embankments were studied (Appendix E; Doré and Jørgensen, 2008).

Figure 2.1 Location of Tasiujaq Airport (orange) and Kangerlussuaq Airport (red) (Wikimedia, 2008)

2.2.1 Tasiujaq Airport

The village of Tasiujaq is located in the southwestern part of Ungava Bay at 58°71' N and 69°82' W, just a few kilometers north of the tree line and in the zone of abundant discontinuous permafrost. The airport has a gravel surface and is built on a Quaternary river terrace covered with fluvial and alluvial deposits (Allard et al., 2007; Beaulac, 2006). The runway embankment consists of a 150 mm granular surface course material ranging 0-20 mm (MG-20b), a 250 mm granular material of size 0-56 mm (MG-56) and finally a 300 mm sub-base layer of a crushed gravel material ranging 0-150 mm (MG-150), on top of fill materials. The shoulder of the runway consists of a 150 mm surface course layer of MG-56 and a 550 mm layer of crushed MG-150 (Beaulac, 2006).

During the 1990s, the entire Nunavik territory experienced an increase in the mean annual air temperature. In the village of Kuujjuaq, which is the village closest to Tasiujaq (approximately 110 km to the southeast) with a long-term temperature series, the mean annual air temperature increased with 3.2°C (from -6.2°C to -3.0°C) from 1992-2000 (Beaulac, 2006). During 1993-2005 soil temperatures was monitored under natural circumstances in a borehole 42 m from the runway at Tasiujaq Airport. The recorded data showed an increase in permafrost temperature at 11 m depth of approximately 1.3°C (from -4.0°C to -2.7°C). In the same period the thickness of the active layer increased from 1.3 m to 2.0 m (Allard et al., 2007).

In the summers 2004 and 2005, several depressions were observed along the shoulders of the runway at Tasiujaq Airport, caused by an accelerated thaw of the permafrost underneath and adjacent to the runway. Stagnant water, which was observed along the foot of the embankment (Beaulac and Doré, 2006-A), has led to an increased heating of the underlying geological deposits and thereby increased the thickness of the thaw depth, which could lead to a situation with shoulder rotation and longitudinal cracking (similar to the situation illustrated on figure 1.1) along the sides of the runway. In the beginning of September 2007, a test-site was constructed along the southeastern shoulder of the runway (Doré et al., 2007). The total length of the test-site is 200 m, consisting of a reference section and three test-sections: air convection embankment, heat drain and gentle slope (Appendix E). Each section was instrumented with thermistors to measure the thermal regime of the embankments and the underlying geological deposits.

2.2.2 Kangerlussuaq Airport

Kangerlussuaq Airport is built on a Quaternary river terrace (altitude 30-50 m) at the head of the 170 km long fjord, Kangerlussuaq (Søndre Strømfjord), located just north of the Arctic Circle at 67°00' N and 50°42' W. In the western part of the area, the terrace is made up of fine-grained glaciomarine sediments, partly covered with fluvial deposits of sand and gravel. In the eastern part, fine-grained marine deposits are absent. The southern parking area of Kangerlussuaq Airport is built up of a surface and intermediate course with a total asphalt thickness of 150-200 mm, approximately 250 mm of crushed aggregate base course and a sub-base of varying thickness with materials ranging 0-300 mm (United States Air Force Corps of Engineers, 1971; United States Air Force Civil Engineering Center, 1984).

The climatic conditions in Kangerlussuaq are arctic continental, determined by its northern location and its position in a 2-3 km wide valley surrounded by mountains (plateau altitude 400-600 m). To the east, the Greenlandic ice sheet, with altitudes up to 3 km, has a dominant influence on precipitation and winds. These conditions result in a dry sub-arctic climate with winter temperatures down to -40°C and summer temperatures up to 20°C. During 1977-99, the mean annual air temperature was -5.7°C and the mean annual precipitation was 151 mm (Danish Meteorological Institute, 2008). Since the middle of the 1990s, the mean annual temperature in Kangerlussuaq has increased to -4.0°C. Nevertheless, Kangerlussuaq is still underlain by 100-150 m of continuous permafrost (Tatenhove and Olesen, 1994). The entire active layer is frozen during winter, but in late summer the depth of the frost table reaches 3.0 m in the open terrain (Ingeman-Nielsen et al., 2007).

On the southern parking area of the airport, a number of depressions have developed throughout the last 5-10 years. In autumn 2000, three test areas were painted white, to reduce further development of depressions in the asphalt pavement. One of these areas has been used to study and compare the annual variations of the frost table underneath a normal dark asphalt surface, to that below a more reflective surface (Appendices A and C).

2.3 Air Convection Embankment

The idea of constructing embankments of large porous rock, was first reported in the Russian literature (Esch, 1996). During the 1990s the method was further developed at the University of Alaska, Fairbanks, USA. Series of computer modeling studies were carried out and full-scale test embankments were constructed in areas near Fairbanks. Results from the test embankments showed that the air convection embankment generated a passive cooling and

that the mean annual temperature at the base of a test-section was decreased with 4˚C compared to the reference embankment (Saboundjian and Goering, 2003).

2.3.1 Description

The air convection embankment technique involves the use of a highly-permeable granular material to construct the core or the shoulder of a road embankment. The high permeability, of such a material, allows natural convection of the pore air to occur in the embankment during the winter months, when unstable air density gradients exist (Goering, 1996; Saboundjian and Goering, 2003; Goering and Kumar, 1996). During winter months, cold air from the upper part of the embankment will tend to settle downwards towards the lower part due to its greater density. At the same time warm air will rise from the base of the embankment, which will result in circulation of the pore air and enhanced wintertime heat transfer by speeding the cooling of the underlying permafrost (Esch, 1996; Saboundjian and Goering, 2003). During summer months, the air density gradients are stable, the warmer air will stay in the upper part of the embankment, and circulation will not occur (Goering, 1996; Goering and Kumar, 1996). The air convection embankment will thus produce a cooling effect, which reduces the mean annual air temperature in the embankment and thereby help preventing thaw of underlying permafrost.

Theoretically the system can be modeled by a horizontal layer of porous material, which is heated from below. That system will experience natural convection of the pore air if a critical Rayleigh number is exceeded. The Rayleigh number, Ra, is defined as (Nield and Bejan, 1992):

$$Ra = \frac{C\beta gKH\Delta T}{vk} \tag{2.1}$$

where C is the volumetric heat capacity of the pore fluid (air, $J/m^3 \cdot K^{-1}$), β is the expansion coefficient of the pore fluid (air, K^{-1}), g is the acceleration due to gravity (9.8 m/s^2), K is the intrinsic permeability of the material, H is the height of the layer (m), ΔT is the temperature difference between the top and the bottom of the layer (K), v is the kinematic viscosity of the pore fluid (air, m^2/s) and k is the thermal conductivity of the material (J/s·m·K).

A stability analysis shows, that a horizontal layer with impermeable boundaries of uniform temperature at its base and upper surface will start to experience natural convection once the Rayleigh number exceeds $4\pi^2$ (39.48 ≈ 40). Using the limit, it is possible to define a critical ΔT (Saboundjian and Goering, 2003):

$$\Delta T = \frac{40vk}{C\beta gKH} \tag{2.2}$$

When the critical ΔT is exceeded, a series of circulation cells will arise, which will transport the warmer pore air from the base upwards, whereas the cooled air will be going downwards. Under natural field conditions, where the system is not ideally horizontal, convection will normally begin at smaller Rayleigh numbers as much as ½ or ¼ of the value listed above (Saboundjian and Goering, 2003).

2.3.2 Laboratory studies

The laboratory testing was carried out at l'Université Laval in the fall 2006 (Appendix B). The tests were carried out in a cold room, which maintained a constant temperature at -17˚C (precision ± 1˚C). The refrigeration system was programmed to shut down every 10 h for deicing purposes. This process has slightly affected the results of the test. For the test a small-scale (25-50 % of a full-scale road embankment) shoulder of an air convection embankment and a reference embankment was constructed (Figure 2.2). The reference embankment consisted of a natural gneissic granular material (≤ 18.75 mm) from a gravel-pit located near Québec City, Québec, Canada (Voyer, 2008). The bulk density of the material was determined to approximately 2.0 g/cm^3 and the water content to 6.0 %. The air convection embankment was assembled using sorted rounded boulders (approximately 100 mm in diameter) of gneissic origin.

Figure 2.2 Embankment box with the two small-scale embankments, air convection embankment and reference embankment

The box used for the laboratory testing included two sections, thus two small-scale embankments could be constructed, tested and compared at the same time. The embankments were insulated by covering the outside of the box with a 50 mm polystyrene layer. A 100 mm layer of polystyrene was placed between the two sections to avoid heat losses and a layer of 300 mm glass wool was placed on the top of the embankments to recreate the insulating effect from a snow cover. In each section, 5 thermistors were installed to continuously monitor the thermal regime. The dimensions of the box and the location of the thermistors are shown in figure 2.3. At the bottom of the box, the temperature was maintained constant at 0˚C by a heating system.

Three tests were carried out in the laboratory to study the temperature differences between a closed and an open embankment. During the first test the embankment was totally covered with glass wool. In the second test the glass wool was removed from the top of the embankment (over a distance of 23 cm), while the glass wool was removed from both the top and the bottom (over a distance of 23 cm) of the embankment during the third test (Figure 2.3).

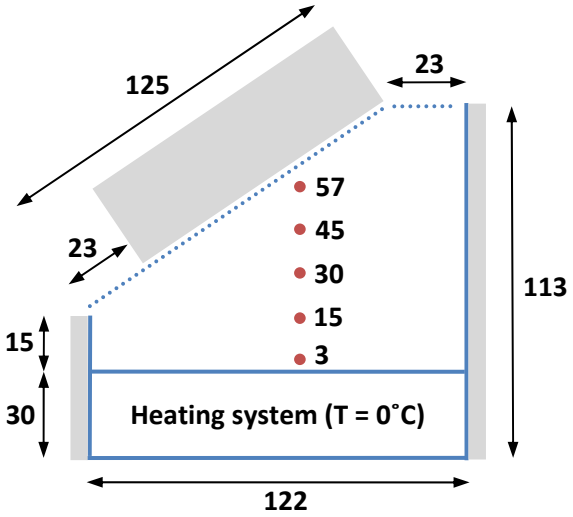

Figure 2.3 Dimensions of embankment box (all units are shown in cm). The position of the thermistors (red circles) is shown as the distance from the bottom of the embankment

2.3.3 Field studies

In September 2007, a test-section was established along 50 m of the southeastern orientated shoulder on the runway in Tasiujaq Airport. The construction of the air convection embankment section required an excavation of the existing shoulder of the runway. To minimize the disruption of the thermal regime in the underlying geological deposits the first part of the embankment was constructed immediately after finishing the excavation. At the same stage a borehole was carried out in the middle of the section for the installation of thermistors. The embankment was then built up of crushed rock, and ventilation pipes were installed at the top and the bottom of the shoulder (Figure 2.4) (Doré et al., 2007).

To prevent granular material from the runway to fall into the embankment and fill the pores between the blocks, a geotextile was placed in the upper part of the embankment (Figure 2.5). The final structure of the embankment is shown on figure 2.6.

The section was instrumented with 16 thermistors, which were installed in the borehole and the embankment. The thermistors were placed with an interval of 30 cm. In one of the pair of chimneys, two sets of thermistors were installed to measure the temperature difference between the temperatures of the air intake and air outlet. Since the completion of the construction, the thermistors has stored the thermal regime of the embankment and the underlying geological deposits every 6 h.

Figure 2.4 Construction of the air convection embankment along the runway at Tasiujaq Airport. The intake ventilation pipe, which will allow cold air to penetrate the embankment, is seen in the bottom of the picture (Doré et. al, 2007)

Figure 2.5 Installation of geotextile in the upper part of the air convection embankment (Doré et. al, 2007)

2.3.4 Results

Several laboratory tests of the air convection embankment were carried out to study the temperature differences between a closed and an open embankment (Appendix B). The embankment was placed in a cold room and brought to steady state condition (stabile temperature regime), while the entire surface was covered with 300 mm of glass wool. When steady state was reached, the glass wool was removed from the top of the embankment to allow cold air to penetrate into the embankment. The effect of opening the top is seen on figure 2.7. It is seen, that the temperature at the bottom of the embankment decreases with approximately 4°C after the embankment is opened at the top. The actual effect is probably a couple of degrees less, since the glass wool was removed before the steady state condition was completely obtained.

When the embankment again had obtained steady state condition, the glass wool was removed from the bottom to allow a heat flow through the embankment, where cold air will penetrate the embankment from the bottom, while warm air is expelled at the top. These conditions resulted in an inversion of the temperatures in the embankment (Figure 2.7). The bottom, which used to be the coldest part of the embankment, was now the warmest, while the top was the coldest. The temperatures in the bottom of embankment were decreased by approximately 1°C, when the bottom was opened, while the temperature changes in the top were in the order of 5°C. The heat flows for the open air convection embankment and the reference embankment are illustrated in figure 2.8. It is seen, that the temperatures in the air convection embankment are significantly lower in the entire embankment (over 4˚C), compared to the temperatures in the reference embankment.

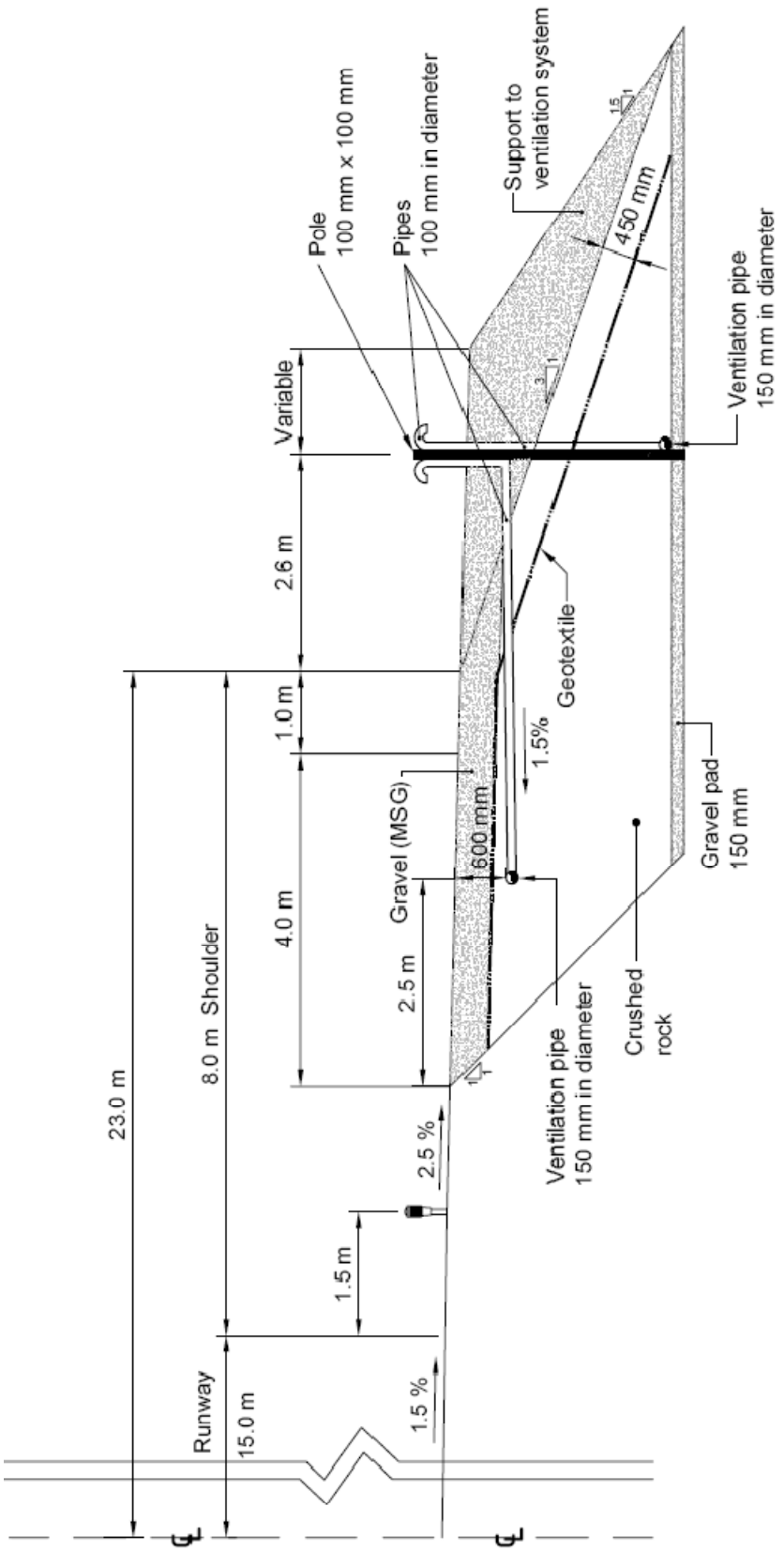

Figure 2.6 Structure of the air convection embankment at Tasiujaq Airport (based on Doré et al., 2007)

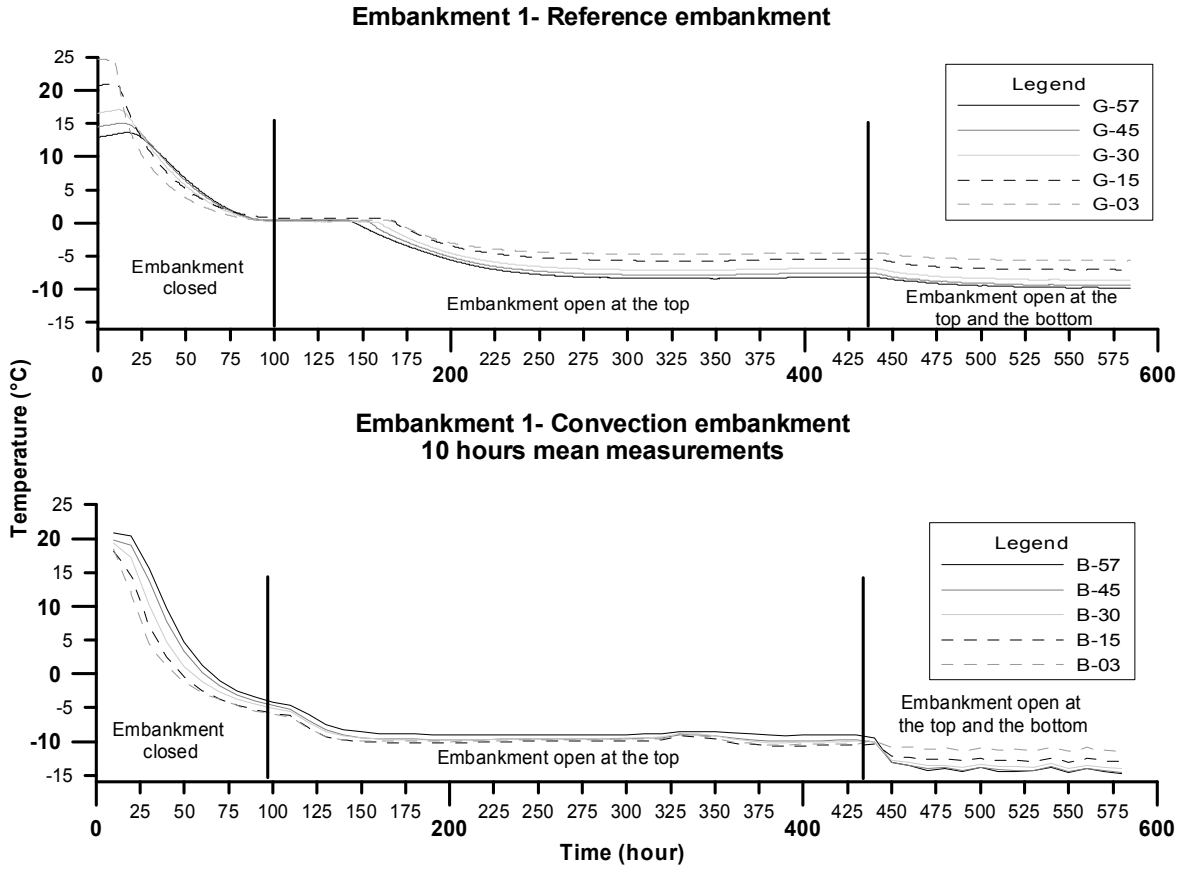

Figure 2.7 Change in temperature regime in the reference embankment (top) and air convection embankment (bottom) with time and situation type. Three different situations were tested; closed top and bottom, open top and closed bottom, and finally open top and bottom. The height of the thermistors is shown in the legend as centimeters from the bottom of the embankments

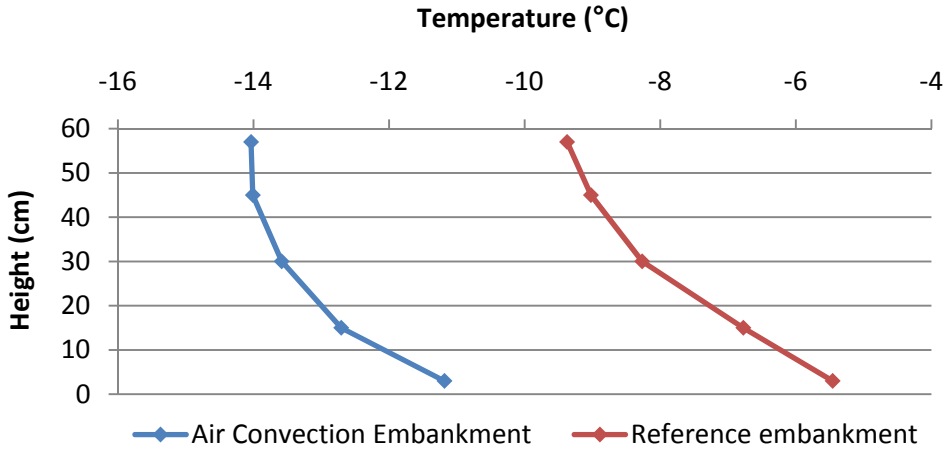

Figure 2.8 Temperatures during steady state conditions with an open top and an open bottom. The height is shown from the bottom of the embankments

Figure 2.9 illustrates the hypothetical mechanism believed to be responsible for the temperature inversion in the embankment as a result of the opening at the bottom of the embankment.

The laboratory results showed that it is possible to increase the effectiveness of the air convection embankment technique by opening the top and the bottom of the embankment, and allowing cold air to penetrate into the embankment from the bottom, while warm air is dissipated at the top. The results obtained, on the small-scale embankment, are similar to those obtained in the Chinese studies using numerical modeling, where a model of an open and closed full-scale air convection embankment has been investigated (Lai et al., 2004; Lai et al., 2006).

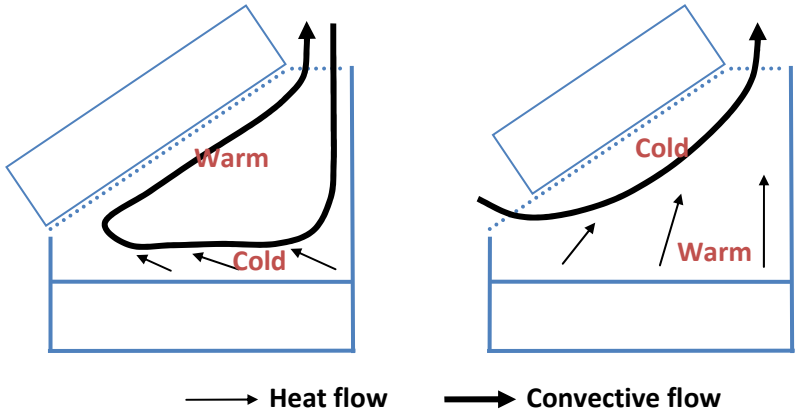

Figure 2.9 Hypothetical heat flow and convective flow of the air convection embankment with an open top (left), and with an open top and an open bottom (right)

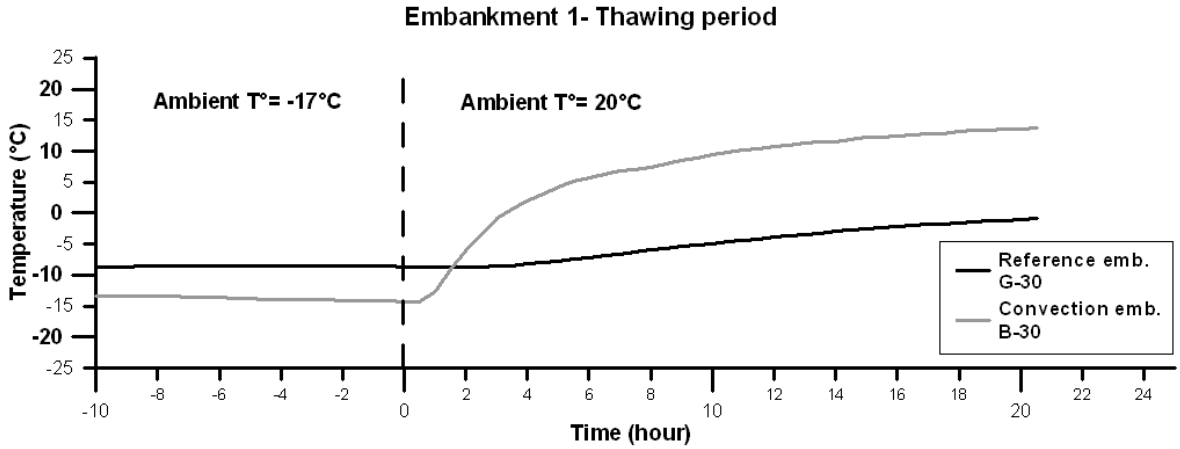

Figure 2.10 Progression of temperature with time in the reference embankment and the air convection embankment

In the laboratory a warming process was simulated to assess the rate of temperature increase in the air convection embankment compared to the reference embankment. This was achieved by moving the embankments out of the cold room and into a room with an air temperature around 20°C. The temperatures observed with the thermistor located at mid-depth in the air convection embankment and the reference embankment is shown in figure 2.10.

The results shows that the temperature in the middle of the air convection embankment rises almost immediately and 3 h after the embankment was removed from the cold room, the temperature is above 0°C. During the same period the temperature in the reference embankment has only increased by 0.3°C (from -8.7°C to -8.4°C). With the results from this test, it can be concluded that the open air convection embankment is much more sensitive to temperature changes than the reference embankment. A cold air flow could be observed at the bottom of the embankment, showing that dense cold air rapidly drains out of an unprotected air convection embankment at the toe of the slope. This will make the air convection embankment vulnerable to rapid warming during the summer months, when warm air can be forced by wind into the embankment and contribute to the rapid raise of embankment temperature together with the rapid drainage of cold air. A solution to this problem could be to place a gravel liner, which is separated from the open graded material using a geotextile, on top of the air convection embankment and to assure proper ventilation of the air convection embankment using air intakes installed along the embankment shoulders. It is expected that, while assuring air intake in the system during winter, this system will trap the cold air at the bottom of the embankment during summer, limiting thus heat intake by conduction only. This solution was used in the construction of the test-section along the shoulder of the runway at Tasiujaq Airport.

The thermal regime in the air convection embankment and reference embankment during the first year of monitoring at Tasiujaq Airport is illustrated as trumpet diagrams in figure 2.11 (Appendix E). It is clearly seen, that the annual temperature variations in the air convection embankment are smaller than what was monitored in the reference embankment, and that the geological deposits underneath the air convection embankment are kept considerably colder than underneath the reference embankment.

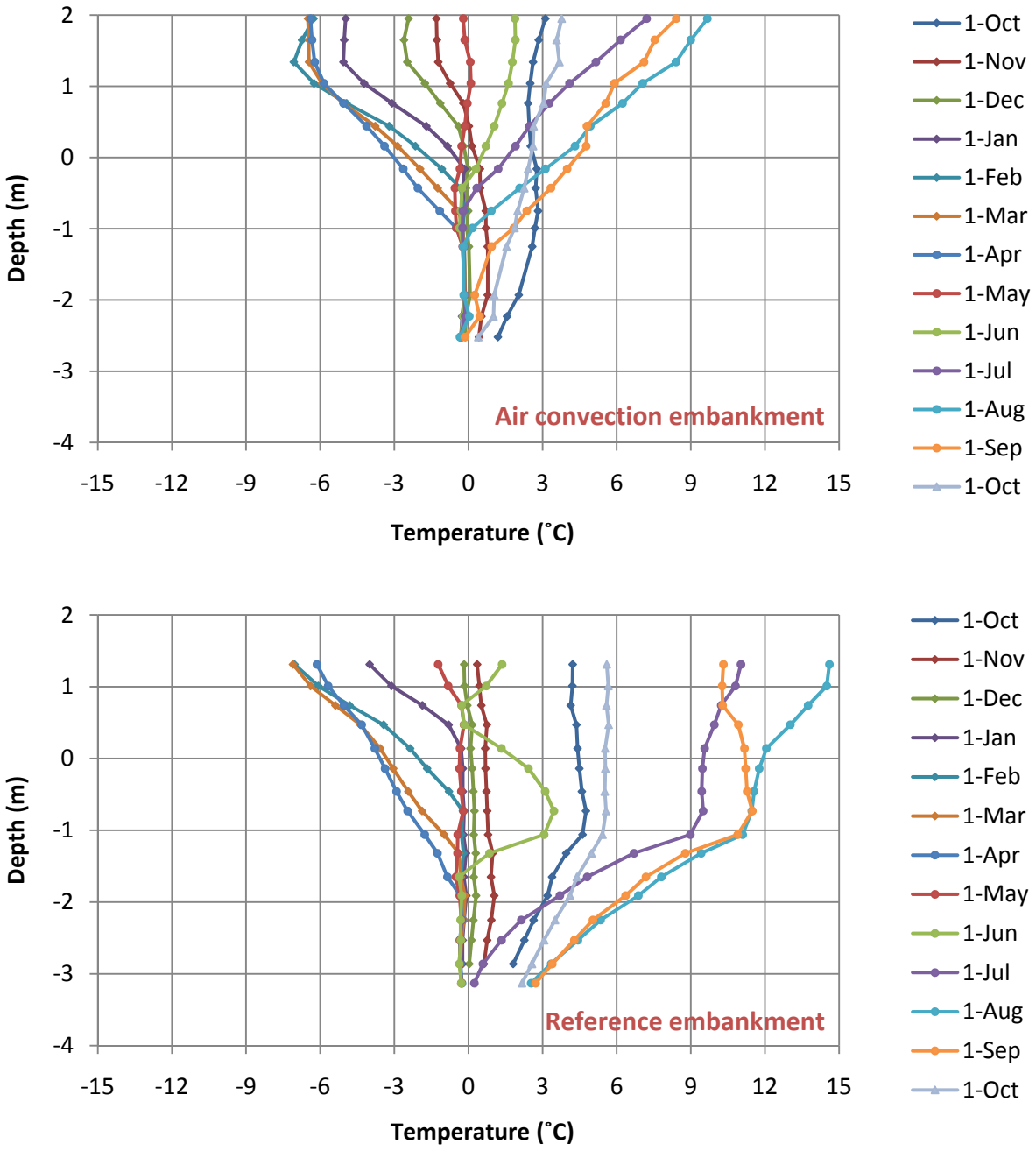

Figure 2.11 Trumpet diagrams of the thermal regime in air convection embankment (top) and the reference embankment (bottom) during the period from October 2007 until October 2008

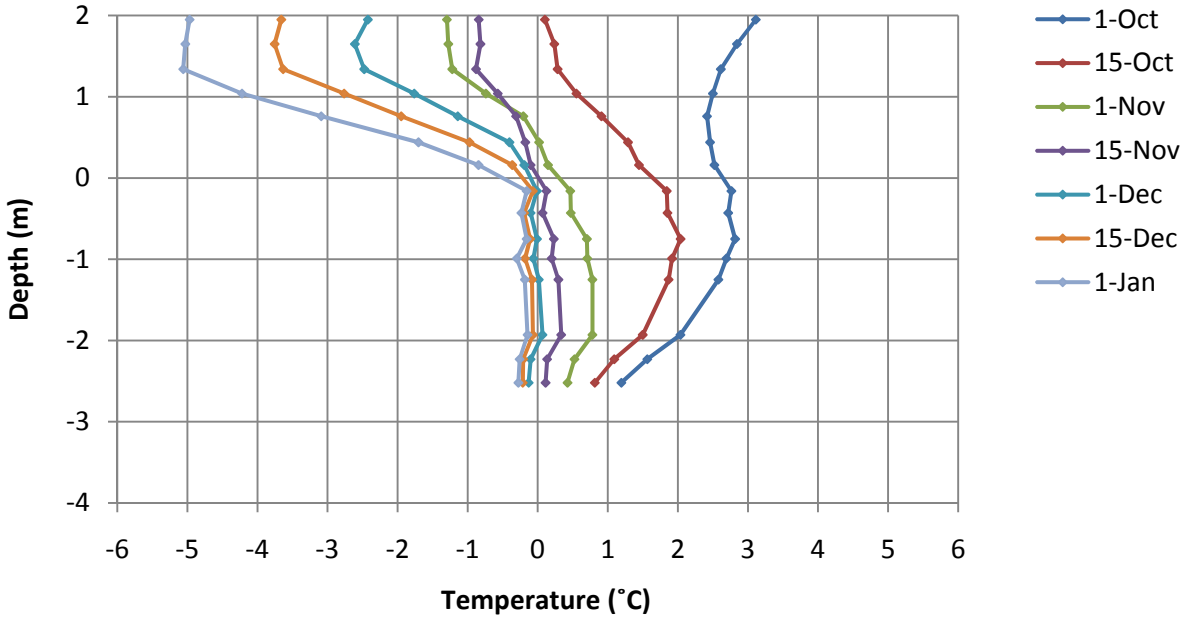

Figure 2.12 Thermal regime of the air convection embankment during the first months (from October 1, 2007 until January 1, 2008) after construction

Looking at a plot of the results from just the first months after the construction of the air convection embankment (Figure 2.12), it is seen that the measured temperatures in the geological deposits were disturbed (especially in the period until November 15) during the excavation and the installation of the thermistors. Heat seems to be trapped in the upper part of the geological deposits. The heat has been accumulated during the construction period, and the system doesn't seem to be able to extract all the heat out of the ground. During the winter period the geological deposits seem to progressively cool down and return to their intended thermal regime.

After the daily average air temperature drops below 0˚C, the air convection embankment is cooled down significantly faster than the reference embankment (Figure 2.11). At the level +1.3 m the temperature difference is approximately 2.5˚C by the beginning of December. From December, the air convection embankment seems to become less effective, and by the beginning of February the thermal regime in two embankments is almost alike. It is also worth to note that an inversion of the temperatures seems to appear in the upper part of the air convection embankment in the beginning of February (Figure 2.11). This is probably caused by the ventilation pipes and their lack of potential to expel warm air at the top of the embankment. A higher amount of drainage holes in the ventilation pipes would probably have increased the effectiveness of the system.

During spring the thermal regime of the two embankments continue to be alike, whereas from June a significant difference is observed. The air convection embankment is kept significantly colder during the entire summer period, which reduces the temperature variation of the underlying geological deposits (Figure 2.11).

The annual temperature variation at the sub-grade level is shown in figure 2.13. It is seen that the temperature at the sub-grade level, in the two embankments, are quite similar during the freezing period. Thus the temperature in the air convection embankment is significantly lower during the thawing period, which will lead to a decreased thaw-depth underneath the air convection embankment compared to that below the reference embankment. The mean annual sub-grade temperature is approximately 1.0˚C for the air convection embankment, whereas it is approximately 2.7˚C for the reference embankment.

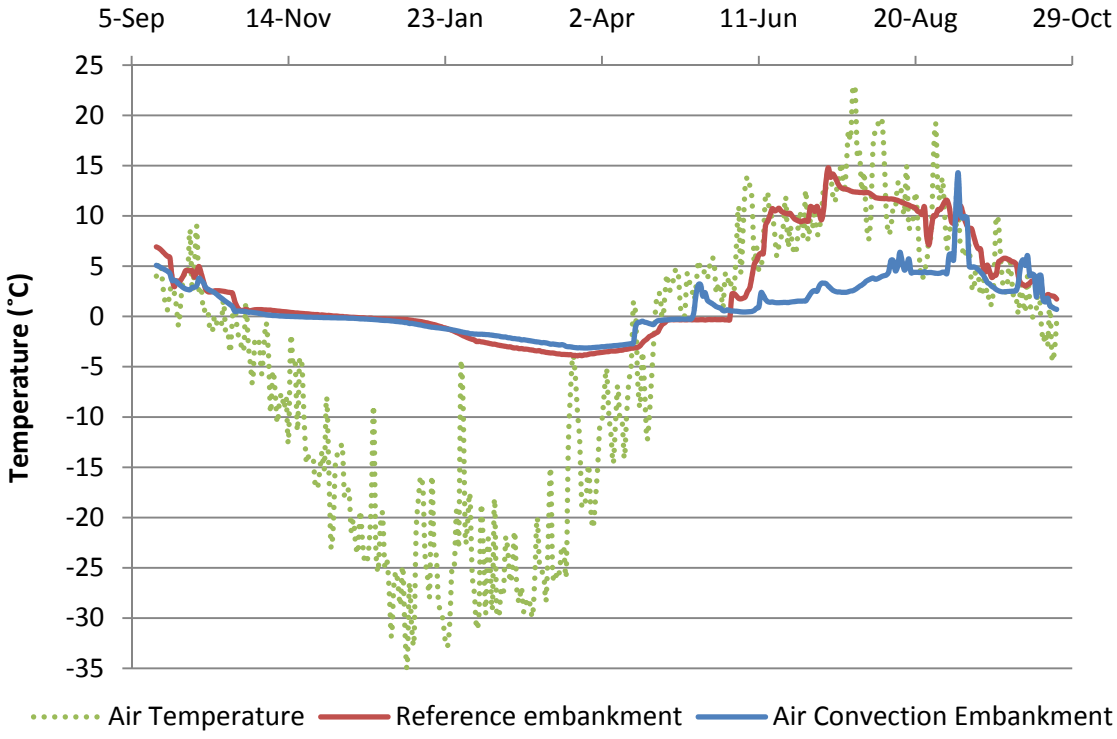

Figure 2.13 Temperature variation at sub-grade level and air temperature. The sub-grade temperatures for the first months are misleading because of the changes in the thermal regime, which was disturbed during construction

The thermal regime of the air convection embankment and the reference embankment at minimum and maximum temperature conditions is illustrated on figure 2.14. It is obviously that the thermal regime in the reference embankment and the air convection embankment is quite similar during winter conditions. The temperature difference between the thermal regimes, which was observed under controlled conditions in the laboratory tests (figure 2.8), is not obtained under the natural conditions at the test-section in Tasiujaq Airport. Comparing the thermal gradients, during minimum temperature conditions (figure 2.14), it seems like the sought heat flow doesn't occur. This is, as earlier mentioned, probably caused by the poor performance of the ventilation pipes. The thermal regime of the geological deposits is also quite similar below the two embankments. This scenario is assumed to be different from the winter 2009, since the temperature variations in the air convection embankment have shown (figure 2.13 and 2.14) to be significantly lower during the summer period. A decrease in the temperatures of the geological deposits underneath the air convection embankment is therefore expected to occur.

The thermal regime at maximum temperature conditions is quite different for the air convection embankment compared with the reference embankment (Figure 2.14). Cold air seems to be trapped in the air convection embankment during the summer period. This situation results in a reduction of the temperature conditions in the entire air convection embankment and in the upper part of the geological deposits. At sub-grade level the temperature difference between the two embankment types is approximately 8˚C (Figure 2.14). The thaw depth, at this time of year, is approximately 1.0 m below the air convection embankment, whereas the thaw depth underneath the reference embankment is more than 3.0 m. The maximum thaw depth is registered to be more than 3.0 m for both embankment types by the beginning of October (Figure 2.11). However, the thermal regime of the air convection embankment and the geological deposits is significantly colder than the thermal regime in the reference embankment. The difference is approximately 2.5-3.0˚C.

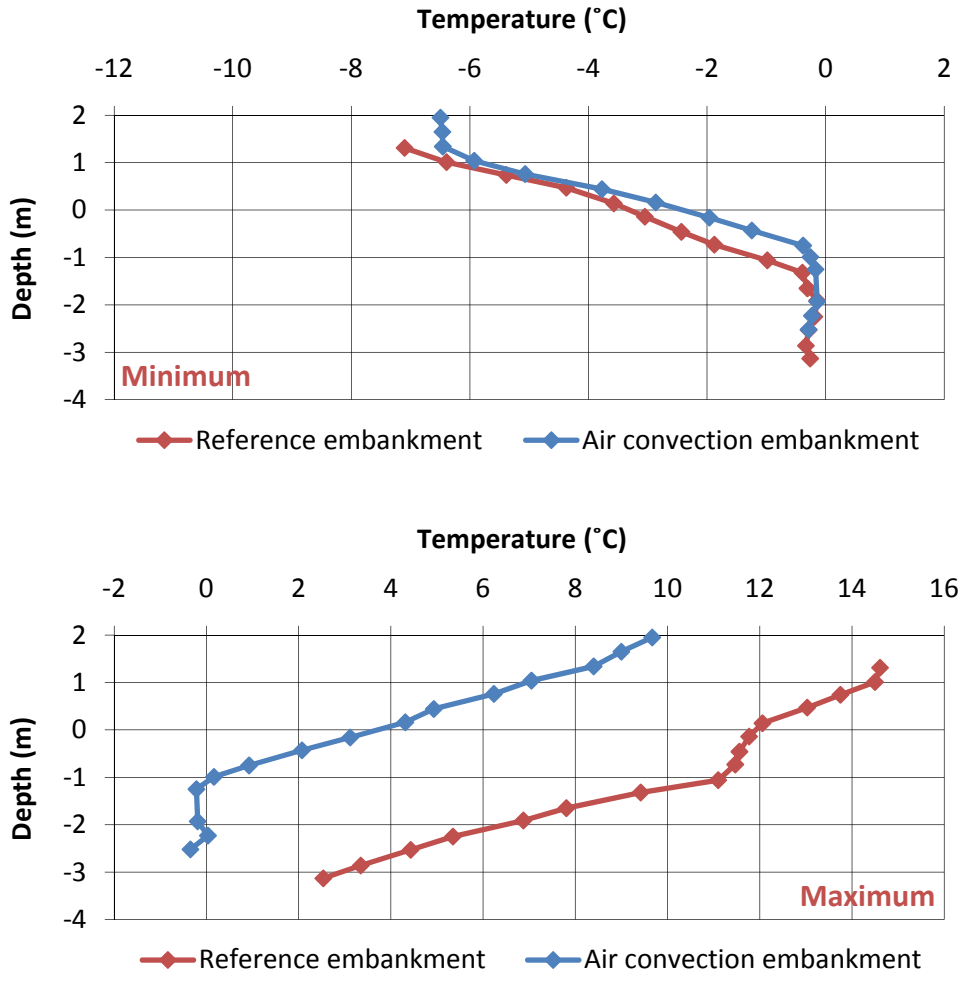

Figure 2.14 Thermal regime of the air convection embankment and the reference embankment during minimum (top) and maximum temperature conditions (bottom)

2.4 Heat Drain

The heat drain is an innovative system, developed at l'Université Laval in order to protect the side-slopes of road and airfield embankments. The heat drain is placed in the shoulder and an air intake is installed at the foot of the embankment to allow upwards circulation of air in the membrane during winter months (Figure 2.15). The main purpose of this method is to extract heat from the embankment in order to raise the permafrost table in the ground at that critical location (Beaulac and Doré, 2006-B).

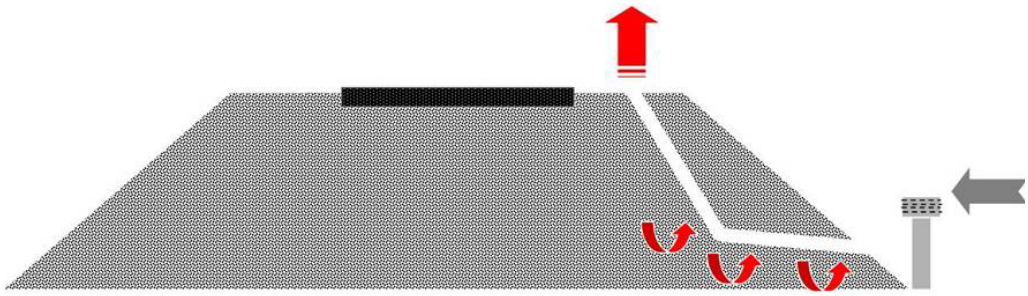

Figure 2.15 Heat drain placed in the shoulder of a road embankment (Beaulac, 2006)

2.4.1 Description

The heat drain technique consists of a drainage geocomposite with high permeability, placed in the shoulder of a road embankment. The geocomposite is composed of a corrugated plastic core covered by geotextile layers with a total thickness of 25 mm, allowing air to flow into the embankment (Figure 2.16). An air intake system is installed at the base in order to allow an upward movement of air in the membrane (Beaulac, 2006). This movement of air, also called the chimney effect, is a result of a lower density caused by the change in temperature. The drain is designed to facilitate heat extraction. The heat initially flows towards the heat drain by conduction and is then expelled of the embankment by convection. The purpose of the method is to extract heat from the ground and the embankment in order to rise or, at the minimum, to prevent a depression in the permafrost level.

Figure 2.16 The geocomposite, which is used to extract heat out of the embankment (Beaulac and Doré, 2006-B)

Heat conduction occurs in all soil constituents and involves a transfer of kinetic energy from molecules in a warm area to a cooler area of the material. Considering a prismatic element of a given soil, having a cross-sectional area A, at right angles to the heat flow q, the conduction is given as (Andersland and Ladanyi, 1994):

$$Q = -\mathrm{k_u A}\frac{\mathrm{dT}}{\mathrm{dx}} \tag{2.3}$$

$$q = \frac{\mathrm{Q}}{\mathrm{A}} = -\mathrm{k_u}\frac{\mathrm{dT}}{\mathrm{dx}} = \mathrm{k_u i} \tag{2.4}$$

where Q/A = q is the rate of heat flow per unit area (J/m^2·s or W/m^2), k_u the unfrozen thermal conductivity (J/s·m·K or W/m·K), dT/dx = i is the thermal gradient (K/m), and A is the area (m^2). The negative sign indicates that the heat flow is going from a high to a low temperature.

Heat transfer by convection is a process, which removes heat from the surface, when the latter is exposed to a fluid (liquid or gas) by the temperature difference from surface (Krahn, 2004). The convection can be either natural or forced. The transfer of heat is defined as:

$$q = \mathrm{h}(\mathrm{T_s} - \mathrm{T_\infty}) \tag{2.5}$$

where q is the heat flux (W/m^2), h is the convection coefficient (W/m^2·K), T_s is the temperature of the surface (K) and T_∞ is the temperature of the fluid (K). The convection coefficient is often given from theoretical or empirical equations based on the Nusselt number, Rayleigh number, Prandtl number and the properties of the fluid.

2.4.2 Laboratory studies

During the winter 2007 a laboratory test were carried out in a cold room at l'Université Laval (Appendix B). A small-scale shoulder of a road embankment (25-50 % of a full-scale road embankment) with and with-out (reference embankment) a heat drain were constructed. The embankments were built of a natural gneissic granular material (≤ 18.75 mm) from a gravel-pit located near Québec City, Québec, Canada (Voyer, 2008). The bulk density of the material was determined to approximately 2.0 g/cm^3 and the water content 6.0 %. In the section with the heat drain, a geocomposite was installed in the middle of the embankment (between the thermistors located at 15 cm and 30 cm from the bottom of the embankment), while ventilation pipes (100 mm in diameter) were placed along the top and toe of the embankment to allow air to circulate (Figure 2.17).

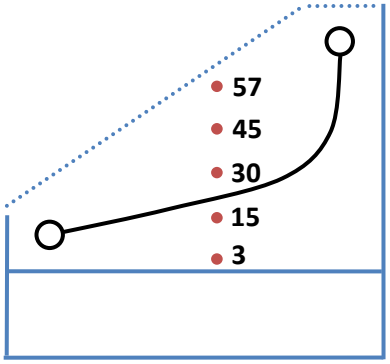

Figure 2.17 Installation of geocomposite and ventilation pipes in the heat drained embankment. The position of the thermistors is shown as the distance from the bottom of the embankment

The box, used for the laboratory testing, included two sections. The box was insulated by covering the outside with a 50 mm polystyrene layer and a 100 mm layer of polystyrene was placed between the two sections to avoid heat losses. Finally, a layer of 300 mm glass wool was placed on the top of the embankments to recreate the insulating effect from a snow cover. In each section, 5 thermistors were installed to continuously monitor the thermal regime of the embankments. The dimensions of the box and the location of the thermistors are shown in figure 2.3.

2.4.3 Field studies

A test-section was established in September 2007 along 50 m of the southeastern orientated shoulder of the runway in Tasiujaq Airport. Before construction, the original shoulder of the runway was removed by excavation. To minimize the period of disruption of the temperature regime in the underlying geological deposits, the construction of the embankment began immediately after completion of the excavation. A borehole was established in the middle of the section for the installation of thermistors in the underlying geological deposits. After that, a thin sand layer was placed at the bottom and on the side, before geocomposite and ventilation pipes were installed (Figure 2.18). The final structure of the embankment is illustrated in figure 2.19.

The borehole was instrumented with 16 thermistors, which were placed with an interval of approximately 300 mm in different heights above and below the natural ground level. Furthermore, two sets of thermistors were installed in one of the pairs of chimneys, which were used as intake and outlet for respectively the cold air and warm air (Doré et. al, 2007). Since the completion of the construction, the thermal regime of the embankment and the underlying geological deposits have been stored every 6 h.

Figure 2.18 Installation of the geocomposite into the shoulder of the runway at Tasiujaq Airport (Doré et. al, 2007)

2.4.4 Results

The laboratory test of the heat drain technique was carried out to study the effect of the method with ventilation pipes installed at the top and bottom of the embankment (Appendix B). The embankment box was placed in the cold room and brought to steady state conditions. The heat flow inside the embankment during steady state conditions are shown in figure 2.20. It is clearly seen that the installation of the heat drain system has a significant effect on the thermal conditions and causes a decrease in temperatures compared to the conditions observed in the reference embankment. The effect is concentrated around the geocomposite (between the thermistors at 15 cm and 30 cm) and in the upper part of the test embankment. The temperatures at the bottom are only slightly colder than the temperatures in the reference embankment (the difference is approximately 1˚C). This situation is however normal, considering that a 0˚C temperature is imposed at the bottom of the embankments and the presence of a normal granular material below the heat drain. This observation shows that the heat drain will have a maximum effectiveness if placed near the bottom of the embankment. At the test-site in Tasiujaq Airport the heat drain has been placed as low as possible in the embankment, there is only a thin sand layer between the sub-grade and the heat drain.

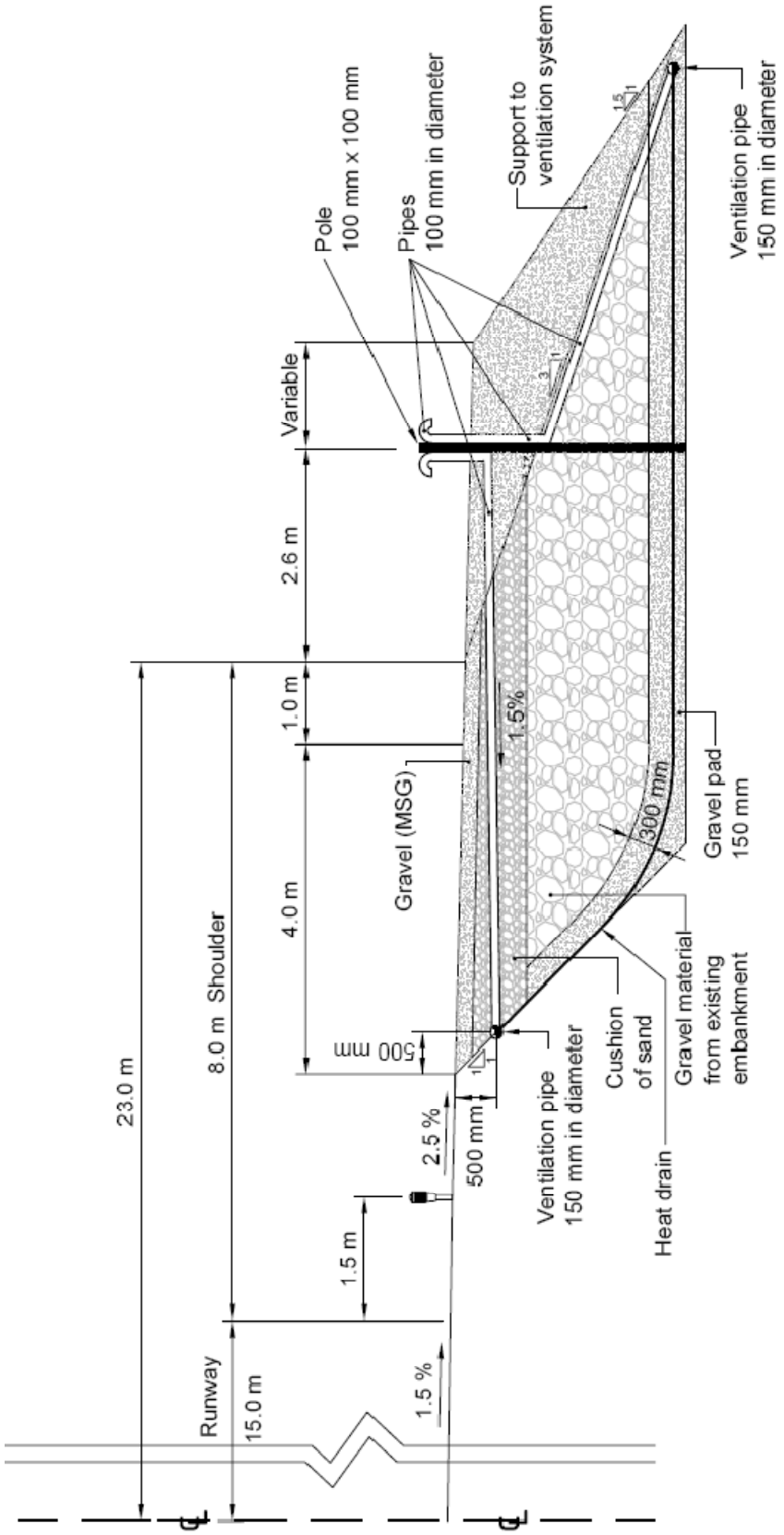

Figure 2.19 Structure of the heat drained embankment at Tasiujaq Airport (based on Doré et al., 2007)

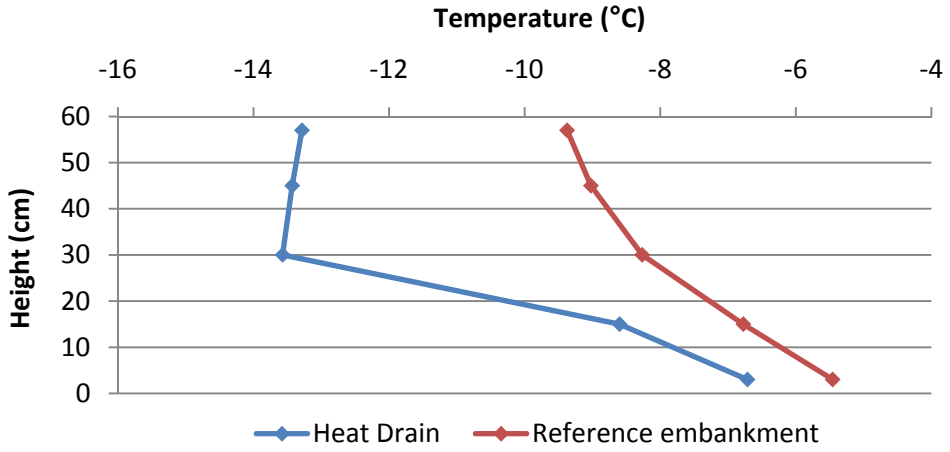

Figure 2.20 Heat flow during steady state conditions with an open top and an open bottom. The height is shown from the bottom of the embankments

The temperature results from the first year of monitoring at the test-site in Tasiujaq Airport are illustrated as trumpet diagrams in figure 2.21 (Appendix E). It is clearly seen, that the annual temperature variations in the heat drained embankment is significantly smaller than the temperatures monitored in the reference embankment. The thickness of the annual thaw depth underneath the heat drained embankment is also significanly smaller. Below the heat drain, the maximum thaw depth reaches down to approximately -1.5 m, whereas underneath the reference embankment the thickness is greater than -3.0 m. So by installing the heat drain into the shoulder of the runway, the thaw depth has been reduced by minimum 1.5 m.

The thermal regime of the geological deposits underneath the heat drained embankment were disturbed during the construction phase. Heat seems to be trapped in the middle of the embankment (November and December) and in the upper part of the geological deposits. During the winter period the thermal regime seems to progressively return to more natural temperature conditions.

From the period, where the daily average temperature drops below 0˚C, it is seen, that the heat drain technique contribute to an increased cooling of the embankment during the winter period (January, February, March and April) compared to what is measured in the reference embankment (Figure 2.21). At the level +1.0 m the installation of heat drain have induced a cooling of approximately 3-4˚C during the winter period.

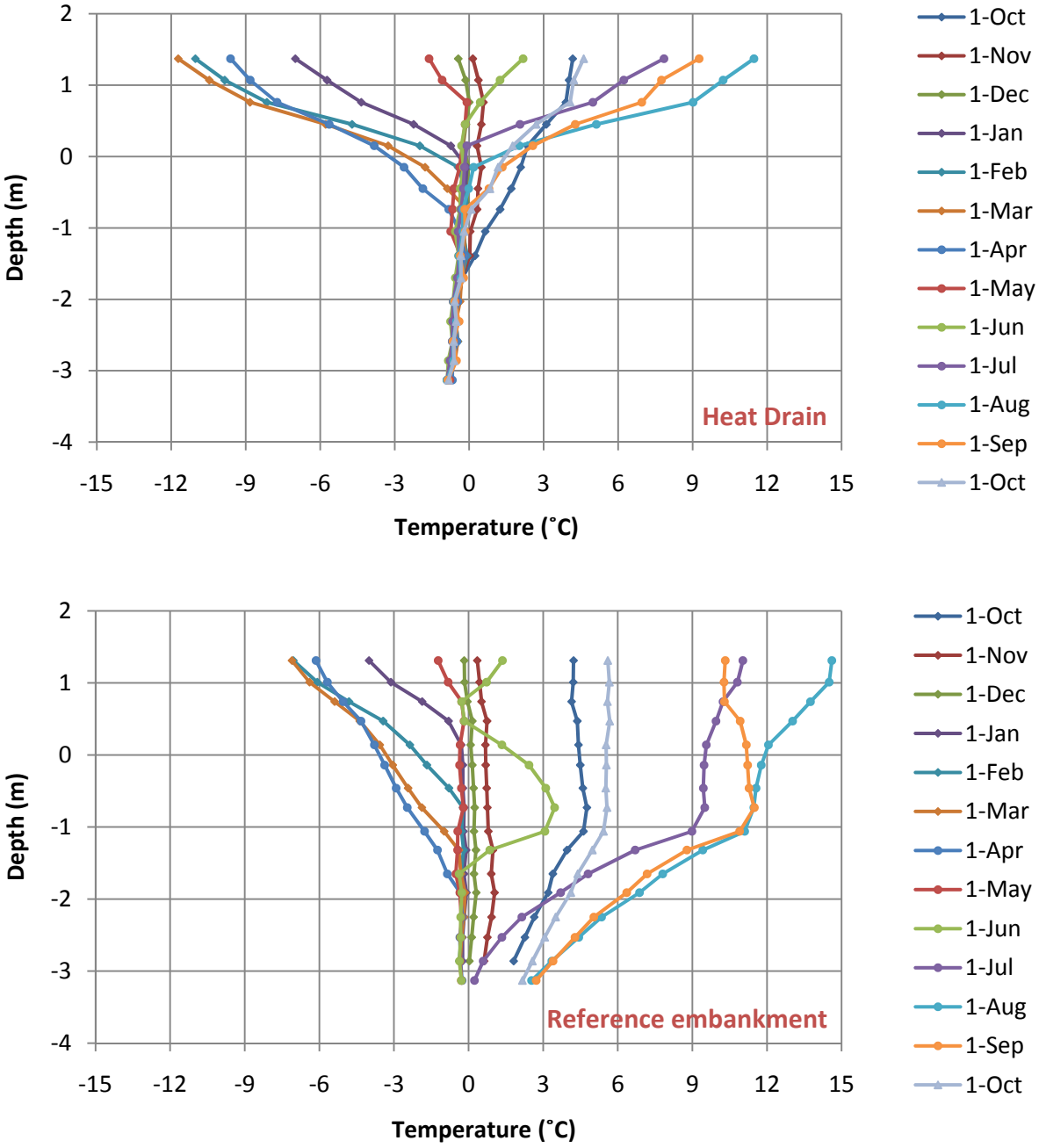

Figure 2.21 Trumpet diagrams of the thermal regime in the heat drain (top) and the reference embankment (bottom) during the period from October 2007 until October 2008

During the summer period a significant difference in the thermal regime of the two embankment types is observed. The heat drained embankment and the underlying geological deposits is significantly colder than compared to the reference section. Especially the temperature regime from the depth of the installed heat drain and down is considerable. At the level -1.0 m the temperature difference is up to 10-12˚C in the late summer months (Figure 2.21).

The temperature variations at the sub-grade level are illustrated in figure 2.22. It is clearly seen, that the heat drained embankment is significantly colder during the summer period, which will lead to reduced thaw in the underlying geological deposits compared to that below the reference embankment. Whereas the mean annual sub-grade temperature is approximately 2.7˚C for the reference embankment, this value is approximately 0.1˚C for the section with the heat drain.

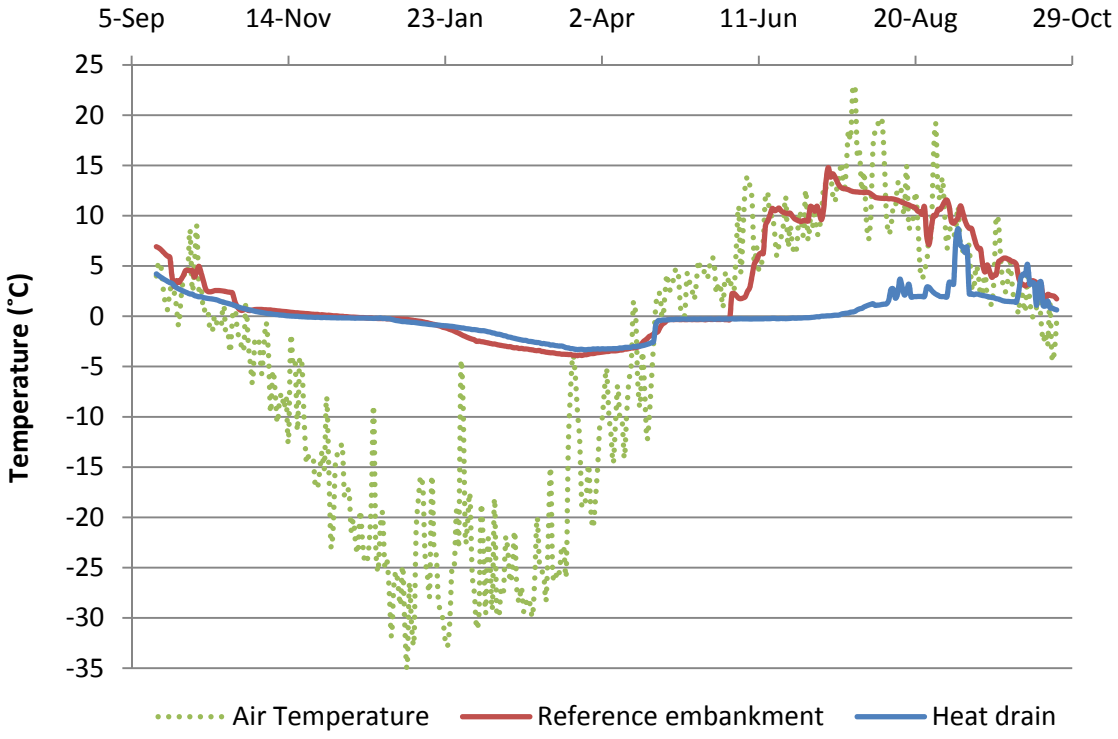

Figure 2.22 Temperature variation at sub-grade level and air temperature. The sub-grade temperatures for the first months are misleading because of the changes in the thermal regime, which was disturbed during construction

The thermal regime of the heat drained embankment and reference embankment at minimum and maximum temperature conditions is illustrated on figure 2.23. During minimum temperature conditions it is seen that the thermal gradient (temperature change per meter depth) in the heat drained embankment is nearly twice the size in comparison to the one obtained in the reference embankment. Although the heat drained embankment is colder than the reference embankment, the thermal regime of the geological deposits is warmest underneath the heat drained embankment. This situation is probably caused by the thermal disturbances, which occurred during the construction of the test-sections. Looking at the thermal regime at figure 2.23, it seems like heat is still trapped in the geological deposits between level -0.5 and -2.0 m. The thermal regime of the sub-grade soils underneath the heat drained embankment is anticipated to be different from the winter 2009; the cooling of the embankment should lead to a progressively cooling of the permafrost.

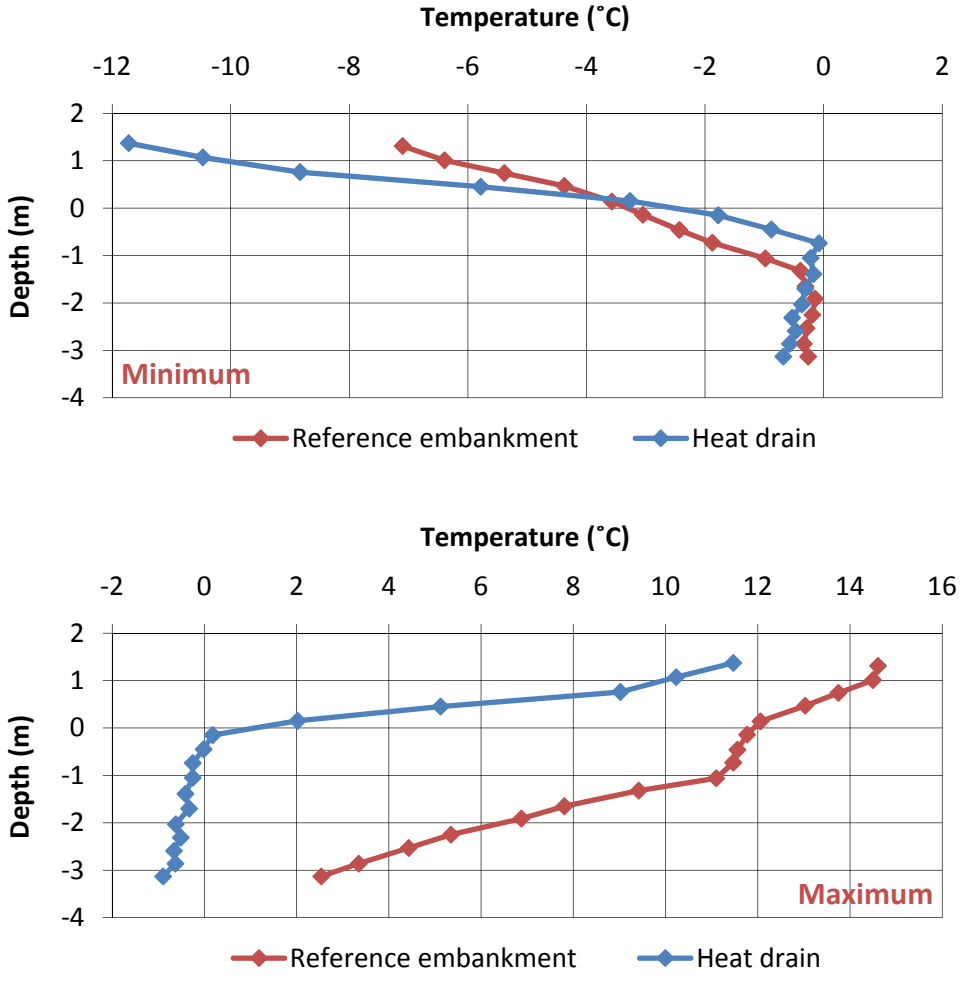

Figure 2.23 Thermal regime of the heat drained embankment and the reference embankment during minimum (top) and maximum temperature conditions (bottom)

During maximum temperature conditions the heat drained embankment is significantly colder than the reference embankment (Figure 2.23). Around the installation of the heat drain (just above the sub-grade level), the thermal differences is approximately 10˚C, whereas the difference is only about 3˚C at the top of the embankments. Already at a depth of approximately -0.5 m the temperature drops below 0˚C underneath the heat drained embankment, whereas the temperature at this time of year is still above 11˚C underneath the reference embankment. This observation constitutes a huge difference in the thermal regime of the two embankments, and a notable reduction in the annual thaw depth by installation of the heat drain technique.

2.5 Reflective surface

The surface temperature of black asphalt can be reduced by white paint or other reflective materials, which will increase the albedo of the surface and thereby lead to a reduced thickness of the active layer in permafrost areas underneath a road embankment. The first reported use of white paint, to increase the albedo of a surface, was reported in 1963, when paint was successfully used to reduce the annual thaw depth underneath the runway at Thule Air Base in northern Greenland (Esch, 1996). Despite the benefit of a reduced thaw depth, the use of reflective surfaces has not gained popularity, because of problems with low skid resistance and high maintenance costs. Today new reflective materials, with higher skid resistance, are available. This can lead to an increased use of reflective surfaces on road embankments in arctic regions.

2.5.1 Description

The mean annual temperature of a given surface differs from the mean annual air temperature with no constant difference between them. The difference accounts on several factors including net radiation, vegetation, snow cover, ground thermal properties, surface relief, subsurface drainage, surface type, and wind speeds (Andersland and Ladanyi, 1994). Average temperatures for the entire freezing or thawing seasons are used to estimate the air freezing (I_{af}) and air thawing (I_{at}) indices. Surface indices are estimated using an empirically determined surface n-factor defined as:

$$n_t = \frac{\mathrm{I_{st}}}{\mathrm{I_{at}}} \tag{2.6}$$

$$n_f = \frac{\mathrm{I_{sf}}}{\mathrm{I_{af}}} \tag{2.7}$$

where n_t is the n-factor for a given surface during the thawing season and n_f is the n-factor during the freezing season. I_{st} is the ground surface thawing index and I_{sf} is the ground surface freezing index. The warming of soil beneath paved roads is attributable to several causes as removal of vegetation, reduction in evaporation due to the presence of pavement, loss of shading due to clearing for a road and reduction of albedo caused by dark surfaces (Reckard, 1985).

Use of reflective surfaces can reduce the n-factor and has proven to be effective in reducing the thaw depth in permafrost regions. Reflective surfaces, based on the use of white painting applied on pavement surfaces, have been tested in several experimental projects in Alaska (Berg and Esch, 1983; Esch, 1988; Reckard, 1985). In 1982, a comparison of a white-painted, a yellow-painted and a normal asphalt pavement was carried out in Fairbanks, Alaska. Results from this test showed a reduced n-factor for the yellow-painted surface of 15 %, while the n-factor for the white painted surface was reduced by 20 % (Berg and Esch, 1983).

2.5.2 Field studies

During the summer months in 2005-2008 a total of 15 Ground Penetrating-Radar (GPR) investigations were carried out at the southern parking area of Kangerlussuaq Airport (Figure 2.24) (Appendix C). The objectives of the measurements were to study the variations in the depth of the frost table throughout a complete thaw-freeze season and to compare the differences in the depth underneath a normal dark asphalt surface and a more reflective surface (white paint). The GPR method was chosen because the method has proved to be useful for mapping the distribution of permafrost and near-surface geological structures (Annan, 2002; Annan and Davis, 1976; Pilon et al., 1992). Especially the frost table is often observed as a strong reflection in the GPR data (Appendix A; Ingeman-Nielsen, 2005; Arcone et al., 1998).

GPR systems produce a short pulse of high frequency electromagnetic energy which is transmitted into the ground. The propagation of the signal depends on the electrical properties of the ground, which are mainly controlled by the water content of the investigated materials. Changes in the dielectric properties will cause a reflection of parts of the transmitted signal, while the rest of the signal will continue to propagate into the ground. Reflection will occur at each successive interface in the ground, until the signal has been damped by losses in the ground. The reflected signal is detected by the GPR receiver and travel times for the individual radar waves can be used to display the results in a radargram, in terms of received amplitude as a function of travel time (Daniels, 2004).

Results from a GPR investigation give insight into the structural changes in the ground, but do not directly show the composition or type of the materials investigated. To calibrate the GPR

results from Kangerlussuaq Airport, a borehole was drilled and a trench was dug in August 2005 (Figure 2.25). The borehole was terminated to a depth of 15 m and provided data on the thicknesses of the different layers in the embankment and subsurface, water content and grain size, while the trench was dug just beside the border of the asphalt area to determine the depth of the frost table. To determine the n-factor for both the normal dark asphalt surface and the reflective surface, temperature sensors were installed in the pavement on the southern parking area in June 2007.

Figure 2.24 Kangerlussuaq Airport with location of test area (blue circle)

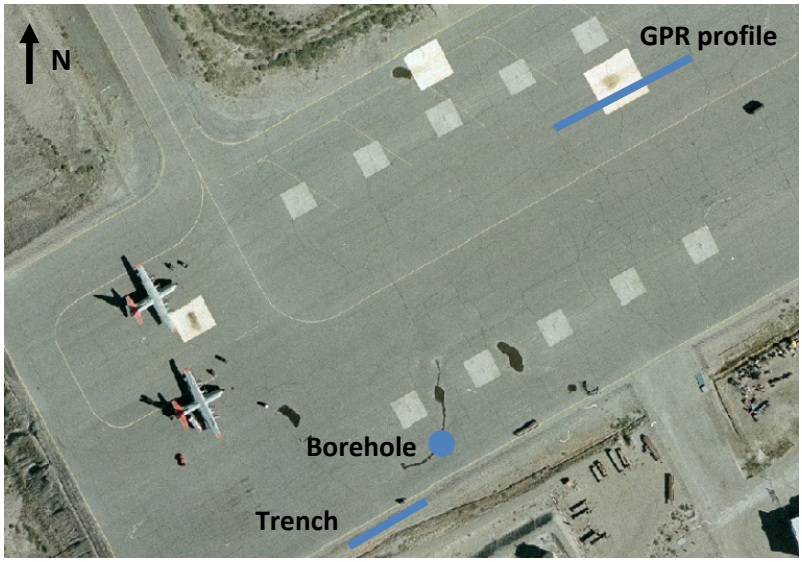

Figure 2.25 Placement of the GPR measurements and location of the trench and the borehole

2.5.3 Thermal modeling

A thermal model of the embankment at the southern parking area in Kangerlussuaq Airport was used to study the changes in the thickness of the active layer, underneath a normal dark asphalt surface and a more reflective surface, as a result of the increase in the recorded air temperatures from 1992-2007 (Figure 2.26) (Appendix D). The modeling was carried out with the finite element software TEMP/W from GEO-SLOPE International Ltd.

The temperature data used in the modeling are mean monthly air temperatures from the period 1992-2007 (Danish Meteorological Institute, 2008). The mean monthly air temperatures for the winter months can vary in excess of 10-20°C on a year-to-year basis, while the summer months are much more consistent. Surface temperature for the two surfaces investigated was recorded from June 2007 until September 2008. The measured temperatures were used to estimate the n-factors, which were used in the modeling (Table 2.1).

A five layered model of the original geological deposits and the embankment construction was established using the information obtained from the borehole, established in August 2005.

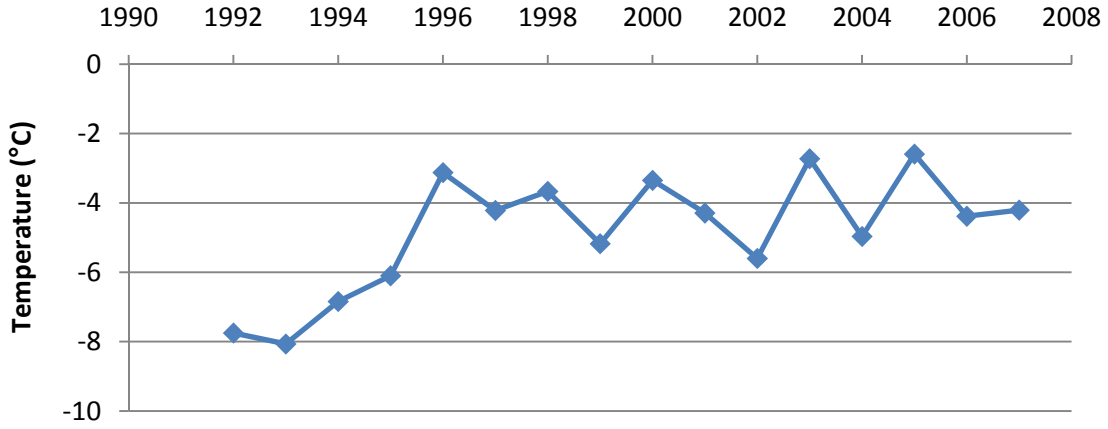

Figure 2.26 Mean annual air temperature in Kangerlussuaq, 1992-2007 (Danish Meteorological Institute, 2008)

Surface	n_f	n_t
Normal dark asphalt surface	0.90	1.65
Reflective surface (white paint)	1.00	1.20

Table 2.1 Estimated n-factors for each of the two investigated surfaces in Kangerlussuaq Airport. The n_f-values was used for the freezing seasons (T < 0˚C) and n_t-values was used for the thawing seasons (T > 0˚C)

2.5.4 Results

Figure 2.27 illustrates the difference in the depth of the frost table underneath the normal dark asphalt surface and the more reflective surface (white painted area). The variations in the depth of the frost table throughout the thaw-freeze season are illustrated in figure 2.28 (Appendices A and C). Based on borehole information, the measured depth of the frost table (produced by trench excavation) and GPR data, collected at the locations of the borehole and the trench in August 2005, the radar wave velocity in the unfrozen sediments was found to be 0.13 m/ns, which correspond to a permittivity on 5.3. The top soils at the borehole location were unsaturated sorted sand until a depth of 3.5 m with water content in the range of 2-5 %. Using a calibration curve, empirically determined by Topp et al. (1980) and soil parameters (dry-density 2.70 g/cm^3 and porosity 30 %), generally used for sandy materials in the area, a permittivity on 5.3 result in a water content on 4.75 % for the material. This value lies within the interval of the water content measured in the soil samples from the borehole.

The low water content and well sorted sandy material, which result in a low adherence of the water particles, gives a situation close to dry conditions and temporal changes in the velocity due to changing pore-water content in the unfrozen sediments were therefore neglected in the present study. An increase in water content will result in an increased permittivity of the material, which will have lead to a decreased velocity of the radar waves.

The GPR results (Figure 2.28) illustrate the lowering of the frost table with time. The results also show the effect of the white surface on the depth of the frost table. The fact that the changes in depth to the strong reflection on the radargrams are aligned with the boundaries of the painted area (26 m wide) confirms that this reflection is actually the interface between the frozen and unfrozen ground (Figure 2.27).

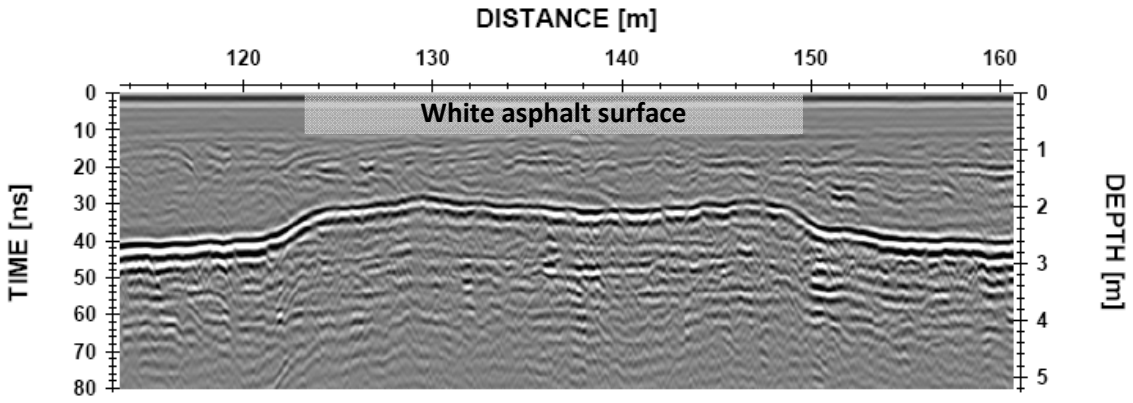

Figure 2.27 Radargram from July 2007 showing the depth of the frost table. The frost table is seen as a strong reflector in the depth of approximately 2.7 m underneath the normal dark asphalt surface (left and right parts of the radargram) and 2.1 m underneath the white painted area (middle of the radargram)

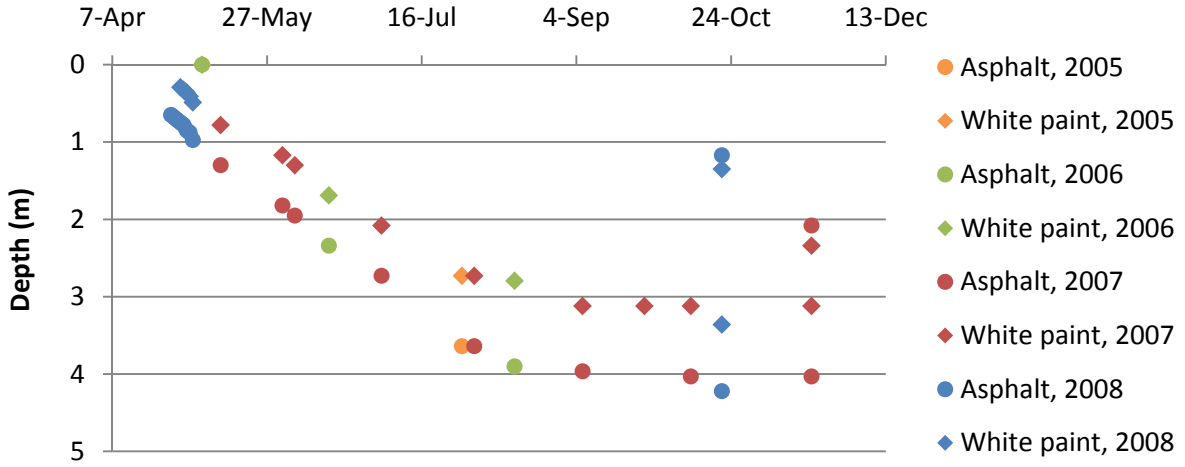

Figure 2.28 Variations in the depth of the frost table underneath the normal dark asphalt surface and the white painted area

During the period 1992-2007 the mean annual air temperature in Kangerlussuaq has increased by approximately 2.5˚C (Figure 2.26). To gain insight into what impact the air temperatures has on the annual thickness of the active layer, a thermal model was constructed for the 15 year time period (Appendix D). The modeling was carried out for each of the two surfaces, a normal dark asphalt surface and a more reflective surface (white paint), which has been investigated with the GPR. The results of the modeling showed, that the average modeled maximum thaw depth underneath both surfaces has increased with approximately 0.5-0.7 m during the period 1992-2007 (Figure 2.29).

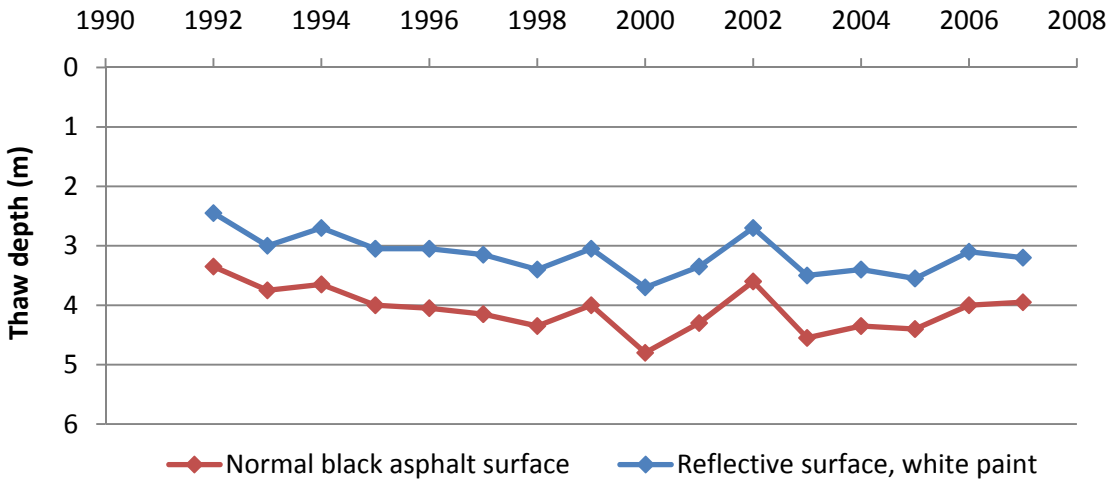

Figure 2.29 Modeled thaw depths under the southern parking area in Kangerlussuaq Airport, 1992-2007

The results, from both the GPR and the thermal modeling, have shown that the present change in active layer thickness due to the increased reflectivity of surface amounts to approximately 0.8-1.0 m in late summer (Appendices A, C and D). This constitutes a major difference in the thermal conditions below the reflective surface and the normal dark asphalt surface. The results should promote the interest in the development and use of light-colored pavement materials to reduce settlements under arctic infrastructures caused by the annual thaw-freeze cycle and increasing thickness of the active layer.

Chapter 3: Discussion

3.1 Strengths and weaknesses in analysis

The promising laboratory results of the heat drain and air convection embankment techniques have lead to the construction of a full-size test-site at Tasiujaq Airport, Nunavik, Québec, Canada. The test-site was constructed in September 2007 and the results from the first year of monitoring have been very promising. To get a more reliable picture of the effectiveness of the two techniques, data should be collected for a longer time period, minimum 2-3 years with continued monitoring.

The use of reflective surfaces has been monitored throughout the thaw-freeze seasons at Kangerlussuaq Airport, Greenland, in the years 2005-2008. The Ground Penetrating-Radar (GPR) method has been used to measure the annual variation in the depth of the frost table underneath a dark asphalt surface and a reflective surface (white paint). The GPR results have been very useful in following the changes between the frozen and unfrozen materials in the ground. To calibrate the GPR results a borehole was drilled and a trench was dug in August 2005. Only one borehole was established caused by limited funding and time. Additional boreholes could have helped to give a more reliable picture of the geological deposits underneath the airfield embankment and thermistors should have been installed in the boreholes, so the thermal regime of the ground could have been measured. This information could have helped to give an even better understanding of the annual changes of the ground.

All three investigated mitigation techniques have shown to have a positive impact on the protection of permafrost. They all lead to a decrease in the thickness of the active layer compared to what have been observed underneath the reference embankments, which again should lead to a decrease in the problems with instability and thaw settlements.

3.2 Recommendations for implementation

The implementation of the air convection embankment or the heat drain technique into the construction of a road embankment will lead to a small increase in construction costs. However the implementation of the techniques will lead to a decrease in maintenance costs, and to a higher stability of the embankment structure. For the implementation of the air convection embankment, it is essential that boulders or rocks of an adequate size are accessible close to the building site. The heat drain technique requires the same type of granular material as an ordinary embankment. The implementation of the heat drain technique also requires geocomposite and ventilation pipes, which should be built into the shoulder of the embankment. The transportation of the geocomposite to the remote location in the Arctic can be complicated, but should be possible with cargo ships or planes.

The use of reflective surfaces have until now been kept to a minimum because of problems with very low skid resistance and high maintenance costs (repainting of the surfaces). Today new reflective materials with a higher skid resistance and lighter-colored asphalt pavements are available, which can lead to an increased use of the reflective surfaces on road embankments in arctic regions.

Based on the experiences obtained during the field investigations it could be recommended to implement the studied mitigation techniques into embankments constructed on thaw sensitive sedimentation soils to minimize problems with decreasing permafrost.

3.3 Recommended additional research

Test sections with respectively the air convection embankment and the heat drain techniques have been constructed as a part of a new test-site on a highway in Yukon Territory, Canada, in the summer 2008. This project is carried out by l'Université Laval and the University of Alaska Fairbanks, in cooperation with the Yukon Highways and Public Works.

In Sisimiut, western Greenland, two smaller test-sites were established in August 2008 and September 2008, respectively. On an existing road the effect of a light-colored asphalt pavement will be studied and compared with the performance of a normal dark asphalt. The light-colored asphalt pavement contains 46.75 % regular granite materials, 46.75 % calcined flint and 6.50 % binder. The second test-site was established during the construction of a new road. This test-site includes a section with an air convection embankment. Both projects are carried out by the Arctic Technology Centre, Technical University of Denmark, in cooperation with the former Municipality of Sisimiut (Sisimiut Kommunianut, from January 2009 a part of

the new Qeqqata Kommunianut) and with financial support from the Commission for Scientific Research in Greenland (Kalaallit Nunaani ilisimatuutut misissuinernut kommissioni / Kommissionen for Videnskabelige Undersøgelser i Grønland).

The test-site at Tasiujaq Airport includes a test-section, where the existing shoulder of the runway was extended from having a 2H:1V slope to a gentler slope, 8:1 (Appendix E). The goal was to reduce wind turbulence, resulting in reduced snow accumulation. Results from the first year of monitoring showed a positive effect on reducing the annual temperature variations in the test-embankment and the geological deposits is kept considerably colder during the summer period than underneath the reference embankment. Optimization of this method is therefore of great interest.

Still, in the coming years, it should be attempted to establish a couple of additional test-sites on different field locations in the Arctic. Furthermore the data collection should be carried out throughout a continuous period of minimum 2-3 years. This will help to get a more reliable picture of the actual effect of the three studied mitigation techniques, as well as the gentle slope, and their impact on the thermal regime of the permafrost underneath the test embankments. It could also be of great interest to carry out additional modeling and laboratory tests to optimize the effectiveness of the air convection embankment technique. This should be done by carrying out tests with different geometries and locations of the ventilation pipes, as well as the optimum amount of drainage holes.

Chapter 4: Executive summary

Laboratory testing and field studies of three mitigation techniques: air convection embankment, heat drain and reflective surfaces; have been carried out for permafrost protection underneath Arctic road and airfield embankments. The air convection embankment and heat drain techniques have been tested for the implementation in the shoulders of the embankments, whereas the reflective surfaces have been tested to increase the albedo of road surfaces. To evaluate their potential for minimizing the damages caused by thaw settlements and permafrost degradation the three techniques have been tested in full-scale on field locations in respectively Kangerlussuaq Airport (Greenland) and Tasiujaq Airport (Nunavik, Québec, Canada).

The results from the laboratory tests of the air convection embankment showed that the technique is most effective, when the embankment is open both at the top and at the bottom (Appendix B). This allows cold air to penetrate the embankment from the bottom, while warm air is expelled at the top. When the test-site at Tasiujaq Airport was constructed, ventilation pipes were installed in the shoulder of the embankment to increase the effectiveness of the technique. The results from the first year of monitoring at Tasiujaq Airport have shown a reduction in the mean annual temperature at the sub-grade level by approximately 1.7°C compared to what have been measured underneath the reference embankment. Especially the temperature regime during the summer period is significantly lower, which will result in a decreased annual thaw of the underlying geological deposits (Appendix E).

The heat drain was also tested at Tasiujaq Airport. The results from the first year of monitoring have shown that the technique has a considerable impact on the thermal regime of the underlying geological deposits. The thaw depth is reduced by at least 1.5 m compared to that below the reference embankment, while the mean annual temperature at the sub-grade level is reduced to only just above the freezing point (approximately 0.1°C) and approximately 2.6°C colder than the mean annual temperature measured underneath the reference embankment (Appendix E).

Ground Penetrating-Radar (GPR) has been used to study the variations in the depth of the frost table throughout a complete thaw-freeze season in Kangerlussuaq Airport. A white painted area on the parking area of the airport has been used to compare the variations of the frost table underneath a normal dark asphalt surface and a reflective surface. The results have shown a clear correlation between the use of a reflective surface and a reduced depth of the frost table. The thickness of the active layer is reduced with approximately 0.9 m in late summer (Appendices A and C).

The results from the field investigations of the three studied mitigations techniques have been very promising and it is obvious that the techniques have a positive effect on the thermal regime of the embankments and the underlying geological deposits, which will lead to a reduced thickness of the active layer and decreased degradation of the underlying permafrost.

The construction of a road or airfield embankment usually results in an increased mean annual surface temperature and changes of the thermal regime in the underlying ground. The studied mitigation techniques have shown to keep the ground colder than an ordinary gravel embankment and should therefore be implemented into embankments constructed on thaw sensitive sedimentation soils to avoid or at least minimize the problems with instability and thaw settlements.

Chapter 5: References

Allard, M., Fortier, R., Calmels, F., Savard, C., Guimond, A., Tarussov, A., 2007. L'évaluation de l'impact du réchauffement climatique sur la stabilité des pistes d'atterrissage au Nunavik: première étape vers une stratégie d'entretien. Transports Québec, Consortium Ouranos, Fonds d'action pour le changement climatique de Ressources Naturelles Canada. Remis á Ministére des transports du Québec, Transports Canada, 20 p.

Andersland, O. B., Ladanyi, B., 1994. An Introduction to Frozen Ground Engineering. Ed. Chapman & Hall, New York, USA, 347 p.

Annan, P., 2002. GPR – History, Trends and Future Developments. Subsurface Sensing Technologies and Applications, Vol. 3, No. 4, pp. 253-270.

Annan, P., Davis, J., 1976. Impulse radar sounding in permafrost. Radio Science, Vol. 11, No. 4, pp. 383-394.

Arcone, S. A., Lawson, D. E., Delaneay, A. J., Strasser, J. C., Strasser, J. D., 1998. Ground-penetrating radar reflection profiling of groundwater and bedrock in an area with discontinuous permafrost. Geophysics, Vol. 63, No. 5, pp. 1573-1584.

Arctic Climate Impact Assessment, 2004. Impacts of a warming Arctic. Cambridge University Press, 139 p. Information acquired through www.acia.uaf.edu on October 10, 2007.

Beaulac, I., 2006. Impacts de la fonte du pergélisol et adaptations des infrastructures de transport routier et aérien au Nunavik. Master thesis, Département de Génie Civil, Université Laval, Québec, Canada, 250 p.

Beaulac, I., Doré, G., Shur, Y., Allard, M., 2004. Road and airfields on permafrost, problem assessment and possible solutions. 12th International Conference on Cold Regions Engineering, Edmonton, Alberta, Canada.

Beaulac, I., Doré, G., 2006-A. Airfields and access roads performance assessment in Nunavik, Québec, Canada. 13th International Conference on Cold Regions Engineering, Orono, Maine, USA.

Beaulac, I., Doré, G., 2006-B. Development of a New Heat Extraction Method to Reduce Permafrost Degradation under Roads and Airfields. 13th International Conference on Cold Regions Engineering, Orono, Maine, USA.

Berg, R. L., Esch, D. C., 1983. Effect of color and texture on the surface temperature of asphalt concrete pavements. 4th International Conference on Permafrost, Fairbanks, Alaska, USA, pp. 57-61.

Daniels, D., 2004. Ground-penetrating radar. Ed. The Institution of Electrical Engineers, London, United Kingdom. 726 p.

Danish Meteorological Institute, 2008. Temperature data acquired through www.dmi.dk on October 28, 2008.

Doré, G., Pierre, P., Juneau, S., Lemelin, J.-C., 2007. Experimentation de méthodes de mitigation des effets de la fonte du pergélisol sur les infrastructures du Nunavik – Aéroport de Tasiujaq, Rapport d'étape 1 – Compte rendu des travaux d'instrumentation et de supervision de construction des planches expérimentales de l'aéroport de Tasiujaq, description des planches construites et de l'instrumentation installée. Groupe de recherche en ingénierie des chaussées, Département de Génie Civil, Université Laval, Québec, Canada, 28 p.

Doré, G., Jørgensen, A. S., 2008. Experimentation de méthodes de mitigation des effets de la fonte du pergélisol sur les infrastructures du Nunavik – Aéroport de Tasiujaq, Rapport d'étape 2 – Comportement thermique durant le premier hiver et analyse des données sur le comportement mécanique de la couche active. Rapport GCT-2008-08, Remis á Ministére des transports du Québec, Transports Canada, 40 p.

Esch, D. C., 1978. Road embankment design alternatives over permafrost. Conference on Applied Techniques for Cold Environments, Anchorage, Alaska, USA, pp. 159-170.

Esch, D. C., 1983. Evaluation of experimental design features for roadway construction over permafrost. 4th International Conference on Permafrost, Fairbanks, Alaska, USA, pp. 283-288.

Esch, D. C., 1988. Embankment case histories on permafrost – Embankment Design in Cold Regions. Technical Council on Cold Regions Engineering Monograph, pp. 127-159.

Esch, D. C., 1996. Road and airfield design for permafrost conditions. Roads and Airfields in Cold Regions, Technical Council on Cold Regions Engineering Monograph, pp. 121-149.

Goering, D. J., 1996. Air convection embankments for roadway construction in permafrost zones. 8th International Conference on Cold Regions Engineering, Fairbanks, Alaska, USA, pp. 1-12.

Goering, D. J., Kumar, P., 1996. Winter-time convection in open-graded embankments. Cold Regions Science and Technology, Vol. 24, pp. 57-74.

Goering, D. J., Saboundjian, S., 2004. Design of passive permafrost cooling systems for an interior Alaska roadway. 12th International Conference on Cold Regions Engineering, Edmonton, Alberta, Canada.

Ingeman-Nielsen, T. (2005). Geophysical techniques applied to permafrost investigations in Greenland. PhD-thesis, Arctic Technology Centre, Department of Civil Engineering, Technical University of Denmark, 177 p.

Ingeman-Nielsen, T., Clausen, H., Foged, N., 2007. Engineering geological and geophysical investigations for road construction in the municipality of Sisimiut, West Greenland. Proceedings, International Conference on Arctic Roads, Sisimiut, Greenland, pp. 53-61.

Instanes, A., Mjureke, D., 2005. Svalbard airport runway. Performance during a climate-warming scenario. Proceedings of the 7th International Conference on the Bearing Capacity of Roads and Airfields, Trondheim, Norway, pp. 461-466.

Intergovernmental Panel on Climate Change, 2001. IPCC Third Assessment Report, Climate Change 2001 - Impacts, Adaptation and Vulnerability. Cambridge University Press, www.ipcc.ch

Johnston, G. H., 1981. Permafrost – Engineering Design and Construction. Associate Committee on Geotechnical Research, National Research Council of Canada, Wiley & Sons, New York, 483 p.

Krahn, J., 2004. Thermal Modeling with TEMP/W – An Engineering Methodology. GEO-SLOPE International Ltd, Calgary, Canada. 282 p.

Lai, Y., Wang, Q., Niu, F., Zhang, K., 2004. Three-dimensional nonlinear analysis for temperature characteristic of ventilated embankment in permafrost regions. Cold Regions Science and Technology, Vol. 38, pp. 165-184.

Lai, Y., Zhang, M., Gao, Z., Yu, W., 2006. Influence of boundary conditions on the cooling effect of crushed-rock embankment in permafrost regions of Qinghai–Tibetan Plateau. Cold Regions Science and Technology, Vol. 44, pp. 225-239.

Lunardini, V. J., 1981. Heat Transfer in Cold Climates. Van Nostrand Reinhold, New York, 731 p.

Nield, D. A., Bejan, A., 1992. Convection in Porous Media. Springer-Verlag, New York, 408 p.

Pilon, J. A., Allard, M., Levesque, R., 1992. Geotechnical Investigations of Permafrost in Ungava with Ground Penetrating Radar. Innovation & Rehabilitation, Proceedings of the 45th Canadian Geotechnical Conference, Canadian Geotechnical Society, pp. 19/1-19/9.

Reckard, M. K., 1985. White Paint for Highway Thaw Settlement Control. Alaska Department of Transportation and Public Facilities, Report no. FHWA-AK-RD-85-16, Fairbanks, Alaska, USA, pp. 1-7.

Saboundjian, S., Goering, D. J., 2003. Air Convection Embankment for Roadways – Field Experimental Study in Alaska. Transportation Research Record, Issue 1821, pp. 20-28.

Topp, G. C., Davis, J. L., Annan, A. P., 1980. Electromagnetic determination of soil water content: measurements in coaxial transmission lines. Water Resources Research, Vol. 16, No. 3, pp. 574-582.

United States Air Force Corps of Engineers, 1971. Information's acquired through the Greenlandic Airport Departments achieve in Kangerlussuaq, August 2005.

United States Air Force Civil Engineering Center, 1984. Information's acquired through the Greenlandic Airport Departments achieve in Kangerlussuaq, August 2005.

Van Tatenhove, F. G. M., Olesen, O. B., 1994. Ground Temperature and Related Permafrost Characteristics in West Greenland. Permafrost and Periglacial Processes, Vol. 5, pp. 199-215.

Voyer, É., 2008. Expérimentation de méthodes de mitigation de la dégradation du pergélisol sur les infrastructures de transport du Nunavik, Nord du Québec. Master thesis, Département de Génie Civil, Université Laval, Québec, Canada, 233 p.

Wikimedia Commons, 2008. Picture required through commons.wikimedia.org on November 11, 2008.

Appendix A

Mapping of permafrost surface using ground-penetrating radar at Kangerlussuaq Airport, western Greenland

Authors
Anders Stuhr Jørgensen (corresponding author)
Frank Andreasen

Publication status
Published in Cold Regions Science and Technology, Vol. 48 (2007), pages 64-72

Department of Civil Engineering
Technical University of Denmark

Available online at www.sciencedirect.com
ScienceDirect
Cold Regions Science and Technology 48 (2007) 64–72
cold regions science and technology
www.elsevier.com/locate/coldregions

Mapping of permafrost surface using ground-penetrating radar at Kangerlussuaq Airport, western Greenland

Anders Stuhr Jørgensen [a,*], Frank Andreasen [b]

[a] *Arctic Technology Centre, BYG•DTU, Technical University of Denmark, 2800 Kgs. Lyngby, Denmark*
[b] *Dansk Geoservice, Nakskovvej 16, Veddelev, 4000 Roskilde, Denmark*

Received 8 September 2006; accepted 30 October 2006

Abstract

Kangerlussuaq Airport is located at 67°N and 51°W in the zone of continuous permafrost in western Greenland. Its proximity to the Greenlandic ice sheet results in a dry sub-arctic climate with a mean annual temperature of −5.7 °C. The airport is built on a river terrace mostly consisting of fluvial deposits overlying fine-grained marine melt-water sediments and bedrock.

A ground-penetrating radar (GPR) survey was performed to study the frozen surface beneath the airfield. The measurements were carried out in late July 2005 on the southern parking area in Kangerlussuaq Airport. Five years earlier, in autumn 2000, three test areas were painted white in order to reduce further development of depressions in the asphalt pavement. GPR profiles crossing the white areas show a distinct difference in depth to the permafrost surface under the painted areas compared to the natural black asphalt surface. GPR data also show a correlation between structures in the river terrace and depressions in the paved surface.

The combination of large dark areas of asphalt pavement and perhaps a change in snow removal routines on the southern parking area have caused an increase in solar heating, a lowering of the permafrost surface and the formation of several depressions in the pavement of the southern parking area. The depressions can be clearly seen after rainfall.

To calibrate the GPR survey, sediment samples from a borehole were analyzed with respect to water content, grain size and content of organic material. To find the exact depth of the permafrost a trench was dug down to the frozen surface.

Keywords: GPR; Permafrost; Active layer; Asphalt surface; Albedo

1. Introduction

A very important aspect of civil engineering in permafrost regions is the presence of permafrost and mapping of the annual changes in the active layer. Ground-penetrating radar (GPR) has proved to be a useful method for mapping the distribution of permafrost and near-surface geological structures Annan and Davis, 1976; Arcone et al., 1998a,b; Hinkel et al., 2001; Pilon et al., 1992; Wu et al., 2005). The interface between unfrozen and frozen soil can be clearly seen on GPR profiles in areas with a well-developed boundary between unsaturated and saturated frozen soil. An inversion of phase in the reflected radar signal is characteristic.

This paper is based on GPR results from an investigation carried out in late July 2005 in the southern parking area of Kangerlussuaq Airport, western Greenland (Fig. 1A). The

* Corresponding author. Tel.: +45 45255004; fax: +45 45885935.
E-mail address: asj@byg.dtu.dk (A.S. Jørgensen).

0165-232X/$ - see front matter © 2007 Elsevier B.V. All rights reserved.
doi:10.1016/j.coldregions.2006.10.007

southern parking area used to be used by the U.S. Air Force and plays no role in today's civil use of the airport, which only uses the runway and the northern parking area (Fig. 1B).

Kangerlussuaq Airport is of special interest because of the presence of a number of depressions (Fig. 2A) in the asphalt surface in the southern parking area and the existence of three test areas where the asphalt surface has been painted white (Fig. 2B). Over the last 3–4 years, airport personnel have observed the development of the depressions. The objective for carrying out the GPR survey was to show what has caused the depressions and

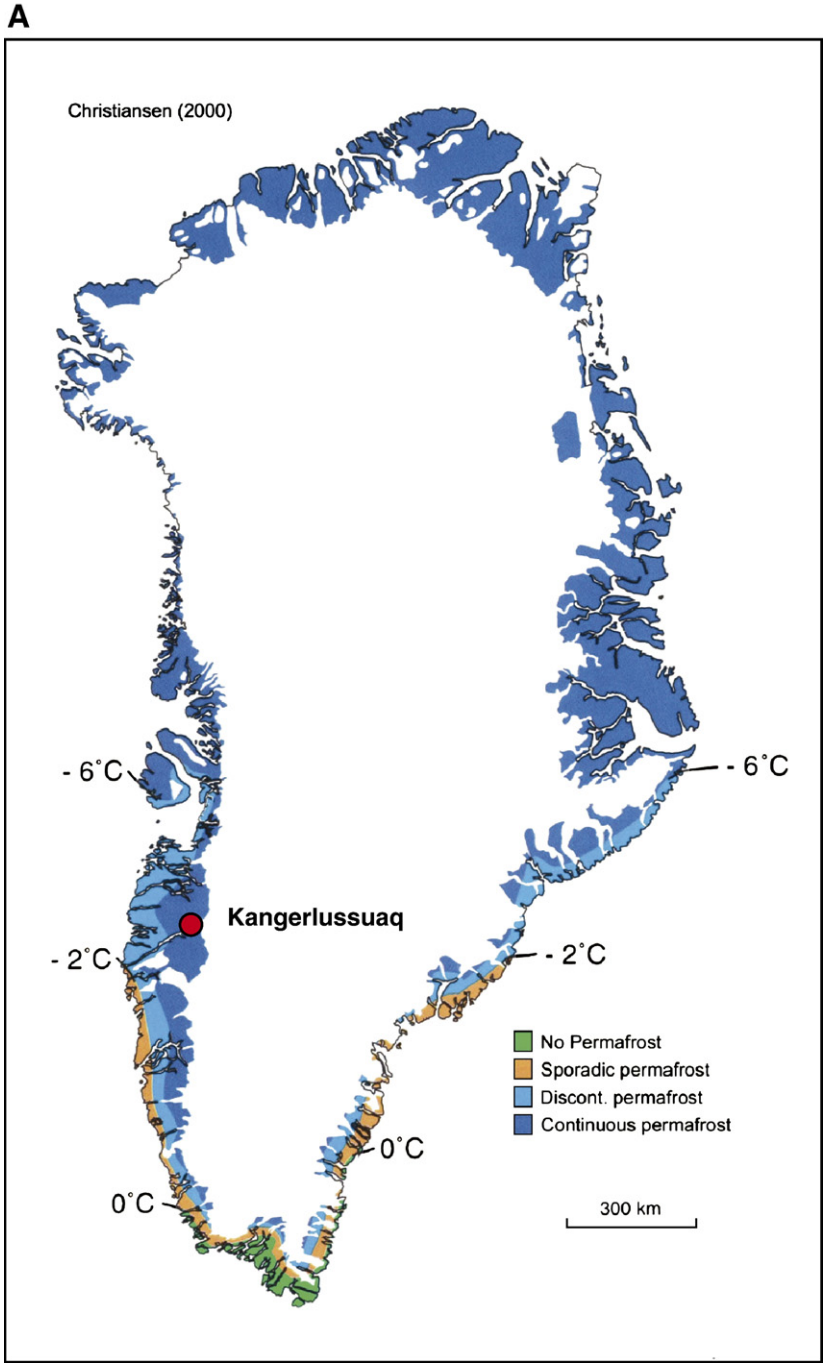

Fig. 1. (A) Location of Kangerlussuaq and permafrost distribution in Greenland (Christiansen and Humlum, 2000). (B) Ortho-photo of Kangerlussuaq Airport.

Fig. 1 (*continued*).

at the same time compare the disposition of the permafrost surface beneath a white-painted asphalt surface and a normal black asphalt surface.

2. Site description

Kangerlussuaq Airport is built on a river terrace (altitude 30–50 m) at the head of the 170 km long fjord, Kangerlussuaq (Søndre Strømfjord), located just north of the Polar Circle at 67°N and 51°W. In the western part of the area the terrace is made up of fine-grained marine melt-water sediments partly covered with fluvial deposits of sand and gravel. In the eastern part the fine-grained marine deposits are absent.

The climatic conditions at Kangerlusssuaq are determined by its northern location and its position in a 2–3 km wide valley surrounded by mountains (plateau altitude 400–600 m). To the east and south the Greenlandic ice sheet, with altitudes up to 3 km, has a dominant influence on precipitation and winds. These conditions result in a dry sub-arctic climate with winter temperatures down to −40 °C (−40 °F) and summer temperatures up to 18–20 °C (64–68 °F). The mean annual temperature is −5.7 °C and the mean annual precipitation is 151 mm (Danish Meteorological Institute, 1977–99). Since the beginning of the 1990s the temperature in Kangerlussuaq has increased by 2–3 °C but the mean annual temperature is still below −4 °C (Danish Meteorological Institute, 2000–05). Despite the increase in temperature, Kangerlussuaq is still in the zone of continuous permafrost estimated to a thickness between 100 and 150 m (Van Tatenhove and Olesen, 1994). The entire active layer is frozen during the winter, but in late summer the depth to the permafrost surface is between 1.5 and 2.0 m in the open terrain (Van Tatenhove and Olesen, 1994). However, under areas covered with asphalt the depth to the frozen surface is greater and in some areas this causes melt water to concentrate under the pavement. From spring to late summer saturated sediments will lead to raised pore-water pressures and decreased sediment shear strength. This is important considering the heavy dynamic loads involved in departing and landing aircraft, particular in early summer when the unfrozen layer is thin.

3. Equipment and methods

The whole investigation was carried out in the southern parking area of the airport (Fig. 3A and B). GPR impulses respond to the physical changes in the ground and show structural changes clearly, but they do not directly show the composition of the material investigated. Further information from boreholes or excavations is needed if the exact composition of materials is of interest. The GPR profiles from the southern parking area were supported by results from a borehole and a trench.

3.1 GPR

The equipment used for the survey was an impulse radar designed and constructed by Geophysical Survey

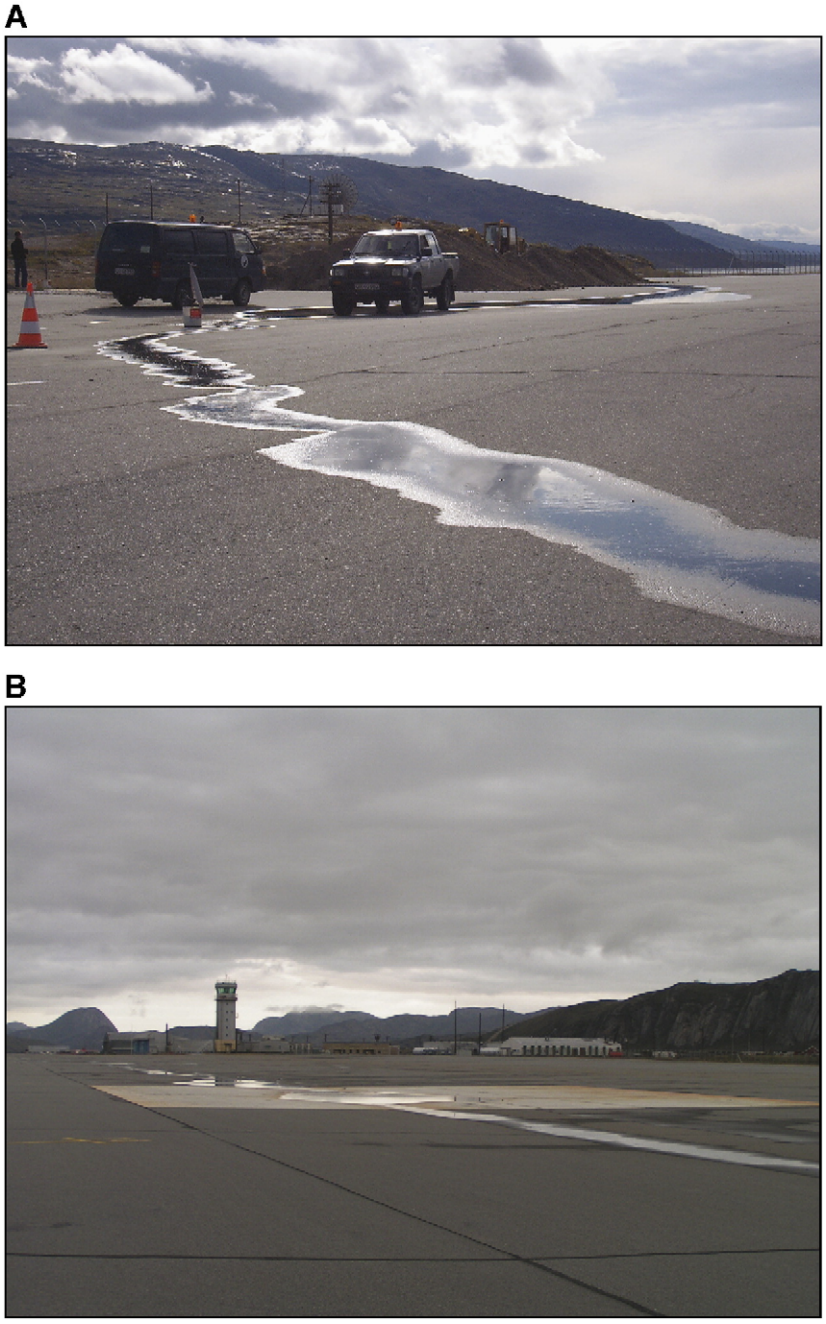

Fig. 2. (A) Depressions with water filled ponds on southern parking area. (B) White-painted asphalt surface on southern parking area.

System, Inc. (GSSI), model SIR-2000. A single ground-coupled antenna was used as both transmitter and receiver (GSSI model 5103) with a center frequency near 350 MHz. All measurements were done with the antenna towed about 3 m behind a car in which the radar control unit was placed. The positioning of the GPR data profiles was done with GPS. Coordinates were found for the start point and end point of each profile.

The GPR profiles were recorded by survey wheel and traces were collected every 0.02 m (50 traces per meter). The density was 512 samples per trace and 16 bits per sample. The range was set to 150 ns and in the field recordings both high-pass (175 MHz) and low-pass filtering (700 MHz) were used. The investigation included 11 GPR profiles all located on Fig. 3A.

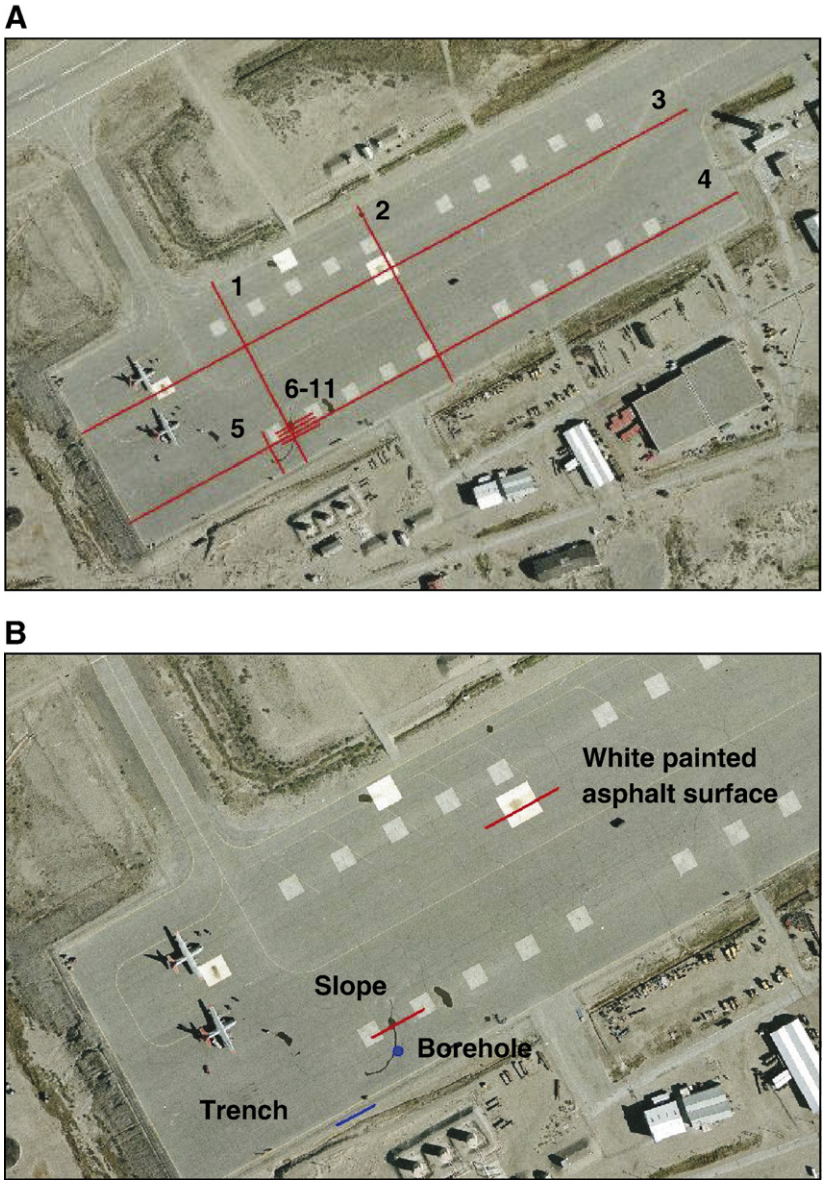

Fig. 3. (A) Picture of all GPR profiles. (B) Positions of the described surveys on the southern parking area.

The post-processing included band-pass trace-filtering to reduce electronic and antenna-to-ground coupling noise, spatial filtering to remove coherent background noise, and a running average to make a horizontal smoothing of the recorded signal. The processing was carried out using the program ReflexW from Sandmeier Scientific Software.

3.2. Borehole and trench

The borehole was made next to one of the depressions in the southwestern part of the parking area (Fig. 3B) and bored to a final depth of 15 m. Samples were taken every 0.5 m (sometimes with a smaller distance) so altogether 41 samples were taken. The trench was dug south of the southwestern part of the parking area (Fig. 3B) just beside the border of the asphalt area. This position was chosen so that the embankment under the asphalt pavement would not be damaged. The trench was 20 m long and excavated down to the permafrost surface at a depth of about 4.0 m.

The borehole logs provided data on the depths of the different layers in the construction and subsurface, water

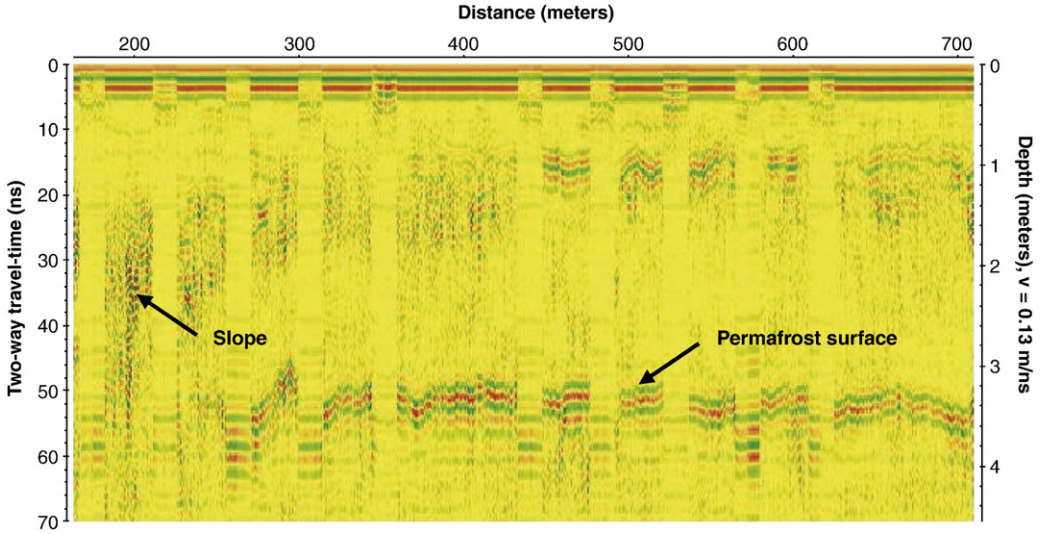

Fig. 4. Radargram of GPR profile 4 which is the profile closest to the trench. The profile crosses 10 tank stations of reinforced concrete which is seen on the radargrams as ringing.

content and grain size. The top soils were unsaturated, but sediments at the drilling location were saturated below a depth of 3.5 m. Analysis of the soil samples from between 4.0 and 5.5 m showed frozen fine-grained silty sand containing organic sediment holding a large percentage of water (20–80%).

The trench was used to find the exact depth of the permafrost surface. At the location of the trench, the sediments appeared to be well-drained right down to the frost surface. The frost surface was at a depth of about 4.0 m. This depth was used to estimate the velocity of the radar waves (v=0.13 m/ns) and make depth scales on the radargrams. Fig. 4 shows the radargram of GPR profile 4 (Fig. 3A), which is the profile closest to the trench (Fig. 3B).

4. Field results

In this section, two examples of the collected GPR profiles are interpreted (Fig. 3B). One of the profiles shows the difference in depth to the permafrost surface under a white-painted asphalt area compared to the ordinary black asphalt surface. The other example shows the geological structures under the embankment

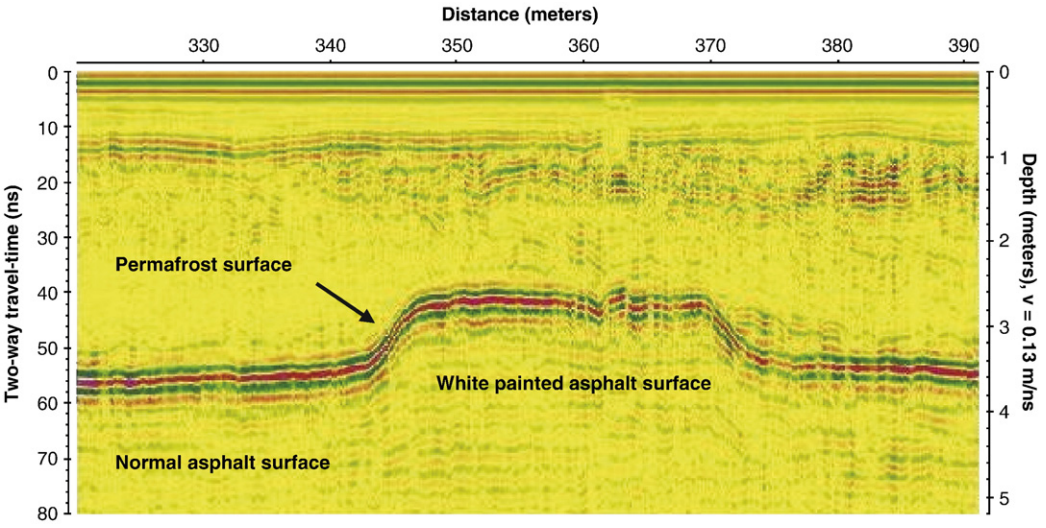

Fig. 5. Radargram showing the variations in the depth to the permafrost surface.

where it crosses one of the depressions in the asphalt surface.

4.1. Surface colour

In autumn 2000 three test areas were painted white on the southern parking area with the purpose of reducing surface subsidence (Holm, K. W., pers. comm., 2006). The radargram in Fig. 5 illustrates the effect of the white surface on the depth to the frozen surface. The perfect match between the boundary of the white area which is 26.6 m wide and the anomaly in the radargram confirms that the anomaly shown is actually the interface between unfrozen and frozen sand. Under the white-painted area the frost surface is approximately 0.75 m higher compared to the rest of the profile. This indicates a lower heat flow (a lower temperature at a specific depth) under the white surface compared to the normal black asphalt surface. Previous investigations carried out by the consulting engineering company, NIRAS Greenland A/S, have shown that the use of white surface paint reduces the asphalt temperature in Kangerlussuaq Airport by about 20% (Petersen, P. V., pers. comm., 2005).

4.2. Depressions

In the southwestern part of the parking area a number of depressions in the surface can clearly be seen. Over the last 3–4 years a number of typically elongated small and larger pools of water can be seen after rainfall, the large ones up to approximately 20 m in diameter.

Because of these depressions parts of the area are not in use today. In the area with the deepest depressions (20–25 cm deep) a hole was bored and a number of GPR profiles were recorded. The GPR profiles showed a clear connection between structures in the original deposits and the shape of the surface depressions (Fig. 6). The maximum depth of the surface conforms to the structure in the sediments. The interface between unfrozen and frozen soil is not clearly visible in well-drained areas, and it is not visible in the profiles crossing the gully shown in Fig. 6. The soil samples from the borehole show that the soil filling up the gullies creates a potential risk for the further development of surface depressions if the frost surface continues to get lower. The borehole log is shown in Fig. 7A and the water content is shown in Fig. 7B.

5. Conclusion

The survey has shown a clear connection between the areas with white-painted asphalt and a reduced depth to the permafrost surface. Insulation is increased under the areas with white-painted asphalt compared to the areas with a normal black asphalt surface. Reduced snow cover has reduced the total insulation by exposing the black asphalt to the sun at an earlier time of the year. Lowering the permafrost surface has resulted in several depressions in the southern parking area. The depressions are caused by the melting of water in silty layers with a relatively high organic content formed by filling in the gullies that have eroded into the terraces and filled with aeolian sediments.

There is usually freeze-back from the surface in the winter, but the disposition of the permafrost surface at a

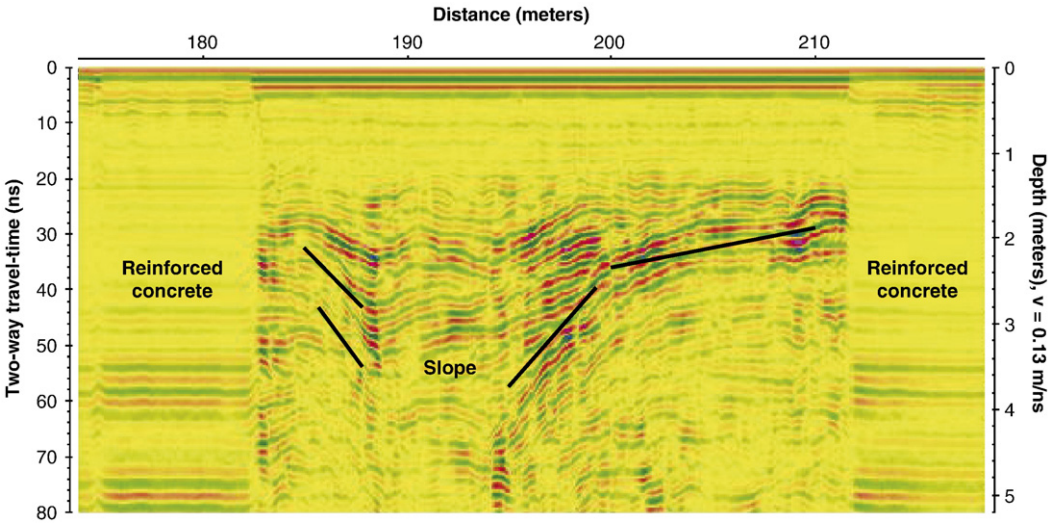

Fig. 6. Radargram illustrating the situation with the original gully.

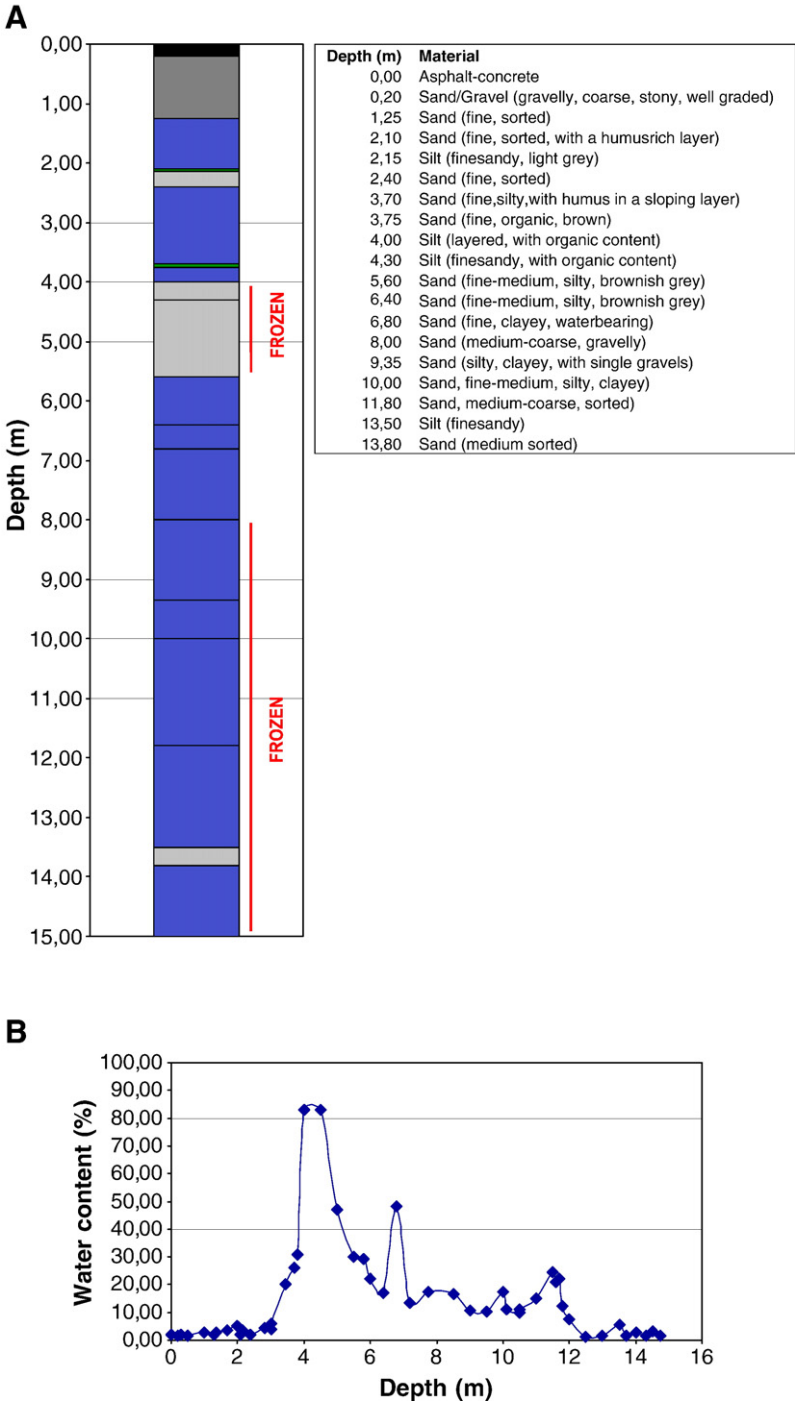

Fig. 7. (A) Bore profile and bore log. (B) Water content in soil samples from borehole.

depth of 3.5–4.5 m makes it doubtful that the entire thaw has occurred in the current year. It could be interesting to follow the annual disposition of the permafrost surface and determine whether the entire active layer freezes in the winter or not.

Acknowledgements

We would like to thank the Greenland Airport Department (Mittarfeqarfiit) for making it possible for us to access the airport area in Kangerlussuaq. We would

also like to thank research manager Professor Niels Nielsen Foged from the Technical University of Denmark for helpful discussions and suggestions, all very valuable in the preparation of the paper.

References

Annan, P., Davis, J., 1976. Impulse radar sounding in permafrost. Radio Science 11 (4), 383–394.

Arcone, S.A., Chacho, E.F., Delaney, A.J., 1998a. Seasonal structure of taliks beneath Arctic streams determined with ground-penetrating radar. Permafrost Seventh International Conference Proceedings, International Permafrost Association, Yellowknife, Canada, pp. 19–24.

Christiansen, H.H., Humlum, O., 2000. Permafrost. In: Jakobsen, B.H., Bôcher, J., Nielsen, N., Guttesen, R., Humlum, O., Jensen, E. (Eds.), Topografisk Atlas Grønland. Det Kongelige Danske Geografiske Selskab og Kort & Matrikelstyrelsen.

Arcone, S.A., Lawson, D.E., Delaney, A.J., Strasser, J.C., Strasser, J.D., 1998b. Ground-penetrating radar reflection profiling of groundwater and bedrock in an area of discontinuous permafrost. Geophysics 63 (5), 1573–1584.

Danish Meteorological Institute (1977–99): Climate data acquired through www.dmi.dk.

Danish Meteorological Institute (2000–05): Climate data acquired through www.dmi.dk.

Hinkel, K.M., Doolittle, J.A., Bockheim, J.G., Nelson, F.E., Paetzold, R., Kimble, J.M., Travis, R., 2001. Detection of subsurface permafrost features with ground-penetrating radar, Barrow Alaska. Permafrost and Periglacial Processes 12, 179–190.

Pilon, J.A., Allard, M., Levesque, R., 1992. Geotechnical investigations of permafrost in Ungava with ground penetrating radar. Innovation and Rehabilitation, Proceedings of the 45th Canadian Geotechnical Conference. Canadian Geotechnical Soc, pp. 19/1–19/9.

Van Tatenhove, F.G.M., Olesen, O.B., 1994. Ground temperature and related permafrost characteristics in West Greenland. Permafrost and Periglacial Processes 5, 199–215.

Wu, T., Li, S., Cheng, G., Nan, Z., 2005. Using ground-penetrating radar to detect permafrost degradation in northern limit of permafrost on the Tibetan Plateau. Cold Regions Science and Technology 41, 211–219.

Appendix B

Assessment of the effectiveness of two heat removal techniques for permafrost protection

Authors
Anders Stuhr Jørgensen (corresponding author)
Guy Doré
Érika Voyer
Yohann Chataigner
Louis Gosselin

Publication status
Published in Cold Regions Science and Technology, Vol. 53 (2008), pages 179-192

Department of Civil Engineering
Technical University of Denmark

Available online at www.sciencedirect.com
ScienceDirect
Cold Regions Science and Technology 53 (2008) 179–192
cold regions science and technology
www.elsevier.com/locate/coldregions

Assessment of the effectiveness of two heat removal techniques for permafrost protection

Anders Stuhr Jørgensen [a,*], Guy Doré [b], Érika Voyer [b], Yohann Chataigner [c], Louis Gosselin [c]

[a] Arctic Technology Centre, Department of Civil Engineering, Technical University of Denmark, 2800 Kgs. Lyngby, Denmark
[b] Department of Civil Engineering, Université Laval, Québec (Québec), Canada, G1K 7P4
[c] Department of Mechanical Engineering, Université Laval, Québec (Québec), Canada, G1K 7P4

Received 24 May 2007; accepted 6 December 2007

Abstract

Two mitigation techniques, an air convection embankment and an embankment of a granular material with an integrated heat drain, have been tested for the implementation in the shoulders of road and airfield embankments in permafrost regions. Both techniques will allow cold air to penetrate the embankment from the bottom, while warm air is dissipated at the top. The techniques have been tested in the laboratory, where a small-scale embankment (SSE) was build and placed in a cold room to measure the embankment temperatures during winter conditions. A numerical modeling has been developed and calibrated on the SSE to verify the effects on the thermal regime of full-scale embankments. The results have shown that both techniques will cause a decrease in temperature, which will minimize or even possibly avoid permafrost degradation underneath the embankments. The laboratory results have also shown that the effectiveness of the air convection embankment technique can be increased during winter conditions by ventilating the top and the bottom of the embankment shoulders. Installation of air intakes along the shoulders will facilitate air flow into the system during winter and will trap the cold air in the bottom of the embankment through the summer period. This solution has been verified using the numerical model.

Keywords: Permafrost degradation; Cooling effect; Heat removal; Mitigation techniques; Air convection embankment; Heat drain

1. Introduction

The presence of permafrost is a very important aspect to take into consideration in civil engineering in arctic regions. Permafrost often has high ice contents, making it susceptible to consolidation if thawing occurs. The construction of engineering structures such as road embankments or buildings will unavoidably change the thermal regime of the frozen ground and lead to permafrost degradation. This problem is now amplified by the effects of warming climate. The construction of a road embankment changes the ground-surface energy balance, which is a complex function of seasonal snow cover, vegetation, solar and long wave radiation, surface moisture content and atmospheric air temperature (Lunardini, 1981). All these factors contribute to produce the mean annual surface temperature, which may

* Corresponding author. Tel.: +45 45255004; fax: +45 45885935.
E-mail address: asj@byg.dtu.dk (A.S. Jørgensen).

0165-232X/$ - see front matter © 2007 Elsevier B.V. All rights reserved.
doi:10.1016/j.coldregions.2007.12.002

differ substantially from the mean annual air temperature. The construction of a road embankment usually results in an increased mean annual surface temperature, which will increase the thawing of permafrost (Goering, 1996). More specifically the side-slopes of a road embankment are exposed to thaw settlements, inducing longitudinal cracks along the embankment edge and shoulder rotation.

Different mitigation techniques have been developed to avoid or minimize the damages caused by thaw settlements; reflective surfaces, air convection embankment, thermosyphons, geosynthetic reinforcement etc. (Esch, 1996; Beaulac et al., 2004). This paper is based on the results of laboratory tests, where two protection techniques have been tested in a small-scale embankment, and compared to a reference (unprotected) embankment in a cold room. The experimental setting is designed to represent the shoulder of a road embankment and was carried out in a size 25–50% of a full-scale road embankment. In addition to the reference embankment, the two types of protection techniques tested are; the air convection embankment and the heat drain. The main objective was to determine the effectiveness of the two mitigation methods, and to identify factors that are likely to improve the effectiveness of the methods for future full-scale field-testing and implementation in road and airfield embankments in permafrost regions. The small scale experiments lead to an assessment of the effectiveness of the techniques relative to an embankment constituted of standard granular material. They also allowed the determination of heat transfer parameters to be used in thermal modeling studies conducted in parallel. As a result of the laboratory tests and modeling studies, full-scale field-testing is now already in progress on two locations in northern Canada.

The air convection embankment (ACE) was developed in the 1990s at the University of Alaska, Fairbanks, USA. This technique involves the use of an open-graded embankment material, such as crushed rock with a low fines content, which is used to construct the main portion of the embankment (Goering, 1996). During 1996–97 an experimental air convection embankment was constructed on a road in Fairbanks. Temperature data was collected from the test section and an adjacent control section. Results showed that the air convection embankment generated a passive cooling and that the mean annual temperature at the base of the test section was decreased with 4 °C compared to the control section (Saboundjian and Goering, 2003).

The heat drain is an innovative system developed at Laval University, Québec City, Canada, in order to protect the side-slopes of road and airfield embankments. The heat drain is placed in the shoulder and an air intake is installed at the foot of the embankment to allow upwards circulation of air in the membrane during winter months (Fig. 1). The main purpose of this method is to extract heat from the embankment in order to raise the permafrost table in the ground at that critical location (Beaulac and Doré, 2006).

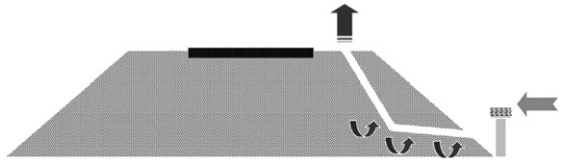

Fig. 1. Heat drain placed in the shoulder of a road embankment (Beaulac, 2006).

A large amount of numerical modeling has been carried out in Lanzhou, China, to implement different mitigation techniques into the construction of road and railway embankments in permafrost regions and to determine the critical embankment height under different temperature scenarios (e.g., Lai et al., 2004; Li et al., 1998; Zhang et al., 2005). The Chinese studies have also included small-scale experimental investigations, where the influence of open and closed boundary conditions on cooling effect in an ACE have been examined (Lai et al., 2006). The investigations showed that an ACE with open boundaries is not able to prevent permafrost degradation caused by increasing temperatures of 2.2–2.6 °C over the next 50 years. However, if a white iron sheet is placed on the top surface the cooling effect is remarkably changed and the embankment is now able to prevent the permafrost from thawing. An ACE with closed boundaries seems to be a method that can be used to eliminate or decrease permafrost degradation under infrastructures in permafrost regions, when the ambient mean temperature is larger than 0 °C (Lai et al., 2006).

2. Methods

In this section the principles and the theoretical background of the two tested mitigation techniques are described.

2.1. Air convection embankment

The ACE technique involves the use of a highly porous, poorly graded material to construct the core or the shoulder of a road embankment. The high permeability of such a material allows natural convection of the pore air to occur in the embankment during winter months, when

unstable air density gradients exist (Goering, 1996; Saboundjian and Goering, 2003; Goering and Kumar, 1996). During winter months, cold air from the upper part of the embankment will tend to settle downwards towards the lower part due to its greater density. At the same time warm air from the base of the embankment will raise, which will result in circulation of the pore air and enhanced wintertime heat transfer by speeding the cooling and refreezing of the underlying permafrost (Esch, 1996; Saboundjian and Goering, 2003). During summer months, the air density gradients are stable, the warmer air will stay in the upper part of the embankment, and circulation will not occur (Goering, 1996; Goering and Kumar, 1996). The air convection embankment will thus produce a cooling effect, which reduces the mean annual temperature and thereby prevents thaw of underlying permafrost.

Theoretically the system can be modeled as a horizontal layer of porous material, which is heated from below. That system will experience natural convection of the pore air if a critical Rayleigh number is exceeded. The Rayleigh number is defined as (Nield and Bejan, 1992):

$$Ra = \frac{C\beta gKH\Delta T}{vk} \tag{1}$$

where

C	Volumetric heat capacity of the pore fluid (air; $J/m^3 \cdot K$)
β	Expansion coefficient of the pore fluid (air; K^{-1})
g	Acceleration because of gravity (9.8 m/s^2)
K	Intrinsic permeability of the material (m/s)
H	Layer height (m)
ΔT	Temperature difference between the top and the bottom of the layer (K)
v	Kinematic viscosity of the pore fluid (air; m^2/s)
k	Thermal conductivity of the material (J/s·m·K)

A stability analysis shows that a horizontal layer with impermeable boundaries of uniform temperature at its base and upper surface will start to experience natural convection once the Rayleigh number exceeds $4\pi^2$ ($39.48 \approx 40$). Using this limit, it is possible to define a critical ΔT (Saboundjian and Goering, 2003):

$$\Delta T = \frac{40vk}{C\beta gKH}. \tag{2}$$

When the critical ΔT is exceeded a series of circulation cells will arise, which will transport the warmer pore air from the base upwards, whereas the cooled air will be going downwards. Under actual field conditions, where the system are not ideal horizontal, convection will normally begin at smaller Rayleigh numbers as much as 1/2 or 1/4 of the value listed above (Saboundjian and Goering, 2003).

During the preparation of this paper, the effects of opening the air convection embankment in the top and the bottom have been examined. This will change the heat flow by allowing cold air to penetrate into the embankment from the bottom.

2.2. Heat drain

The heat drain technique consists of a drainage geocomposite with high permeability, placed in the shoulder of the road embankment (Fig. 1). The geocomposite is composed of a corrugated plastic core covered by geotextile layers with a total thickness of 25 mm, allowing air to flow into the embankment. An air intake system is installed at the base in order to allow an upward movement of air in the membrane (Beaulac, 2006). This movement of air, also called the chimney effect, is a result of a lower density caused by the change in temperature. The drain is designed to facilitate heat extraction. The heat initially flows towards the heat drain by conduction and is then expelled of the embankment by convection. The purpose of the method is to extract heat from the ground and the embankment in order to rise or, at the minimum, to prevent a depression of the level of the permafrost.

Heat conduction occurs in all soil constituents and involves a transfer of kinetic energy from molecules in a warm area to a cooler area of the material. Considering a prismatic element of soil having a cross-sectional area A at right angles to the heat flow q, the conduction is given as (Andersland and Ladanyi, 1994):

$$Q = -k_u A \frac{\mathrm{dT}}{\mathrm{dx}} \tag{3}$$

and

$$q = \frac{Q}{A} = -k_u \frac{\mathrm{dT}}{\mathrm{dx}} = k_u i \tag{4}$$

where $Q/A = q$ is the rate of heat flow per unit area ($J/m^2 \cdot s$ or W/m^2), k_u the unfrozen thermal conductivity (J/s·m·K or W/m·K), $\mathrm{dT/dx} = i$ is the thermal gradient (K/m), and A is the area (m^2). The negative sign indicates that the heat flow is going from a high to a low temperature.

Heat transfer by convection is a process, which removes heat from the surface, when the latter is exposed to a fluid (liquid or gas) by the temperature difference from surface (Krahn, 2004). The convection

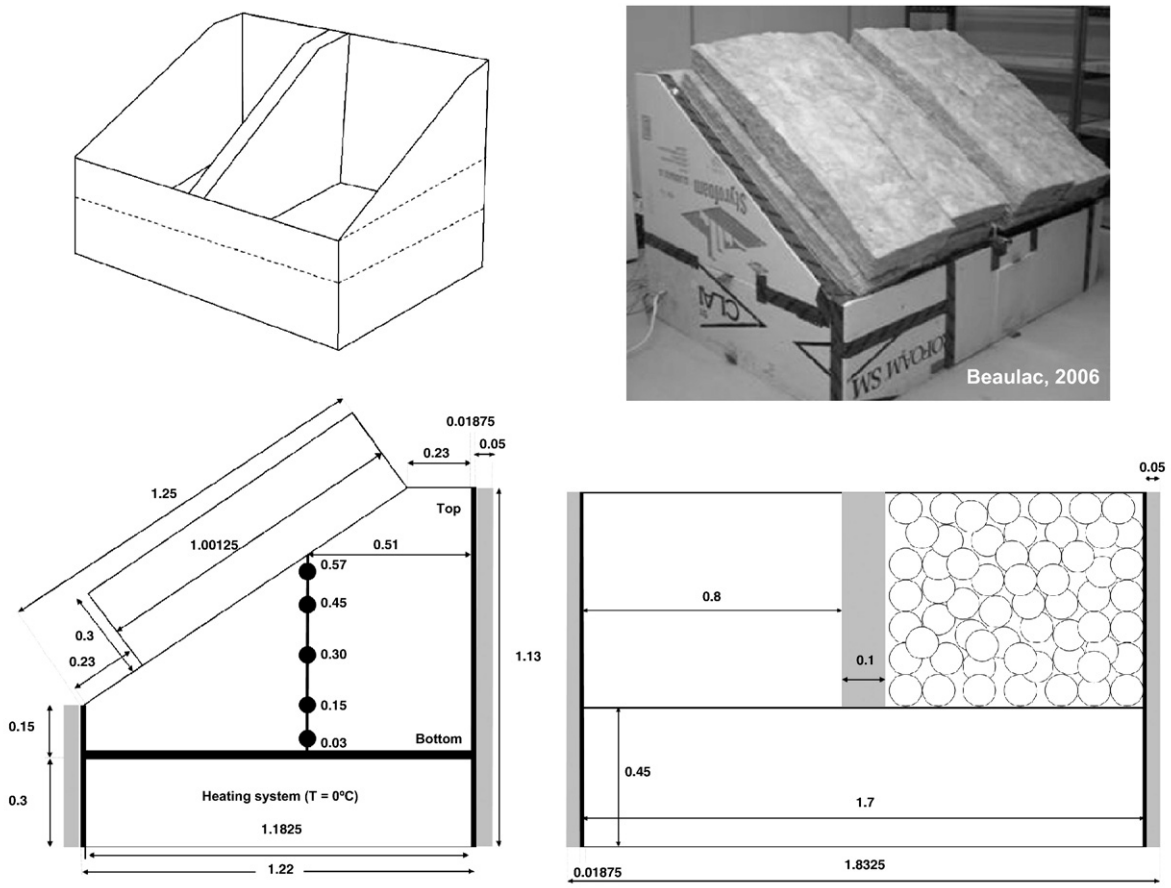

Fig. 2. Dimensions of embankment box. The position of thermistors (black circles) is shown as the distance from the bottom of the embankment. All units are in meters (m).

can be either natural or forced. The transfer of heat is defined as:

$$q = h(T_s - T_\infty) \tag{5}$$

where q is the heat flux (W/m^2), h is the convection coefficient (W/m^{2}K), T_s is the temperature of the surface (K) and T_∞ is the temperature of the fluid (K). The convection coefficient is often given from theoretical or empirical equations based on the Nusselt number, Rayleigh number, Prandtl number and the properties of the fluid.

3. Laboratory testing

3.1. Description of embankment components

3.1.1. Material properties

The reference embankment and the embankment containing the heat drain consisted of a natural gneissic granular material (≤ 18.75 mm) coming from a sand-pit located near Québec City, Québec, Canada. The bulk density of the material was determined to approximately 2.0 g/cm^3 and the water content 6.0%. Throughout the construction the granular material was compacted with a pneumatic air hammer. The air convection embankment was assembled using sorted rounded boulders (approximately 100 mm in diameter) of gneissic origin.

3.1.2. Construction of embankment box

The box used for the tests in the laboratory includes two sections, thus two small-scale embankments could be constructed, tested and compared at the same time. The size of the small-scale embankments is 1/4–1/2 of a real full-scale embankment. The embankments were insulated by covering the outside of the box with a 50 mm polystyrene layer. A 100 mm layer of polystyrene was placed between the two sections to avoid heat losses and a layer of 300 mm glass wool was placed on the top of the embankments to recreate the insulating

effect from a snow cover. The dimensions of the box are shown in Fig. 2. At the bottom of the box the temperature was maintained constant at 0 °C by a heating system.

3.1.3. Data acquisition

Five thermistors were installed vertically in the center of each section to continuously monitor the thermal regime of the embankments every 30 min. The equipment used for the data logging was a DataTaker DT600. The position of the thermistors is shown in Fig. 2.

3.1.4. Test conditions

All tests were carried out in a cold room, which maintained a constant air temperature at approximately −17 °C (precision ±1 °C). The refrigeration system was programmed to shut down every 10 h for deicing purposes. This process has affected slightly the temperature response of the embankments and more specifically of the ACE. This problem can be observed on the experimental data shown in Fig. 9 (last portion of the test). The effect of deicing cycles is attenuated by applying a 10-hour running average to the data shown on Fig. 3.

3.2. Results

3.2.1. Test of an open air convection embankment

This test was done to get insight into the temperature differences between a closed and an open air convection embankment. The embankment was placed in the cold room and brought to steady state conditions, while the entire surface was covered with 300 mm of glass wool. When steady state was reached the glass wool was removed from the top of the embankment to allow cold air to penetrate the embankment. The effect of opening the top is seen on Fig. 3. It can be seen that the temperature in the bottom of the embankment decreases with about 4 °C. The actual effect is probably 1–2 °C less, because steady state condition was not completely obtained when the glass wool was removed.

When the embankment again had obtained steady state condition, the glass wool was removed from the bottom to allow a heat flow through the embankment where cold air will penetrate the embankment from the bottom while warm air is expelled at the top. From Fig. 3 it can bee seen that these conditions resulted in an inversion of the temperatures in the embankment. The bottom, which used to be the coldest part of the

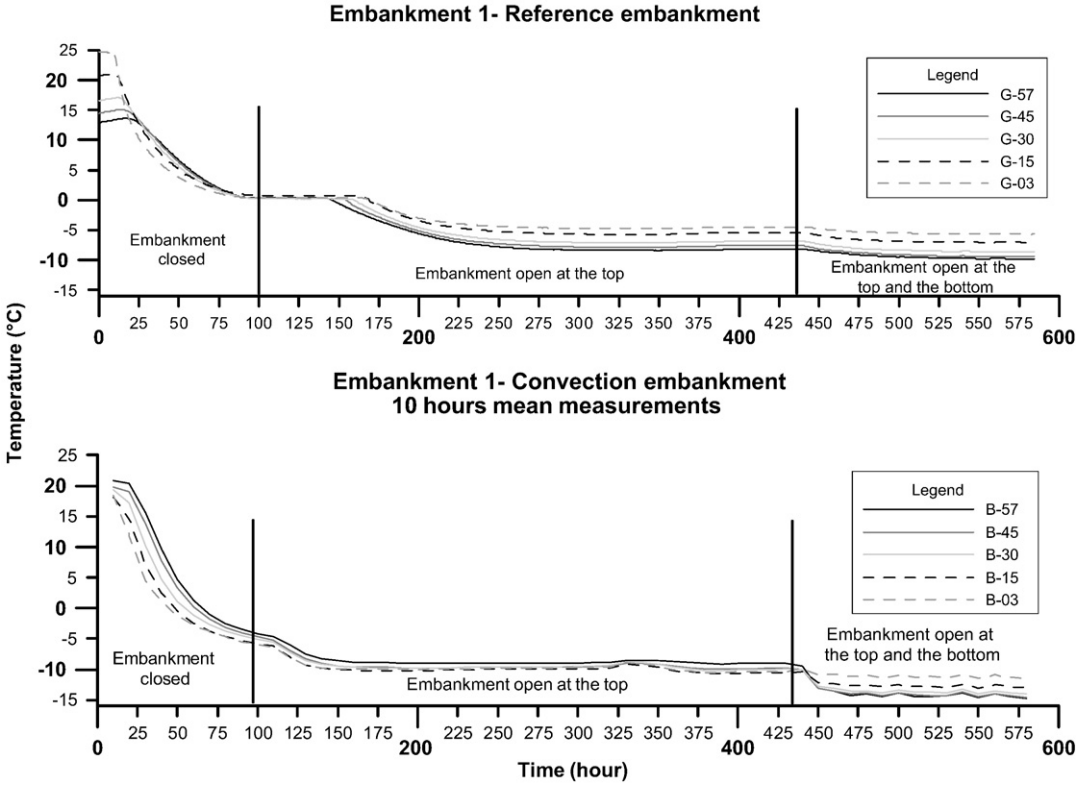

Fig. 3. Change in temperatures according to time; reference embankment (top) and air convection embankment (bottom). The height of the thermistors is shown in centimeters from the bottom of the embankment.

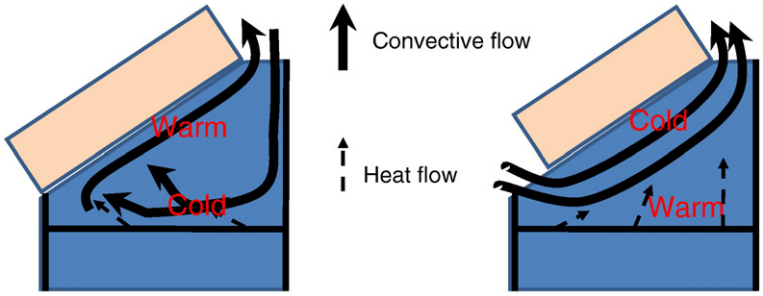

Fig. 4. Hypothetical heat flow and convective flow for an ACE with an open top (left), and an ACE with an open top and an open bottom (right).

embankment, is now the warmest, while the top is the coldest. The temperatures in the bottom of embankment were decreased by approximately 1 °C when the bottom was opened, while the temperature changes in the top were in the order of 5 °C. Fig. 4 illustrates the hypothetical mechanism believed to be responsible for the temperature inversion in the embankment as a result of the opening at the bottom of the embankment.

The results have shown that it is possible to increase the effectiveness of the air convection embankment technique by opening the top and the bottom of the embankment, which will allow cold air to penetrate into the embankment from the bottom, while warm air is dissipated at the top. This can be achieved in a real embankment by providing adequate ventilation to the air convective layer using air inlets and outlets along the embankment.

3.2.2. Comparison of temperature profiles

Temperature profiles at steady state conditions with open top and bottom have been compared for the three investigated embankments; air convection embankment, heat drain and reference embankment. The results are shown in Fig. 5.

It can be clearly seen that the air convection embankment and the heat drain techniques have a significant effect on the thermal conditions and will cause a decrease in temperatures compared to the conditions observed in the reference embankment. Air convection occurring in the ACE seems to have an important

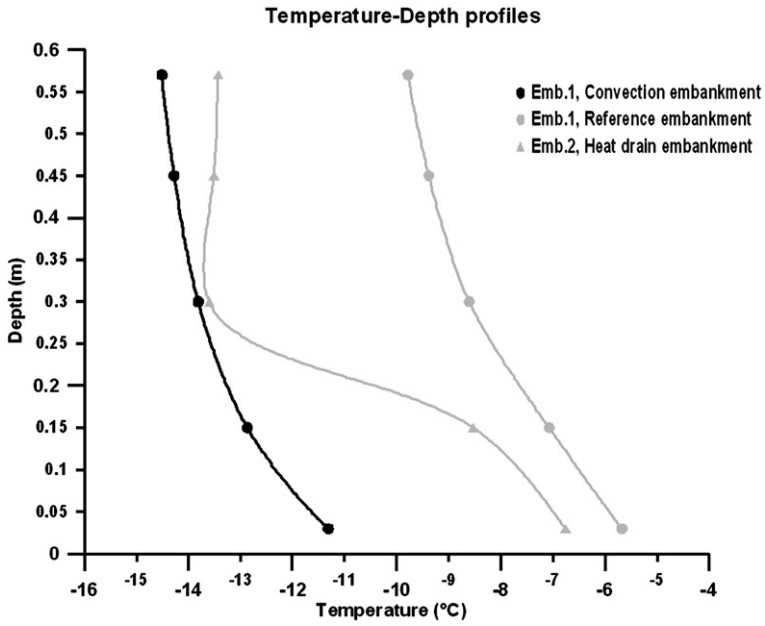

Fig. 5. Heat flow during steady state conditions with an open top and bottom. All three embankment types are shown; reference embankment, air convection embankment and heat drain.

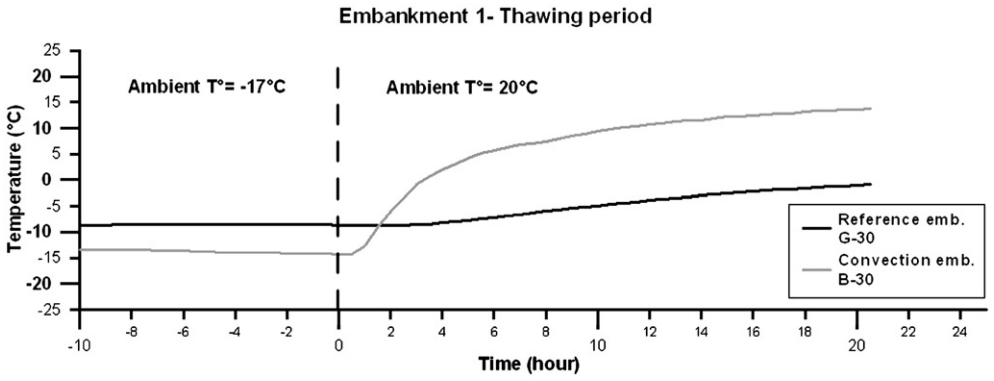

Fig. 6. Progression of thaw according to time; reference embankment and air convection embankment.

influence on the thermal conditions in the entire embankment, while the effect from the heat drain is concentrated around the geocomposite and the upper part of the embankment. The temperatures at the bottom of the heat drain are only slightly colder than the temperatures in the reference embankment (the difference is approximately 1 °C), while the temperatures in the air convection embankment are decreased with 5–6 °C. This situation is however normal considering that a 0 °C temperature is imposed at the bottom of the test embankment and the presence of normal granular material below the heat drain. This observation however suggests that the heat drain would have a maximum effectiveness if placed near the bottom of the embankment.

The temperature reductions obtained in permanent regime in the laboratory testing on a small-scale model are similar to those obtained in the Chinese studies using numerical modeling, where a open and closed full-scale ACE has been investigated (Lai et al., 2004, 2006). The Chinese studies have also shown that the height of an ACE is an important factor, which has to be taking into account to obtain the highest cooling effect in the embankment and the underlying permafrost. For a 2 m high embankment the temperature distributions for open and closed boundary conditions are similar, however the closed embankment is a little better (Lai et al., 2006). If the embankment is high the temperature distributions are completely different for the two types of boundary conditions. The Chinese results have shown that a 5 m high ACE with open boundary is best and that the temperatures beneath the embankment are lower than beneath the embankment with the closed boundaries (Lai et al. 2006).

3.2.3. Rate of warming of the ACE

A warming process was also simulated to assess the rate of temperature increase in the ACE as compared to the reference embankment. This was achieved by moving the embankments out of the cold room and into a room with an air temperature around 20 °C. The temperatures observed with the thermistor located at mid-depth in the ACE and the reference embankment is shown in Fig. 6.

The results shows that the temperature in the middle of the ACE rises almost immediately and 3 h after the embankment was removed from the cold room, the temperature is above 0 °C. At the same time the temperature in the reference embankment has only increased by 0.3 °C (from −8.7 °C to −8.4 °C). With the results from this test it can be concluded that the open ACE are much more sensitive to temperature changes than the reference embankment. A cold air flow could be observed at the bottom of the embankment showing that dense cold air rapidly drains out of an unprotected ACE at the toe of the slope. This will make the ACE vulnerable to rapid warming during the summer months, when warm air can be forced by wind into the embankment and contribute to the rapid raise of embankment temperature together with the rapid drainage of cold air. A solution to this problem could be to place a gravel liner, which is separated from the open graded material using a geotextile, on top of the air convection embankment and to assure proper ventilation of the ACE using air intakes installed along the embankment shoulders, as shown in Fig. 7. It is expected that, while assuring air intake in the system during winter, this system will trap the cold air at the bottom of the embankment during summer, limiting thus heat intake by conduction only. This solution has been tested in the numerical modeling, described in Section 4.

4. Numerical modeling

A numerical model was implemented for solving the governing conservation equations (i.e., mass, x-momentum, y-momentum, and energy equation (Incropera et al., 2006))

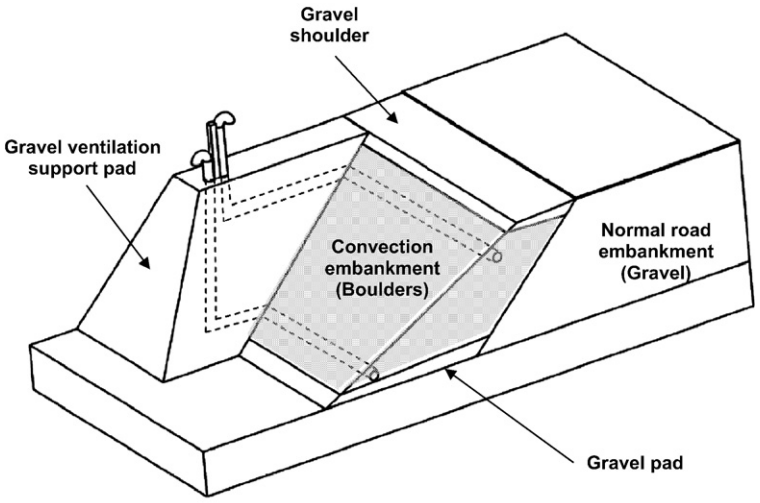

Fig. 7. Possible construction of an air convection embankment with air intakes in the shoulder of a road embankment.

within the embankment. A CFD commercial code from Fluent Incorporated was used to carry out the simulations. This software relies on the finite volumes method (Patankar, 1980); the domain of Fig. 8 is discretized using triangular cells, and then the governing equations are integrated on each cell, yielding a set of algebraic equations. The resulting matrix systems are solved iteratively. In this section, we explain how the numerical model was validated with the experimental data, and then used to simulate an in situ convective embankment subjected to periodic time-varying air temperature.

Three types of embankment materials were considered; reference embankment composed of sand (ρ= 2000 kg/m^3, k=1.95 W/m·K, c_p=1000 J/kg·K), air convection embankment composed of rounded blocks of granite (granite properties; ρ=2630 kg/m^3, k=2.79 W/m·K, c_p=775 J/kg·K) (Incropera et al., 2006), and an embankment of sand with embedded heat drain in which air is flowing (air properties: ρ=1.3947 kg/m^3, c_p=1000 J/kg·K, μ=1.596•10^{-5} N·s/m^2). Temperature gradients in the latter material (i.e., ACE and heat drain) trigger air streams within the embankment, providing beneficial additional heat removal. The reference embankment is conduction-dominated, and is used as a basis of comparison for evaluating the performance of the air convection embankment. Therefore, only the energy equation needs to be solved in the conductive embankment. Darcy flow with local thermal equilibrium was assumed in the convective embankment. The porosity of the convective embankment is estimated at 35%, leading to a permeability of ~6.77*10^{-6} m^2 for a pebble average diameter of 0.1 m. This permeability was estimated with the well-known Ergun's equation (Ergun, 1952). In the embankment with the heat drain, Navier–Stokes equations are solved within the drain, assuming laminar regime.

The general thermal boundary conditions are taken as:

$$-k\nabla_n T = U(T_s - T_\infty) \tag{6}$$

where $\nabla_n T$ is the normal temperature gradient. U is the boundary overall heat transfer coefficient, and accounts for the external convection coefficient and wall thermal resistance as described below. T_∞ is the external air temperature far from the surface. When a boundary is opened, the temperature is that of the incoming air. Because the pressure in the CFD commercial software used is defined as (p-ρgy), the inputs of pressure in the code should not include hydrostatic pressure differences. Therefore, the pressure was set to zero at every opening in

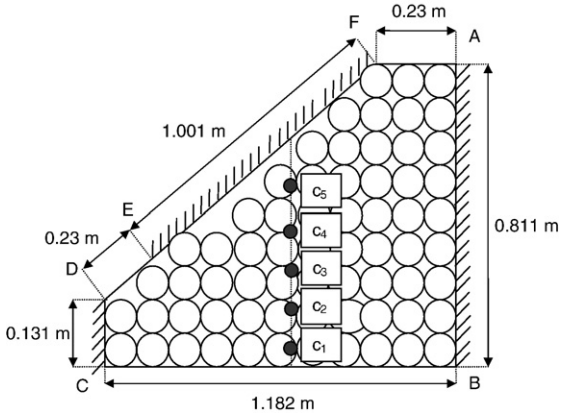

Fig. 8. A schematic representation of the air convection embankment considered.

Table 1
Thermal boundary conditions

Boundary	Step 1	Step 2
AB	$U=0.47$ W/m^{2}K, $T_\infty=-17$ °C	
BC	$U=2.73$ W/m^{2}K, $T_\infty=0$ °C	
CD	$U=0.47$ W/m^{2}K, $T_\infty=-17$ °C	
DE	$U=0.3$ W/m^{2}K, $T_\infty=-17$ °C	$T_\infty=-17$ °C (inflow), $\nabla_n^T=0$ *(outflow)*
EF	$U=0.3$ W/m^{2}K, $T_\infty=-17$ °C	
FA	$T_\infty=-17$ °C (inflow), $\nabla_n^T=0$ *(outflow)*	

order for the flow to be solely self-driven (no forced convection). This approach is well-documented in the heat transfer literature (e.g., Andreozzi and Manca, 2001). Mesh independence was tested extensively until further grid density doubling resulted in variation of the heat flux removed at boundary BC smaller than 1%. The time step was chosen in a similar way.

For the convective embankment, two steps of the experimental study described in Section 3 were reproduced with the numerical model. In the numerical experiment # 1, the boundary DE is closed, and air could enter or exit the embankment through boundary AF. In experiment # 2, both boundaries DE and AF are open, and allow flow penetration or exfiltration. The thermal boundary conditions considered are shown in Table 1. The values of the overall heat transfer coefficients presented were calculated for each interface by summing all the thermal resistances (i.e., wall, insulation, external film) from the interface to the external air. Thermal conduction resistances of each material layer come from Incropera et al. (2006). The convection heat transfer coefficient for quiescent air has been estimated from correlations involving the Rayleigh and Nusselt numbers (Incropera et al., 2006).

The numerical model described above was validated using experimental data collected during laboratory testing. The thermal transient behaviour of the convection and conduction embankment was simulated, and the temperature was recorded at the same positions as in the experimental setup. Fig. 9 compares the evolution of the temperatures resulting from the numerical model and from the experiment, measured at sensor c_5 (see Fig. 8). The agreement could be qualified as very good. The steady-state temperature profile obtained numerically is confronted to the experimental data in Fig. 10. The maximum deviation is less than 1 °C, and therefore, the numerical model is judged satisfactory.

Finally, the numerical model was used for testing the yearly performance of the convection embankment compared to that of the conductive embankment. In that respect, we assumed that the external air temperature varied as follows:

$$T_{\text{air}} = 17\sin\left(1.99\times10^{-7}\times t - 1.7\right) - 4 \qquad (7)$$

in order to reproduce the average air temperature conditions in Beaver Creek, Yukon (Environment Canada, 2007). The time t is in second. In addition, the overall heat transfer coefficient of boundary EF was replaced by a time-varying coefficient including a 20 cm layer of gravel and a variable ground snow thickness, based on

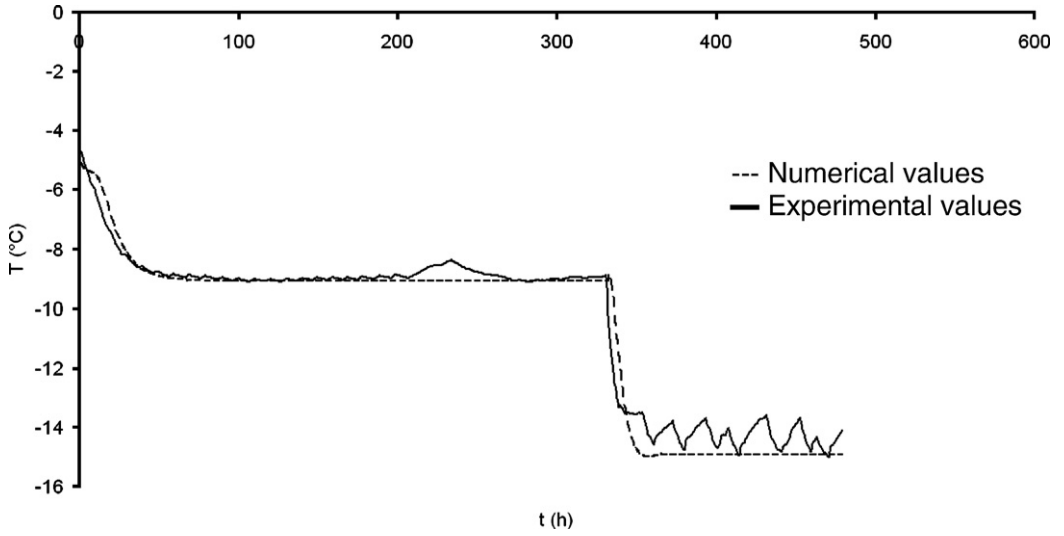

Fig. 9. Evolution of experimental and numerical temperatures at sensor c_5 for the air convection embankment.

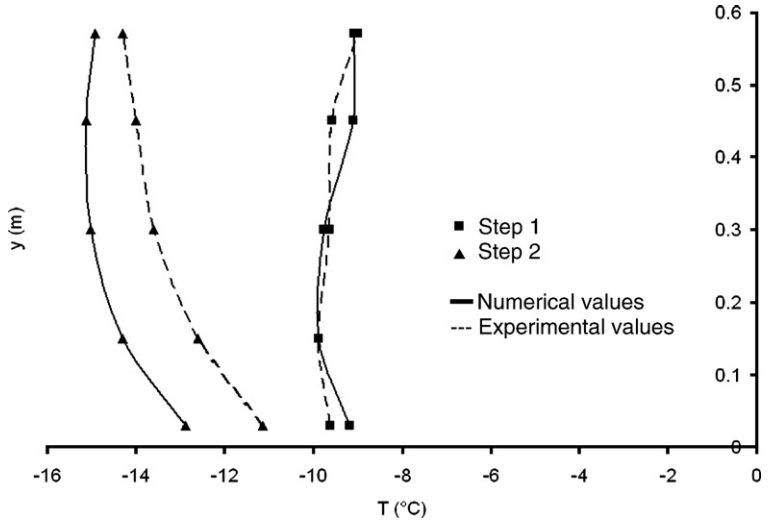

Fig. 10. Steady-state results of experimental and numerical temperatures for the 5 sensors in the air convection embankment.

historical weather data (Environment Canada, 2007) and calculated as follow:

$$\frac{1}{U_{EF}(t)} = \frac{1}{h_{air}} + \frac{e(t)}{k_{snow}} + \frac{L_{gravel}}{k_{gravel}} \quad (8)$$

where U_{EF} is the overall heat transfer coefficient of the EF interface, h_{air} is the convection coefficient of the air, L_{gravel} is the thickness of the gravel layer and k_{gravel} and k_{snow} are the thermal conductivities of the gravel layer and snow, respectively. $e(t)$ corresponds to the variable thickness of snow during the year (Environment Canada, 2007). The overall heat transfer coefficients of the other boundaries were kept as specified in Table 1. Periodic solutions were sought for each simulation.

4.1. Convective embankment

Two convective embankment designs were tested with the numerical model:

1) Air convection embankment where interfaces AF and DE are open to air flow;
2) Air convection embankment with chimney (air intake) as shown in Fig. 11 (the dimensions of Figs. 8 and 11 are the same). Interface AF is open. Interface DE is connected with the chimney, the walls of which are considered adiabatic. The chimney inlet is located at the same height as the outlet of the embankment.

These designs were confronted to a conventional (conductive) embankment which interface AF where covered with 20 cm of gravel and variable snow thickness, and interfaces it DE is subjected to a heat exchange by convection directly with the air (U=20 W/m^{2}K);.

The average heat flux removed or added at interface BC is shown in Fig. 12 for the two convective embankments and the conductive embankment described above. The heat flux is positive when heat is removed from the ground and negative when heat is induced in the ground. Fig. 12 reveals that both configurations of convection embankment allow removing approximately twice as much heat as the reference embankment in wintertime.

In the warmer period, the convection embankment without chimney heats up the ground more than the conduction-dominated embankment by ~2 W/m^2. However, the summertime performance of the convective embankment with chimney is slightly better than the performance of the reference embankment.

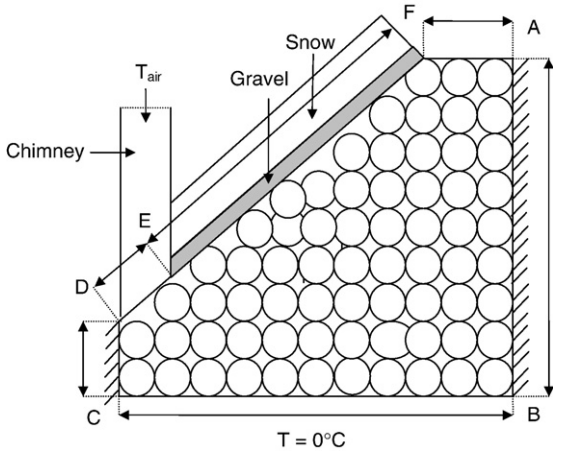

Fig. 11. Air convection embankment with chimney for test 3.

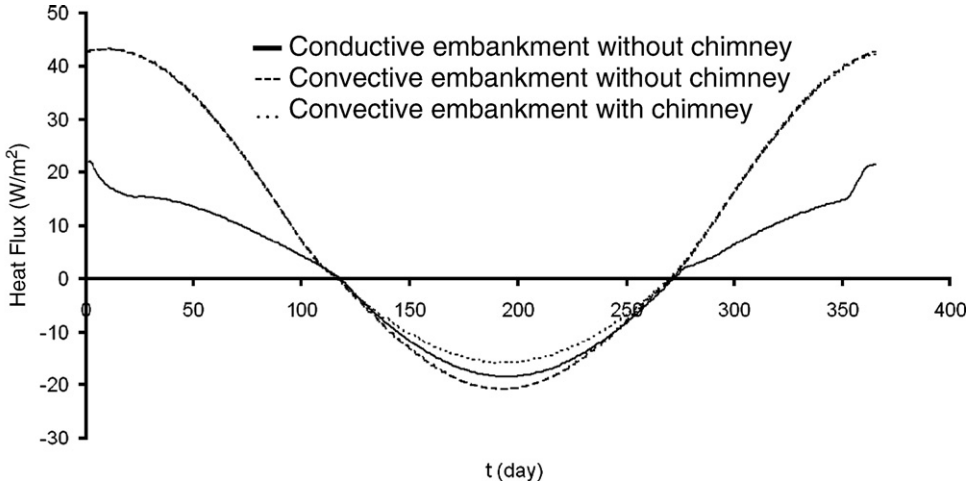

Fig. 12. Annual heat flux evolution at the interface BC for the two air convection embankment designs.

4.2. Heat drain

A second set of numerical simulations was carried out to model the embankment with embedded heat drain. The geometry of this embankment is described in Fig. 13A.

The numerical model with heat drain has two chimneys with the same height. The thermal boundary conditions are shown in Fig. 13B. The boundary overall heat transfer coefficients are as previously. Five numerical sensors are positioned at the same location

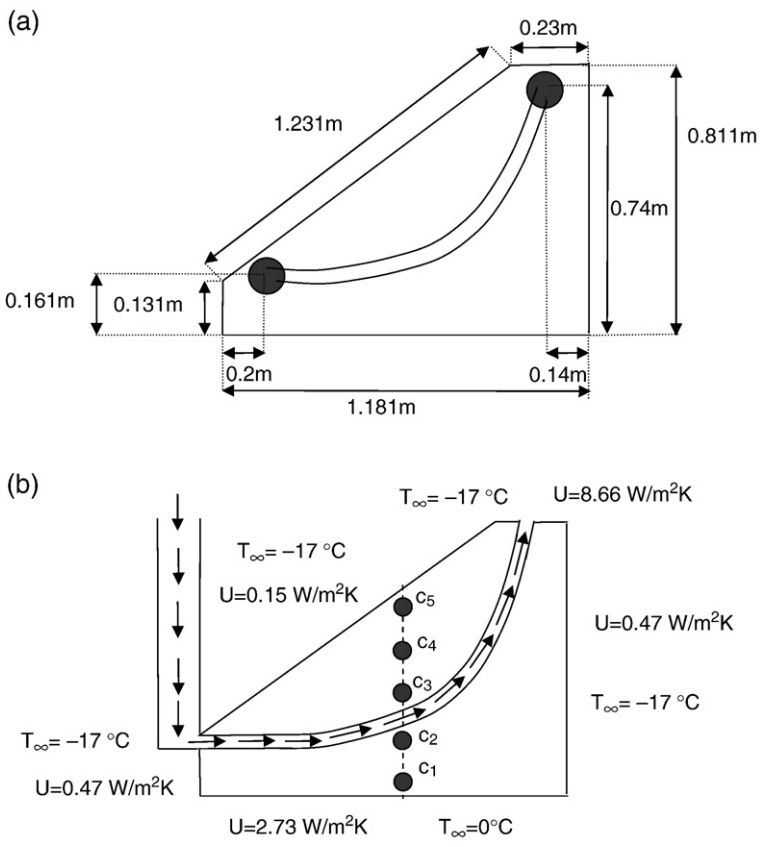

Fig. 13. (a) Geometry of the embankment with embedded heat drain, (b) Boundary conditions for the embankment with heat drain.

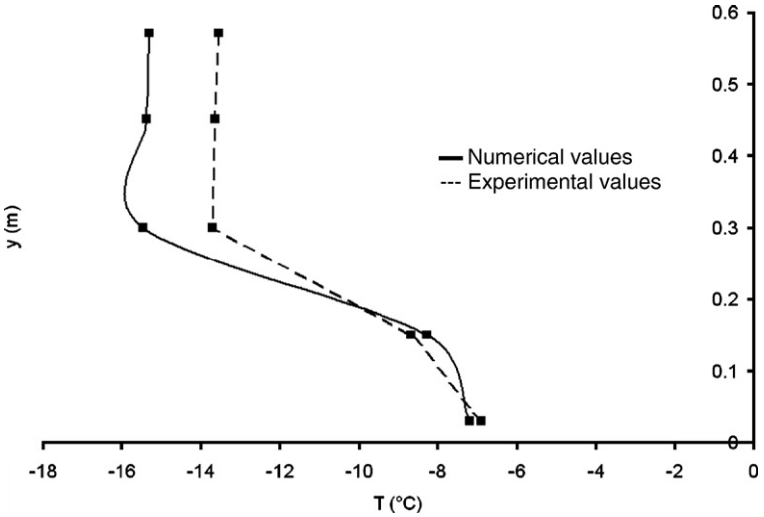

Fig. 14. Steady-state experimental and numerical temperatures for the 5 sensors in the embankment with heat drain.

as in the experiment. Simulation is done in steady-state conditions. A comparison between numerical and experimental results is shown in Fig. 14.

The numerical values obtained are overall very close to the experimental values (less than 0.5 °C of deviation under the drain). However, the difference is more important for the sensors located above the drain. This difference of temperature, which remains rather low (approximately 1.7 °C) can be explained by the fact that the boundary overall heat transfer coefficient is not known precisely, and that the exact positions of the heat drain within the embankment are also unknown. We notice however that for both the numerical and experimental cases, temperatures fall suddenly once below the drain. The drain plays in part the role of a heat insulator, which will be very useful in summer to prevent heat from penetrating in the ground.

Finally, the numerical model of the embankment with embedded heat drain was used for testing the yearly performance of this embankment compared to that of the convective and the conductive embankments. In that respect, we assumed that the external air temperature varied as given by Eq. (7). In addition, the overall heat transfer coefficients were assumed to be the same as those used for the evaluation of the yearly performance of the convective embankment, as described before.

The evolution of the heat flux removed from BC over the year as obtained from the numerical simulations is

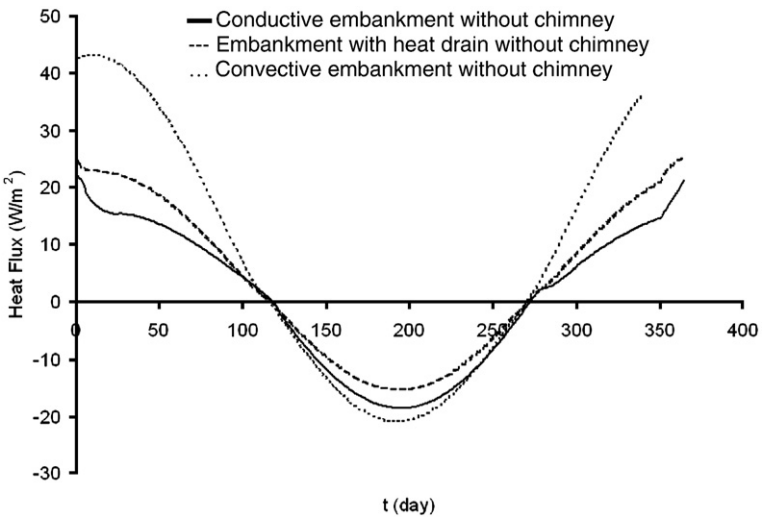

Fig. 15. Annual heat flux evolution at the interface BC for an embankment with embedded heat drain.

shown in Fig. 15. This figure shows that the convective embankment and the embankment with embedded heat drain evacuate more heat from the soil in the winter than the conductive embankment. However, in summer, the convective embankment without chimney heats up the ground more than the conduction-dominated reference embankment and the embankment with embedded heat drain without chimney heats up less than the conduction-dominated embankment. In the warmer period, the heat drain acts as a heat insulator and prevents heat from penetrating into the ground. However, we can notice that the convective embankment evacuates a lot more heat from the soil (70% more) than the embankment with embedded heat drain during the winter.

5. Conclusion

The small-scale embankment tests of the two mitigation techniques, the heat drain and the air convection embankment, have shown that implementing these techniques in the shoulder of a road embankment will result in a significant decrease in temperatures, which will minimize the risk of permafrost degradation underneath the embankment and thereby avoid thaw settlements. The laboratory results have shown that it is possible to increase the effectiveness of the ACE technique during winter conditions by providing proper ventilation at the top and the bottom of the embankment. This allows cold air to penetrate into the embankment from the bottom, while warm air is dissipated at the top. However, the experimentation of a warming process showed that an open air convection embankment is very sensitive to temperature changes and that the cooling effect will be lost rapidly, when air temperature increases. This situation makes an open ACE vulnerable during the summer months, when warm air can be forced into the embankment from the side and raise the temperature significantly. A solution to this problem consists of using a thin gravel layer placed on the slope of the ACE to prevent direct heat exchange. Air intakes installed along the embankment shoulders, allow feeding cold air in the system during winter and limiting warm air intake during summer. Numerical modeling has shown that the embankment with embedded heat drain is better to prevent heat from penetrating into the ground in the warmer period, and that both techniques are very effective to cool permafrost in the winter. The simulations have also shown that the use of a ventilation system improves performance of both protection techniques during summer and winter.

Small scale experiments and numerical modeling however have some limitations. Laboratory models are submitted to idealized conditions and are likely to induce scale effects. Numerical models are, in turn, based on parameters and calibrated on data obtained from the laboratory experiments. Full-scale testing is thus required to calibrate the models to full-scale conditions and improve the robustness of the models. Field testing has been undertaken in Salluit and Tasiujaq, Nunavik, Canada in order to provide field data on the performance of the thermal protection techniques described in this paper.

References

Andersland, O.B., Ladanyi, B., 1994. An Introduction to Frozen Ground Engineering. Ed. Chapman & Hall, New York, USA, 347 pp.

Andreozzi, A., Manca, O., 2001. Thermal and fluid dynamic behavior of symmetrically heated vertical channels with auxiliaty plate. International Journal of Heat and Fluid Flow 22 (4), 424–432.

Beaulac, I., 2006. Impacts de la fonte du pergélisol et adaptations des infrastructures de transport routier et aérien au Nunavik. Master thesis, Département de genie civil, Université Laval, Québec, Canada, 248 pp.

Beaulac, I., Doré, G., 2006. Development of a New Heat Extraction Method to Reduce Permafrost Degradation under Roads and Airfields. Paper. Département de genie civil, Université Laval, Québec, Canada.

Beaulac, I., Doré, G., Shur, Y., Allard, M., 2004. Road and airfields on permafrost, problem assessment and possible solutions. Twelfth International Conference on Cold Regions Engineering (ASCE), Edmonton, Canada. CD-ROM.

Environment Canada, 2007. Experimental data of Beaver Creek acquired through www.climate.weatheroffice.ec.gc.ca on May 22, 2007.

Ergun, S., 1952. Fluid flow through packed columns. Chem. Eng. Prog. 48 (2), 89–94.

Esch, D.C., 1996. Road and airfield design for permafrost conditions. Roads and Airfields in Cold Regions, Technical Council on Cold Regions Engineering Monograph, pp. 121–149.

Goering, D.J., 1996. Air convection embankments for roadway construction in permafrost zones. Proceedings of the Eighth International Conference on Cold Regions Engineering, Fairbanks, Alaska, pp. 1–12.

Goering, D.J., Kumar, P., 1996. Winter-time convection in open-graded embankments. Cold Regions Science and Technology 24, 57–74.

Incropera, F.P., DeWitt, D.P., Bergman, T.L., Lavine, A.S., 2006. Fundamentals of Heat and Mass Transfer, 6th edition. Wiley. 1024 pp.

Krahn, J., 2004. Thermal Modeling with TEMP/W – An Engineering Methodology. GEO-SLOPE International Ltd, Calgary, Canada. 282 pp.

Lai, Y., Wang, Q., Niu, F., Zhang, K., 2004. Three-dimensional nonlinear analysis for temperature characteristic of ventilated embankment in permafrost regions. Cold Regions Science and Technology 38, 165–184.

Lai, Y., Zhang, M., Gao, Z., Yu, W., 2006. Influence of boundary conditions on the cooling effect of crushed-rock embankment in permafrost regions of Qinghai–Tibetan Plateau. Cold Regions Science and Technology 44, 225–239.

Li, D., Wu, Z., Fang, J., Li, Y., Lu, N., 1998. Heat stability analysis of embankment on the degrading permafrost district in the East of the

Tibetan Plateau, China. Cold Regions Science and Technology 28, 183–188.
Lunardini, V.J., 1981. Heat Transfer in Cold Climates. Van Nostrand Reinhold, New York. 731 pp.
Nield, D.A., Bejan, A., 1992. Convection in Porous Media. Springer-Verlag, New York. 408 pp.
Patankar, S.V., 1980. Numerical heat transfer and fluid flow. McGraw-Hill, New York. 210 pp.
Saboundjian, S., Goering, D.J., 2003. Air convection embankment for roadways-field experimental study in Alaska. Transportation Research Record 1821, 20–28.
Zhang, M., Zhang, J., Lai, Y., 2005. Numerical analysis for critical height of railway embankment in permafrost regions of Qinghai–Tibetan plateau. Cold Regions Science and Technology 41, 111–120.

Appendix C

The impact of light-colored pavements on active layer dynamics revealed by Ground-Penetrating Radar monitoring

Authors
Anders Stuhr Jørgensen (corresponding author)
Thomas Ingeman-Nielsen

Publication status
Published in the proceedings to the 9th International Conference on Permafrost, Fairbanks, Alaska, USA (2008), pages 865-868

Department of Civil Engineering
Technical University of Denmark

The Impact of Light-Colored Pavements on Active Layer Dynamics Revealed by Ground-Penetrating Radar Monitoring

Anders Stuhr Jørgensen
Arctic Technology Centre, Department of Civil Engineering, Technical University of Denmark, DK-2800 Kgs. Lyngby, Denmark.

Thomas Ingeman-Nielsen
Arctic Technology Centre, Department of Civil Engineering, Technical University of Denmark, DK-2800 Kgs. Lyngby, Denmark.

Abstract

Ground-penetrating radar (GPR) has been used to study the variations in the depth of the frost table throughout a complete thaw-freeze season at Kangerlussuaq Airport, western Greenland. In autumn 2000, three test areas were painted white on the parking area of the airport in order to reduce further development of depressions in the asphalt pavement. One of these areas has been used in the GPR investigations to compare the variations of the frost table underneath a normal dark asphalt surface to that below a more reflective surface. Results clearly indicate a correlation between the use of the reflective surface and a reduced depth of the frost table. In late summer, the difference in the depths of the frost table is approximately 0.9 m. The results should promote interest in the development and use of light-colored pavement materials.

Keywords: active layer; ground-penetrating radar; permafrost; reflective surface.

Introduction

The presence of permafrost is an important aspect in civil engineering in arctic regions. Thawing of ice-rich permafrost leads to consolidation of the active layer above. The construction of road and airport embankments changes the thermal regime of the ground, and may lead to permafrost degradation under or adjacent to such structures. This problem is now amplified by the effects of climate warming. Mapping the lateral and vertical extent of permafrost as well as actual ice-content is, therefore, an important part of geotechnical site investigations in arctic regions. Ground-penetrating radar (GPR) has proved to be a useful method for mapping the distribution of permafrost (Annan 2002, Annan & Davis 1976, Pilon et al. 1992); especially the frost table is often observed as a strong reflection in the GPR data (Jørgensen & Andreasen 2007, Ingeman-Nielsen 2005, Arcone et al. 1998). Thus, repeated GPR surveys can reveal yearly variations in thickness of the active layer.

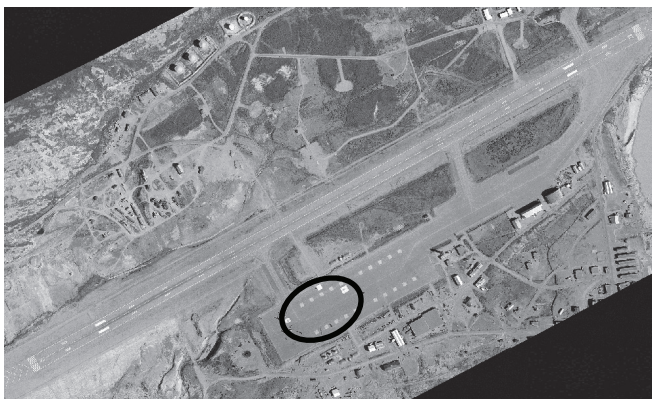

Figure 1. Kangerlussuaq Airport. The investigated area is surrounded by the circle.

This paper is based on repeated GPR investigations from May until October 2007 on the southern parking area at Kangerlussuaq Airport, western Greenland (Fig. 1). The objectives of the measurements were to study variations in the depth of the frost table throughout a complete thaw-freeze season and to compare the differences of the depth underneath a normal dark asphalt and a more reflective surface (a white painted area).

Site Description

Kangerlussuaq Airport is built on a river terrace (altitude 30–50 m) at the head of the 170 km long fjord, Kangerlussuaq (Søndre Strømfjord), located just north of the Polar Circle at 67°00′N and 50°42′W. In the western part of the area the terrace is made up of fine-grained glaciomarine sediments partly covered with fluvial deposits of sand and gravel. In the eastern part fine-grained marine deposits are absent.

The climatic conditions at Kangerlusssuaq are arctic continental, determined by its northern location and its position in a 2-3 km wide valley surrounded by mountains (plateau altitude 400–600 m). To the east the Greenlandic ice sheet, with altitudes up to 3 km, has a dominant influence on precipitation and winds. These conditions result in a dry sub-arctic climate with winter temperatures down to -40°C (-40°F) and summer temperatures up to 20°C (68°F). From 1977–99, the mean annual temperature was -5.7°C and the mean annual precipitation was 151 mm (Danish Meteorological Institute 2007). Since the middle of the 1990s the mean annual temperature in Kangerlussuaq has increased to -4.0°C (Fig. 2). Nevertheless, Kangerlussuaq is still underlain by 100-150 m of continuous permafrost (Tatenhove & Olesen 1994). The entire active layer is frozen during the winter, but in late summer the depth of the frost

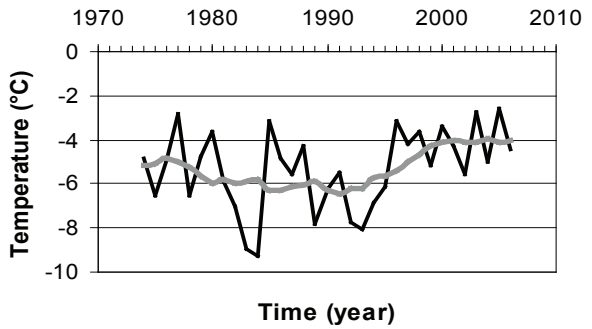

Figure 2. Mean annual air temperature (black) and nine year average temperature (gray) in Kangerlussuaq, 1974-2006 (Danish Meteorological Institute 2007).

table is up to 3.0 m in the open terrain (Ingeman-Nielsen et al. 2007). However, under areas covered with asphalt the depth of the frozen surface is greater, and in some areas this causes melt-water to concentrate under the pavement.

Methodology

In the period from May until October 2007, eight GPR investigations were carried out at the southern parking area of Kangerlussuaq Airport (Fig. 1). In addition, one investigation was carried out in July 2005 and three investigations were carried out in a period from May until August 2006 (Jørgensen & Andreasen 2007, Jørgensen et al. 2007).

GPR systems produce a short pulse of high frequency electromagnetic energy which is transmitted into the ground. The propagation of the signal depends on electrical properties of the ground, which are mainly controlled by the water content of investigated materials. Changes in the dielectric properties will cause a reflection of parts of the transmitted signal, while the rest of the signal will continue to propagate into the ground. Reflection will occur at each successive interface in the ground, until the signal has been damped by losses in the ground. The reflected signal is detected by the GPR receiver, and travel times for individual radar waves can be used to display the results in a radargram, in terms of received amplitude as a function of travel time.

Results from a GPR investigation give insight into the structural changes in the ground but do not directly show the composition or type of the materials investigated. To calibrate the GPR results from Kangerlussuaq Airport, a borehole was drilled and a trench was dug in August 2005.

We applied a GSSI Model SIR-20 with two ground coupled 400 MHz and 900 MHz (GSSI Model 5103 and GSSI Model 3101) antennas. All measurements were conducted along the same profile (Figs. 3A, 3B) with the antennas towed about 3 m behind a car. The GPR profiles were recorded by survey wheel, and traces were collected every 0.05 m (20 traces per meter).

The post-processing included band-pass trace-filtering to reduce electronic and antenna-to-ground coupling noise, spatial filtering to remove coherent background noise, and

Figure 3A. White painted asphalt surface on the southern parking area of Kangerlussuaq Airport.

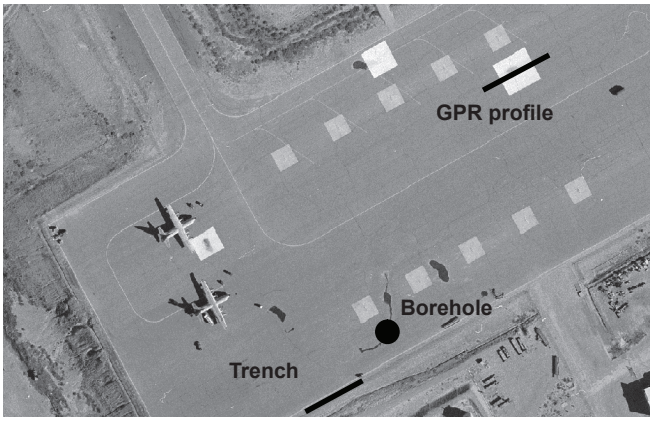

Figure 3B. Placement of GPR measurements across the white painted asphalt surface shown in Figure 3A. The location of the trench and borehole is also shown.

a running average to make a horizontal smoothing of the recorded signal. The processing was carried out using the program ReflexW 3.5 from Sandmeier Scientific Software.

Results

Figure 4 illustrates the difference in the depth of the frost table underneath the normal black asphalt surface and the more reflective surface (white painted area). The variations of the depth of the frost table throughout the thaw-freeze season are illustrated in Figure 5.

According to borehole data from August 2005, top soils were unsaturated and unfrozen until a depth of 3.5 m. The trench revealed a depth of the frost table close to 4.0 m. The velocity of the radar waves in the unfrozen sediments underneath the southern parking area was estimated to be 0.13 m/ns by combining the GPR results with the results from the borehole logs and the trench.

The GPR results (Fig. 5) illustrate the progressive lowering of the frost table. The results also show the effect of the white surface on the depth to the frost table. The fact that the changes in depth to the strong reflection on the radargrams are aligned with the boundaries of the painted area (26 m wide) confirms that this reflection is actually the interface between the frozen and unfrozen ground.

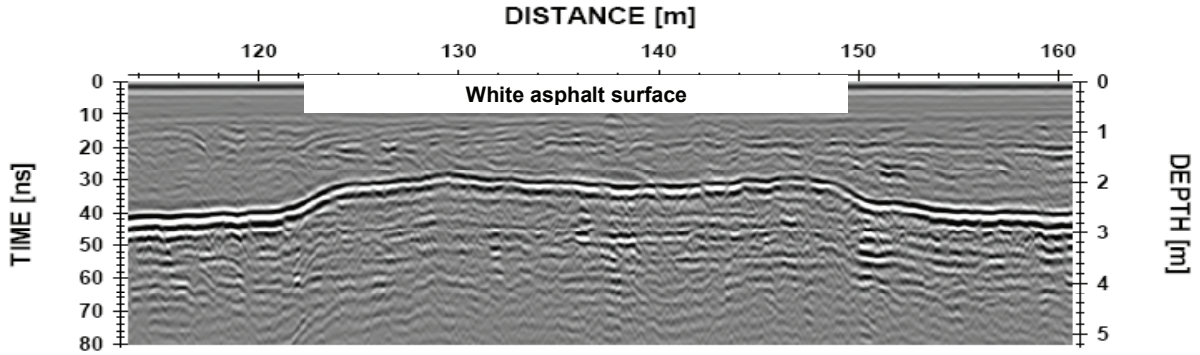

Figure 4. Radargram from July 2007 showing the depth of the frost table. The frost table is seen as a strong reflector in the depth of approximately 2.7 m underneath the normal dark asphalt surface (left and right parts of the radargram) and 2.1 m underneath the white painted area (middle of the radargram).

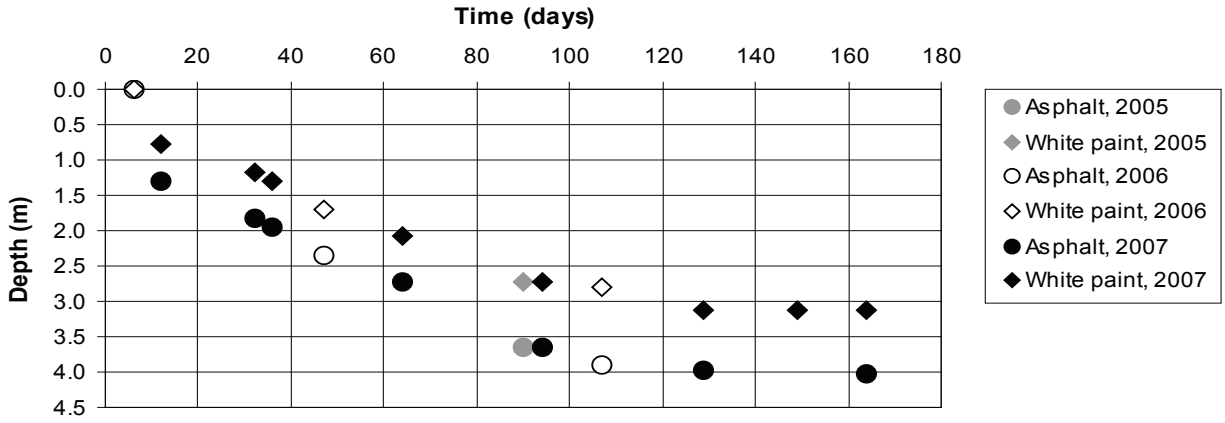

Figure 5. Variations of the depth of the frost table underneath the normal black asphalt surface and the white painted area. The time is shown as number of days from May 1st.

It appears that a stable situation is approached underneath the surfaces between the two measurements carried out in September (Fig. 5). The maximal difference between the depths to the frost table is found as approximately 0.9 m at the end of the thawing period (Fig. 5).

Discussion

We have performed GPR measurements across a reflective surface (white paint) eight times in the period from May until October 2007. The measurements have shown a clear correlation between the use of the reflective surface and a reduced depth to the frost table. At the end of the thawing period the difference in the depths to the frost table is approximately 15 ns.

Based on borehole information, the measured depth of the frost table (procured by the trench excavation) and GPR data collected at the locations of the borehole and the trench in August 2005, the radar wave velocity in the unfrozen sediments was found to be 0.13 m/ns, which corresponds to a permittivity of 5.3. The top soils at the borehole location were unsaturated sorted sand until a depth of 3.5 m with water content in the range of 2%–5% (Jørgensen and Andreasen, 2007). Using a calibration curve empirically determined by Topp et al. (1980) and soil parameters (density 2.70 g/cm^3 and porosity 30%), which is generally used for sandy materials in the area, a permittivity of 5.3 result in a water content of 4.75% for the material. This value lies within the interval of the water content measured in the soil samples from the borehole.

The low water content and well sorted sandy material, which result in a low adherence of the water particles, gives us a situation close to dry conditions and temporal changes in the velocity due to changing pore-water content in the unfrozen sediments were therefore neglected in the present study. An increase in water content will result in an increased permittivity of the material, which will lead to a decreased velocity of the radar waves. A water content of 9.50%, twice the amount of the determined value, would have reduced the maximal difference between the depths to the frost table underneath the two investigated surfaces to approximately 0.2–0.3 m.

Our results have shown that the change in active layer thickness due to the increased reflectivity of surface amounts to approximately 0.9 m in late summer. This constitutes a major difference in the thermal conditions below the reflective surface and the normal dark asphalt surface, and the results should promote interest in the development and use of light-colored pavement materials to reduce settlements under arctic infrastructures caused by the annual thaw-freeze cycle and increasing thickness of the active layer.

Acknowledgments

This research was mainly funded by the Commission for Scientific Research in Greenland (Kalaallit Nunaani ilisimatuutut misissuinernut kommissioni) and partly funded by the Polar Earth Science Program, Office of Polar Programs, National Science Foundation (ARC-0612533).

We would like to thank the Greenlandic Airport Department (Mittarfeqarfiit) for granting us access to the airport area in Kangerlussuaq, and the Municipality of Sisimiut (Sisimiut Kommunianut) for help with accommodation and transportation.

References

Annan, P. 2002. GPR – History, Trends, and Future Developments. *Subsurface Sensing Technologies and Applications* 3(4): 253-270.

Annan, P. & Davis, J. 1976. Impulse radar sounding in permafrost. *Radio Science* 11(4): 383-394.

Arcone, S.A., Lawson, D.E., Delaney, A.J., Strasser, J.C. & Strasser, J.D. 1998. Ground-penetrating radar reflection profiling of groundwater and bedrock in an area of discontinuous permafrost. *Geophysics* 63(5): 1573-1584.

Danish Meteorological Institute 2007. Climate data acquired through www.dmi.dk on August 20, 2007.

Ingeman-Nielsen, T. 2005. *Geophysical Techniques Applied to Permafrost Investigations in Greenland*. Ph.D. Thesis. Technical University of Denmark.

Ingeman-Nielsen, T., Clausen, H. & Foged, N. 2007. Engineering geological and geophysical investigations for road construction in the municipality of Sisimiut, West Greenland. *Proceedings, International Conference on Arctic Roads, Sisimiut, Greenland*: 53-61.

Jørgensen, A.S. & Andreasen, F. 2007. Mapping of permafrost surface using ground-penetrating radar at Kangerlussuaq Airport, western Greenland. *Cold Regions Science and Technology* 48: 64-72.

Jørgensen, A.S., Ingeman-Nielsen, T. & Brock, N. 2007. Annual variations of frost table in Kangerlussuaq Airport, western Greenland. *Proceedings, International Conference on Arctic Roads, Sisimiut, Greenland*: 79-83.

Pilon, J. A., Allard, M. & Levesque, R. 1992. Geotechnical Investigations of Permafrost in Ungava with Ground Penetrating Radar. Innovation & Rehabilitation, *Proceedings of the 45th Canadian Geotechnical Conference*, Canadian Geotechnical Society: 19/1-19/9.

Topp, G.C., Davis, J.L. & Annan, A.P. 1980. Electromagnetic determination of soil water content: measurements in coaxial transmission lines. *Water Resources Research* 16(3): 574-582.

Van Tatenhove, F.G.M. & Olesen, O.B. 1994. Ground Temperature and Related Permafrost Characteristics in West Greenland. *Permafrost and Periglacial Processes* 5: 199-215.

Appendix D

Thermal modeling of variations in the depth of the frost table caused by increasing temperatures in Kangerlussuaq Airport, western Greenland

Authors
Anders Stuhr Jørgensen (corresponding author)

Publication status
To be submitted, 7 pages

Department of Civil Engineering
Technical University of Denmark

Thermal modeling of variations in the depth of the frost table caused by increasing temperatures in Kangerlussuaq Airport, western Greenland

Anders Stuhr Jørgensen

Arctic Technology Centre, Department of Civil Engineering, Technical University of Denmark.
DK-2800 Kgs. Lyngby, Denmark, e-mail: asj@byg.dtu.dk, phone: (+45) 45 25 50 04

Abstract

Kangerlussuaq Airport is located at 67°00' N and 50°42' W in the zone of continuous permafrost in western Greenland. During the period 1992-2007 the mean annual air temperature in the area has increased with approximately 2.5°C. Thermal modeling has been used to study the changes in the maximum thaw depth caused by the increase in temperature. A five layered thermal model of the original geologic deposits and the embankment construction on the southern parking area of the airport has been used in the modeling. Two types of surfaces have been studied; a normal dark asphalt surface and a more reflective surface (white painted asphalt). The modeled results have shown an increase in the maximum thaw depth from 1992 until 2007 of approximately 0.5-0.7 m for both surfaces. The results have shown that the use of a more reflective surface will reduce the maximum thaw depth with up to 1.0 m. This constitutes a major difference in the thermal regimes below the two surfaces. The modeled results have been verified by GPR investigations, which were carried out at the southern parking area in the period 2005-08. The results from this study should promote the interest for the use of more reflective surfaces to keep Arctic roadway and airport embankments stabilized in a changing climate.

Keywords: Climate change, Thaw depth, Permafrost, Reflective surface, Asphalt surface

1. Introduction

Earth's climate is changing with the global temperature rising at an unprecedented rate. The climate changes are most evident in the Arctic, where the average temperature has risen at almost twice the rate as the rest of the world in the past few decades. Widespread melting of glaciers and sea ice and rising of permafrost temperatures present additional evidence of the strong arctic warming (Arctic Climate Impact Assessment, 2004). The rise in temperature will lead to an increased depth of the active layer and permafrost degradation, which again will result in problems with instability of sediments. The projected change in the permafrost boundary is shown in Figure 1.

The climatic changes is already seen in Kangerlussuaq, located in western Greenland just north of the Polar Circle at 67°00' N and 50°42' W. The climate in Kangerlussuaq is dry sub-arctic with winter temperatures down to -40°C and summer temperatures up to 20°C. In the period 1977-99 the mean annual air temperature was -5.7°C (Danish Meteorological Institute, 2007). Since the middle of

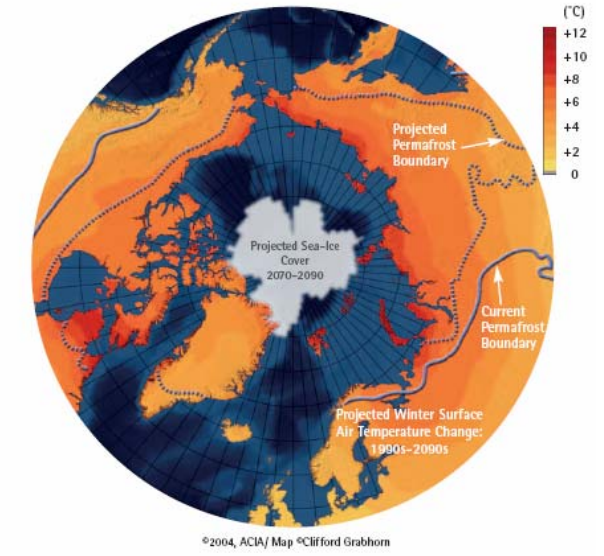

Figure 1: Current and projected (year 2090) permafrost boundary (Arctic Climate Impact Assessment, 2004)

the 1990s the temperature in Kangerlussuaq has increased and the mean annual air temperature is now -4.0°C. Despite the increase in temperature Kangerlussuaq is still in the zone of continuous permafrost (Figure 2) estimated to a thickness between 100-150 m (Tatenhove & Olesen, 1994). The entire active layer is frozen during winter, but in late summer the depth to the frost table is up to 3.0 m in the open terrain (Ingeman-Nielsen et al., 2007) and approximately 4.0 m underneath the asphalt pavement on the southern parking area in Kangerlussuaq Airport (Jørgensen & Andreasen, 2007; Jørgensen & Ingeman-Nielsen, 2008).

Research carried out by the Arctic Climate Impact Assessment (2004) estimates that the mean annual air temperature in the Kangerlussuaq area will raise with approximately 4°C and winter temperatures will increase with up to 6-7°C over the next 80 years.

This paper evaluates the effect of the increase in air temperatures in Kangerlussuaq during the period 1992-2007. A thermal model of the embankment of the southern parking area in Kangerlussuaq Airport has been used to study the changes in the thickness of the active layer. The modeling has been carried out with the finite element software TEMP/W from GEO-SLOPE International Ltd. The thermal model is based on results from a previous borehole drilling, a trench excavation and climate data. Finally the modeling have been compared with results from Ground Penetrating Radar (GPR) investigations, which have been used to study the annual variations of the frost table underneath two different surfaces, a normal dark asphalt surface and a more reflective surface (white paint), on the southern parking area.

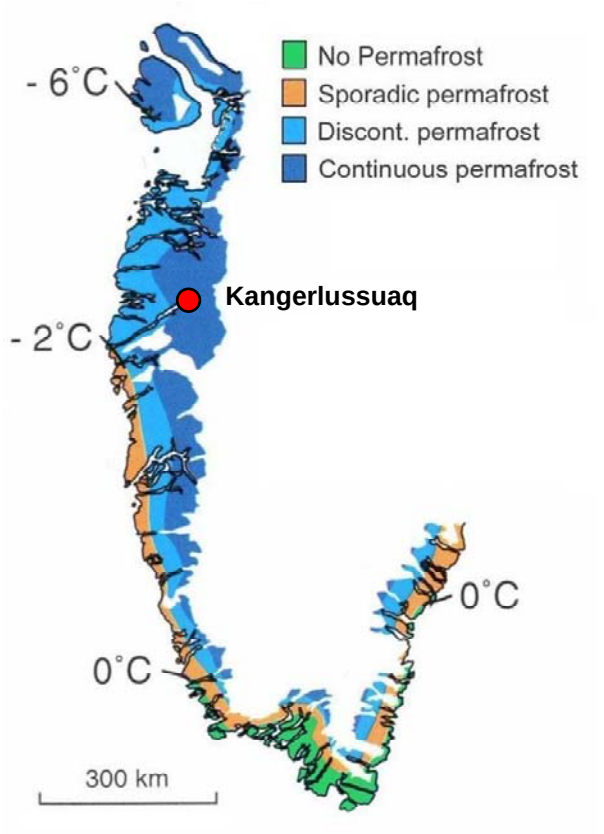

Figure 2: Location of Kangerlussuaq and permafrost distribution in Southwest Greenland (Christiansen & Humlum, 2000)

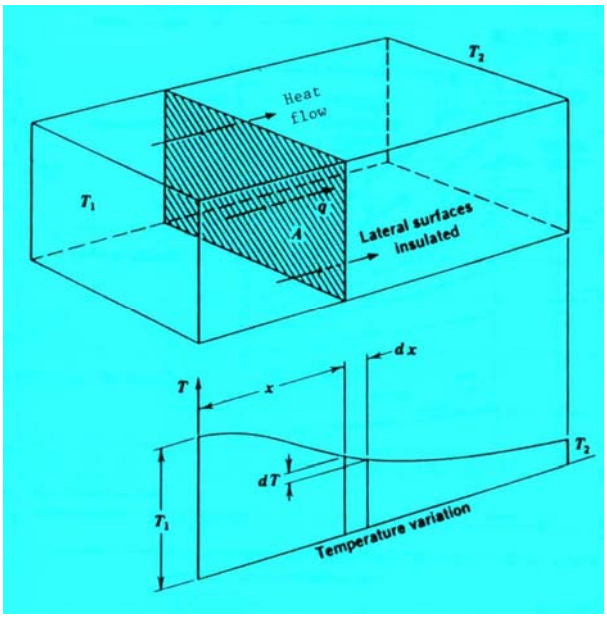

Figure 3: Heat flow through a soil element (Andersland & Ladanyi, 2004)

2. Thermal properties of soils

The response of soil materials to thermal changes requires an understanding of their thermal properties; thermal conductivity, heat capacity, latent heat and thermal diffusivity. These thermal parameters vary with temperature, soil type, water and/or ice content, degree of saturation, and soil density (Andersland & Ladanyi, 1994).

2.1 Thermal conductivity

Heat conduction occurs in all soil constituents and involves a transfer of kinetic energy from molecules in a warm area of the material to a cooler area. Considering a prismatic element of soil having a cross-sectional area *A* at right angles to the heat flow *q* (Figure 3), the conduction is given as (Andersland & Ladanyi, 1994):

$$Q = -k_u A \frac{dT}{dx} \quad (1)$$

and

$$q = \frac{Q}{A} = -k_u \frac{dT}{dx} = k_u i \quad (2)$$

where $Q/A = q$ is the rate of heat flow per unit area (J/m^2·s), k_u the unfrozen thermal conductivity (J/s·m·K or W/m·K), $dT/dx = i$ is the thermal gradient (°C/m), and A is the area (m^2). The minus sign indicates that the heat flow is going from a high to a low temperature.

In general, thermal conductivity of soils depends on density, water content, particle shape, temperature, together with the solid, liquid and vapour constituents, and the state of the pore water (Harlan & Nixon, 1978). The thermal conductivity of ice is much higher than that of water, which results in an increased thermal conductivity when a soil freezes and a decreased thermal conductivity as it thaws. The thermal conductivity of a soil can be computed by (Andersland & Ladanyi, 1994):

$$k_u = \left(k_{sat} - k_{dry}\right)K_e + k_{dry} \quad (3)$$

where k_{sat} and k_{dry} are the saturated and dry thermal conductivities, respectively.

2.2 Heat capacity

Heat capacity is defined as the amount of heat required to raise the temperature of a given material by 1 degree. When expressed on a unit weight basis, the quantity of heat is referred to as the specific heat capacity, c.

Soil consists of various constituents, including solids, water, ice (if frozen), and air. The apparent specific heat capacity, c_a, of a given soil can be expressed as the sum of the heat capacities of the different constituents and a term to account the latent heat (Andersland & Ladanyi, 1994):

$$c_a = c_s + c_i\left(w - w_u\right) + c_u w_u + \frac{1}{\Delta T}\int_{T_1}^{T_2} L \frac{\partial w_u}{\partial T} dT \quad (4)$$

where c_s, c_i and c_u are the heat capacities of the mineral solids, ice and unfrozen water, w is the water content, w_u the unfrozen water content, T the temperature and L the latent heat of the liquid-solid phase change.

2.3 Latent heat

Latent heat is the amount of heat released when a unit mass of a substance (e.g. water) freezes or amount of heat required when a unit mass of a substance (e.g. ice) thaws. For a given soil the total energy involved in the phase change will depend on the total water content and the fraction of this water that changes phase (Andersland & Ladanyi, 1994):

$$L = \rho_d L' \frac{w - w_u}{100} \quad (5)$$

where L is the soil volumetric latent heat of fusion, $L' = 333.7$ kJ/kg is the latent heat for water, ρ_d is the dry density of the soil, w the total water content, and w_u the unfrozen water content of the frozen soil.

2.4 Thermal diffusivity

The rate of which heat is transferred in a soil mass is dependent on the thermal conductivity, k. The rise in temperature that this heat will produce will vary with the heat capacity c and the bulk density ρ of the soil mass. The ratio of these quantities is defined as the soil thermal diffusivity (Andersland & Ladanyi, 1994):

$$\alpha = \frac{k}{c\rho} \quad (6)$$

Values for thermal diffusivities show that α for ice is much higher than that of water. This result in a much higher diffusivity of a frozen soil than that of the same soil in the thawed condition, which mean that the average temperature of a frozen soil will increase more rapidly than an unfrozen soil.

3. Results from borehole and trench

The thermal modeling carried out in connection to this paper is based on results from a borehole and a trench carried out in the southwestern part of the southern parking area in summer 2005 (Figure 4).

3.1 Borehole

The borehole was terminated to a depth of 15 m and provided data on the thicknesses of the different layers in the embankment and subsurface, water content and grain size. The borehole log and the water content are shown in

Figure 4: Location of borehole and trench (red circle), orthophoto of Kangerlussuaq

Figure 5. In August the top soils were unsaturated until a depth of 3.5 m. Analysis of the soil samples between 4.0-5.5 m showed frozen fine-grained silty sand containing organic sediment holding a large percentage of water (20-80% of dry weight).

3.2 Trench

The trench was dug close to the borehole just beside the border of the asphalt area. This position was chosen so that the embankment under the asphalt pavement would not be damaged. The trench was 20 m long and excavated down to the frost surface at a depth of approximately 4.0 m. At the location of the trench, the sediments appeared to be well-drained right down to the frost surface.

4. Climate data

The temperature data used in the thermal modeling are mean monthly air temperatures from the period 1992-2007 (Danish Meteorological Institute, 2007). The mean monthly air temperatures for the winter months can vary in excess of 10-20°C on a year-to-year basis, while the summer months are much more constant. Parts of the temperature data is presented in Figure 6A-6C.

The surface temperature for the two surfaces investigated was found by the use of n-factors (Figure 7). The data used to estimate the values of the n-factors was recorded on a road section in Kangerlussuaq from June until October 2007.

Depth (m)	Thickness (m)	Material
0.00	0.20	Asphalt-concrete
0.20	1.05	Sand/Gravel (gravelly, coarse, stony, well graded)
1.25	0.85	Sand (fine, sorted)
2.10	0.05	Sand (fine, sorted, with a humusrich layer)
2.15	0.25	Silt (finesandy, light grey)
2.40	1.30	Sand (fine, sorted)
3.70	0.05	Sand (fine,silty,with humus in a sloping layer)
3.75	0.25	Sand (fine, organic, brown)
4.00	0.30	Silt (layered, with organic content)
4.30	1.30	Silt (finesandy, with organic content)
5.60	0.80	Sand (fine-medium, silty, brownish grey)
6.40	0.40	Sand (fine-medium, silty, brownish grey)
6.80	1.20	Sand (fine, clayey, waterbearing)
8.00	1.35	Sand (medium-coarse, gravelly)
9.35	0.65	Sand (silty, clayey, with single gravels)
10.00	1.80	Sand, fine-medium, silty, clayey)
11.80	1.70	Sand, medium-coarse, sorted)
13.50	0.30	Silt (finesandy)
13.80	1.20	Sand (medium sorted)

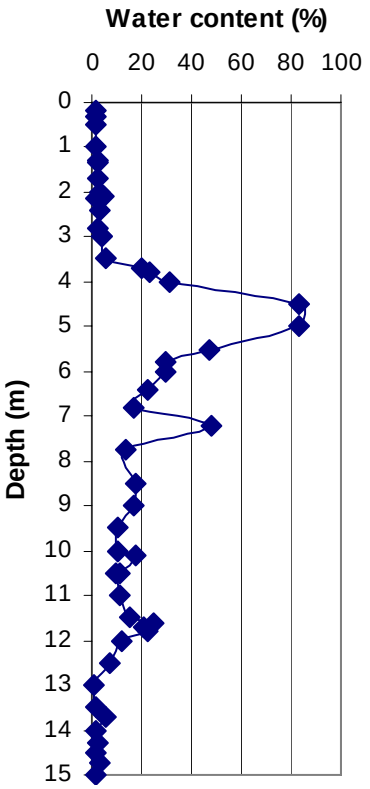

Figure 5: Borehole log and water content (% of dry weight) in soil samples from borehole (Jørgensen & Andreasen, 2007)

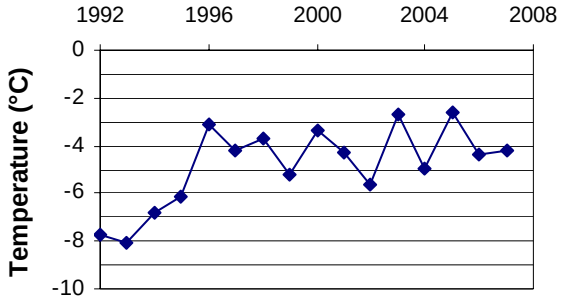

Figure 6A: Mean annual air temperature in Kangerlussuaq, 1992-2007 (Danish Meteorlogical Institute, 2007)

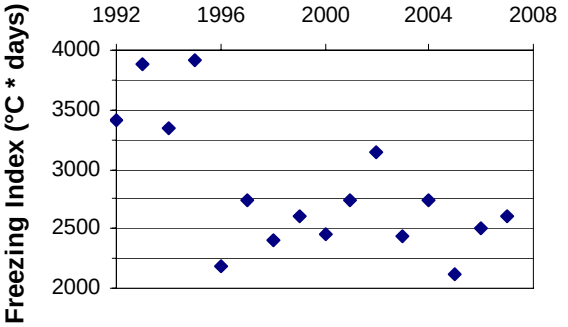

Figure 6B: Freezing index for Kangerlussuaq Airport, 1992-2007. Based on mean monthly air temperatures

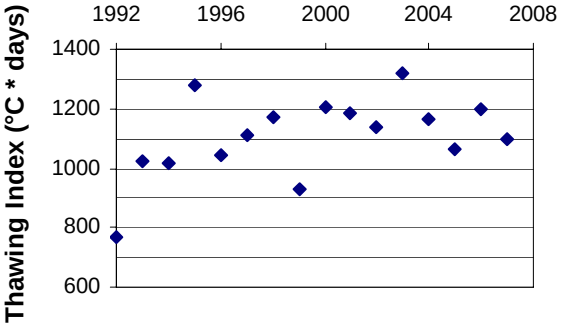

Figure 6C: Thawing index for Kangerlussuaq Airport, 1992-2007. Based on mean monthly air temperatures

Surface	n_f	n_t
Normal black asphalt surface	0.90	1.65
Reflective surface (white paint)	1.00	1.20

Figure 7: Estimated n-factors for each of the two investigated surfaces in Kangerlussuaq Airport. The n_f-values have been used for the freezing seasons (T < 0°C) and n_t-values have been used for the thawing seasons (T > 0°C)

In 2005 a temperature station was established in Kangerlussuaq, results from this station have shown that the temperature of the permafrost is approximately -2.5°C (Ingeman-Nielsen et al., 2007). This value was also used in the modeling.

5. Soil properties

The soil properties used in the thermal modeling are the frozen and unfrozen thermal conductivities, the frozen and unfrozen volumetric heat capacities, the volumetric water content and the unfrozen water content of the different materials. The soil properties were mainly found by using the results from the borehole (Figure 5) and partly from table values (Smith, 1996). A five layered model of the original geologic deposits and the embankment construction was established and used in the thermal modeling (Figure 8). The thermal properties and water content for the five layers are listed in Figure 9. The unfrozen water content was estimated by TEMP/W, based on the materials grain size.

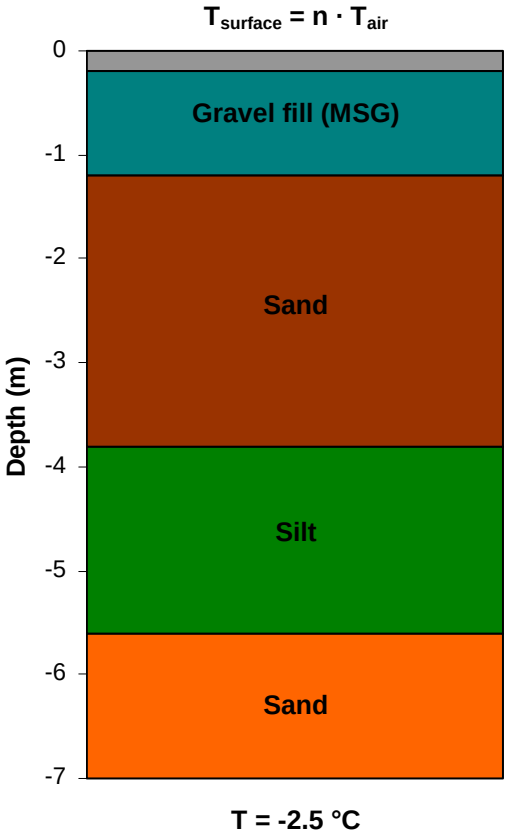

Figure 8: Soil profile used in the thermal modeling with TEMP/W. The first 0.20 m is asphalt (grey)

Layer	Thickness [m]	Thermal conductivity [J/(sec·m·°C]		Vol. heat capacity [kJ/m^3·°C]		Vol. w [%]
		Frozen	Unfrozen	Frozen	Unfrozen	
Asphalt	0.20	0.7	0.7	2200	2340	5.3
Gravel fill (MSG)	1.00	1.2	1.7	1470	1580	5.7
Sand	3.00	1.2	1.7	1510	1660	3.8
Silt	1.60	2.0	1.8	2490	3620	46.0
Sand	-	1.2	1.7	1510	1660	6.5

Figure 9: Thermal properties and water content for each of the five layers used in the thermal modeling

6. Results

In this section the results from the thermal modeling are described and compared with results from GPR investigations carried out on the southern parking area at Kangerlussuaq Airport in the summer periods of 2005-08.

Figure 10 shows the calculated maximum thaw depths underneath the two investigated surfaces, a normal dark asphalt surface and a more reflective surface (white painted asphalt). The maximum modeled thaw depths generally occur in September or October. The modeling results show a clear correlation between the annual variation in the thaw and freeze indices, and the maximum annual thaw depth. The modeled results have shown a progressively lowering of the frost table as a consequence of the increase in air temperatures, which has been seen in the area. During the studied period, 1992-2007, the mean annual air temperature in Kangerlussuaq has increased with approximately 2.5°C. This increase in temperature has lead to a change in the thermal conditions below the two investigated surfaces on the southern parking area, which has lead to an increase in the maximum annual thaw depth. The average modeled maximum thaw depth underneath both surfaces has increased with approximately 0.5-0.7 m during the period 1992-2007 (Figure 10).

The modeled thaw depths compare with the results from GPR investigations carried out during the summer months in 2005-08 (Figure 11). The GPR results from this period have shown that the maximum thaw depth underneath the reflective surface is approximately 3.1 m, whereas the maximum thaw depth is approximately 4.0 m underneath the normal dark asphalt surface (Jørgensen & Andreasen, 2007; Jørgensen & Ingeman-Nielsen, 2008).

7. Conclusion

Thermal modeling have been carried out to get insight into the possible impact of climate warming on the thaw depth penetration underneath the southern parking area at Kangerlussuaq Airport, western Greenland. The results have shown a clear correlation between the annual variation in

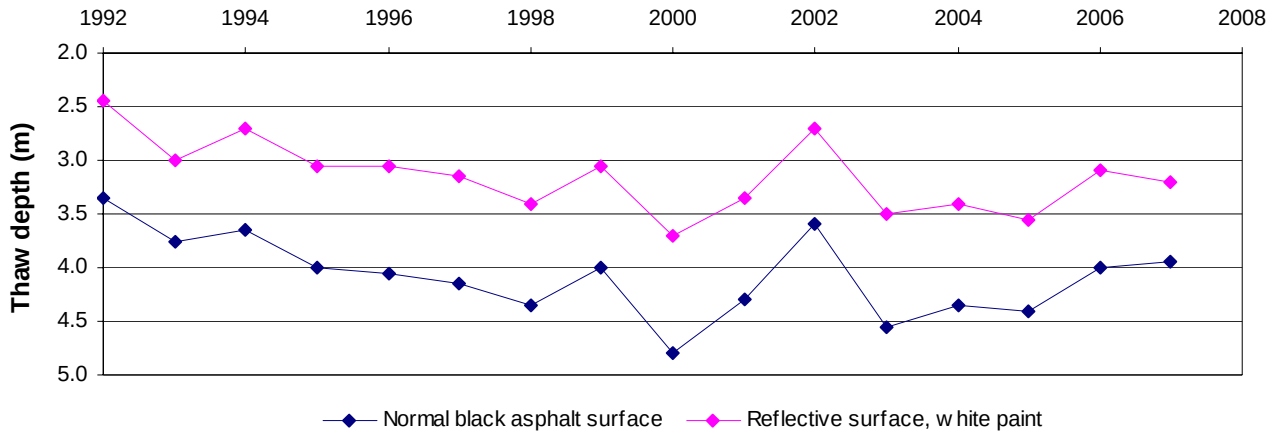

Figure 10: Modeled thaw depths under the southern parking area in Kangerlussuaq Airport, 1992-2007

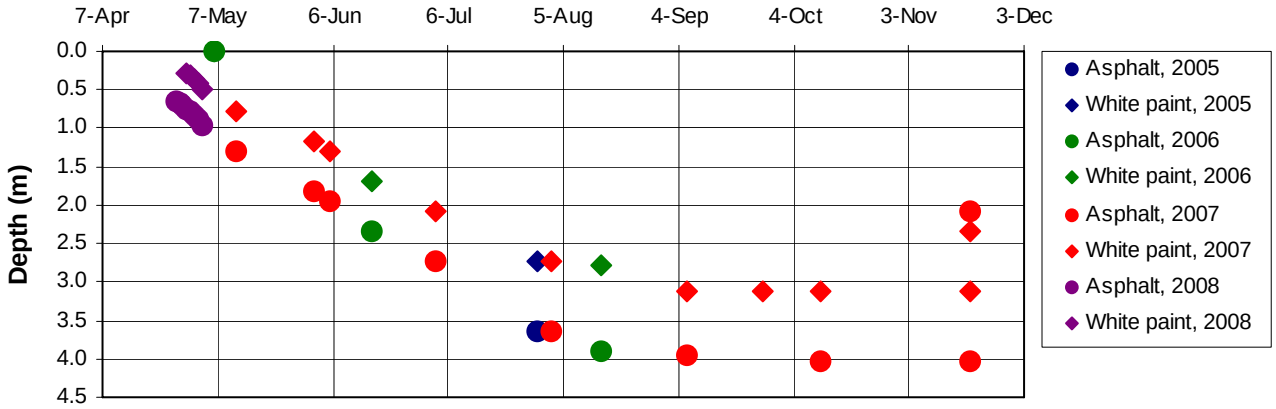

Figure 11: Variations of the depth of the frost table underneath the normal black asphalt surface and the white painted asphalt surface (Jørgensen & Ingeman-Nielsen, 2008)

thaw and freeze indices, and the maximum annual thaw depth. During the studied period the mean annual air temperature in the area has increased with approximately 2.5°C. The increase in temperature has lead to an increase in the maximum annual thaw depth underneath the two investigated surfaces of approximately 0.5-0.7 m. The results have also shown that the use of a more reflective surface will reduce the maximum thaw depth with up to 1.0 m. This constitutes a major difference in the thermal regimes below the two kinds of surfaces. The results should promote the interest for the use of more reflective surfaces to keep Arctic roadway and airport embankments stabilized in a changing climate.

References

Andersland, O. B. & Ladanyi, B. (1994): An Introduction to Frozen Ground Engineering. Chapman & Hall, New York, United Stated of America (ISBN 0-412-98201-3).

Arctic Climate Impact Assessment (2004): Impacts of a warming Arctic. Cambridge University Press. Information acquired through www.acia.uaf.edu on October 10, 2007.

Christiansen, H. H. & Humlum, O. (2000): Permafrost. In: Topografisk Atlas Grønland (B.H. Jakobsen, J. Böcher, N. Nielsen, R. Guttesen, O. Humlum, E. Jensen, Ed.),. Det Kongelige Danske Geografiske Selskab og Kort & Matrikelstyrelsen.

Danish Meteorological Institute (2007): Climate data acquired through www.dmi.dk on October 15, 2007.

Harlan, R. L. & Nixon, J. F. (1978): Ground thermal regime. In: Geotechnical Engineering for Cold Regions (O.B. Andersland, D.M. Anderson, Ed.), Chapter 3, p. 103-163. McGraw-Hill Book Co., New York, United States of America.

Ingeman-Nielsen, T., Clausen, H. & Foged, N. (2007): Engineering geological and geophysical investigations for road construction in the municipality of Sisimiut, West Greenland. Proceedings, International Conference on Arctic Roads, Sisimiut, Greenland, pp. 53-61.

Jørgensen, A. S. & Andreasen, F. (2007): Mapping of permafrost surface using ground-penetrating radar at Kangerlussuaq Airport, western Greenland. Cold Regions Science and Technology, Vol. 48, pp. 64-72.

Jørgensen, A. S. & Ingeman-Nielsen, T. (2008): The impact of light-colored pavements on active layer dynamics revealed by Ground-Penetrating Radar monitoring. Proceedings, Ninth International Conference on Permafrost, Fairbanks, Alaska, USA, pp. 865-868.

Krahn, J. (2004): Thermal Modeling with TEMP/W – An Engineering Methodology. GEO-SLOPE International, Alberta, Canada.

Smith, D. W. (1996): Cold Regions – utilities monograph. 3rd edition. American Society of Civil Engineers and the Canadian Society for Civil Engineering, United States of America (ISBN 0-7844-0192-6).

Van Tatenhove, F. G. M. & Olesen, O. B. (1994): Ground Temperature and Related Permafrost Characteristics in West Greenland. Permafrost and Periglacial Processes, Vol. 5, pp. 199-215.

Appendix E

Experimentation of several mitigation methods in Tasiujaq Airport to minimize the effects caused by the melting of permafrost

Authors
Anders Stuhr Jørgensen (corresponding author)
Guy Doré

Publication status
Abstract accepted to the 14th Conference on Cold Regions Engineering, Duluth, Minnesota, USA (2009). The paper is currently under revision

Department of Civil Engineering
Technical University of Denmark

Experimentation of several mitigation methods in Tasiujaq Airport to minimize the effects caused by the melting of permafrost

Anders Stuhr Jørgensen [1] and Guy Doré [2]

[1] Arctic Technology Centre, Department of Civil Engineering, Technical University of Denmark, 2800 Kgs. Lyngby, Denmark; phone +45 45255004; fax +45 45885935; email: asj@byg.dtu.dk

[2] Department of Civil Engineering, Université Laval, Québec City, Québec, Canada, G1K 7P4; phone (418) 656-2203; email: guy.dore@gci.ulaval.ca

ABSTRACT

Since the beginning of the 1990s an important increase in the mean annual air temperatures has been recorded in Nunavik, Québec, Canada. This has lead to the degradation of permafrost, which is threatening the stability of airport and road embankments in the region. In the summer of 2007 a test-site was established at Tasiujaq Airport to study the effect of three different mitigations methods: heat drain, air convection embankment, and gentle slope (8:1). The methods were constructed in the shoulder of the runway embankment, each method over a distance of 50 m. In each section thermistors were installed to study the annual variations of the thermal regime inside the different embankments. After one year of monitoring, interesting cooling trends have been observed in the different test-sections and a substantially reduced maximum thaw depth have been registered during the thawing season.

INTRODUCTION

The presence of permafrost is an important aspect in civil engineering in arctic regions. Permafrost often has high ice content, making it susceptible to consolidation if thawing occurs. The construction of road and airport embankments will change the thermal regime of the ground, and may lead to permafrost degradation under or adjacent to such structures. This problem is now amplified by the climate warming. The construction of a road embankment changes the ground-surface energy balance, which is a complex function of seasonal snow cover, vegetation, solar and long wave radiation, surface moisture and atmospheric air temperature (Lunardini, 1981). All these factors contribute to produce the mean annual surface temperature, which may differ substantially from the mean annual surface temperature. The construction of a road embankment usually results in an increased mean annual surface temperature, which will increase the thawing of permafrost (Goering, 1996). More specifically the side-slopes of a road embankment are exposed to thaw settlements, inducing longitudinal cracks along the embankment edge and shoulder rotation.

Figure 1. Location of Tasiujaq Airport (red circle) (Wikimedia, 2008)

Different mitigation methods have been developed to avoid or minimize the damages caused by thaw settlements: reflective surfaces, air convection embankment, thermosyphons, geosynthetic reinforcement etc. (Esch, 1996; Beaulac et al., 2004). This paper is based on field results from the first year of monitoring at a test-site in Tasiujaq Airport (Nunavik, Québec, Canada), which includes test-sections of three mitigation methods: gentle slope, air convection embankment and heat drain. The construction of the test-site was based on results from laboratory studies, which included cold room tests of different types of small-scale embankments (Jørgensen et al., 2008). The main objective of establishing the test-site at Tasiujaq Airport has been to determine the effectiveness of the three mitigation methods for permafrost protection in full-scale and under natural conditions.

SITE DESCRIPTION

The village of Tasiujaq is located in the southwestern part of Ungava Bay at 58°71' N and 69°82' W (Figure 1), just a few kilometers north of the tree line and in the zone of abundant discontinuous permafrost. The airport is built on a river terrace covered with fluvial and alluvial deposits (Beaulac, 2006).

During the 1990s the entire Nunavik territory has experienced an increase in the mean annual air temperature. In the village of Kuujjuaq, which is the community closest to Tasiujaq (approximately 110 km to the southeast) with a long-term temperature series, the mean annual air temperature has increased by approximately 3.0°C between 1990 and 2000 (Beaulac, 2006). In the summer periods of 2004 and 2005 several depressions were observed along the shoulders of the runway in Tasiujaq Airport. Another problem, which was observed, is the presence of stagnant water along the foot of the embankment (Beaulac and Doré, 2006). This situation could lead to accelerated thaw of the permafrost underneath and adjacent to the runway.

METHODS

In September 2007 a test-site was constructed along the southeastern orientated shoulder of the runway in Tasiujaq Airport. The total length of the test-site is 200 m, consisting of a reference section and three test-sections: gentle slope, air convection embankment and heat drain. Each section is instrumented with thermistors to measure the thermal regime of the embankments and the underlying geological deposits. The four sections will be described in the following paragraphs.

Reference embankment (section A)

The reference section is used to compare the thermal regime measured in the three test-sections with mitigation methods together with a standard section of the existing runway.

Gentle slope (section B)

The existing shoulder of the runway was extended from having a 2H:1V slope (30 degrees) to a gentler slope, 8:1 (Figure 2). The goal is to reduce wind turbulence, resulting in reduced snow accumulation at the toe of the slope. By reducing or eliminating the insulation effect of snow accumulation the heat extraction is increased during the winter months, reducing the risk of permafrost thawing during the subsequent summer.

Figure 2. Construction of the gentle slope, 8:1 (Doré et al., 2007)

Air convection embankment (section C)

The air convection embankment method involves the use of a highly porous granular material, which was used to construct a new shoulder. The high permeability of such a material allows natural convection of the pore air to occur in the embankment during the winter months, when unstable air density gradients exist (Goering, 1996; Saboundjian and Goering, 2003; Goering and Kumar, 1996). During winter months, cold air from the upper part of the embankment will tend to settle downwards towards the lower part due to its greater density. At the same time warm air will raise from the base of the embankment, which will result in circulation of the pore air and enhanced wintertime heat transfer by speeding the cooling and refreezing of the underlying permafrost (Esch, 1996; Saboundjian and Goering, 2003). During summer months, the air density gradients are stable, the warmer air will stay in the upper part of the embankment, and circulation will not occur (Goering, 1996; Goering and Kumar, 1996). Past experience show that this lead to a reduced mean annual air temperature in the embankment and thereby prevents thaw of the underlying permafrost.

The air convection system as proposed by Goering has been modified for the Tasiujaq experiment on the basis of laboratory tests and numerical simulations. A ventilation system has been added to the convective material to feed cold air at the bottom of the system and to extract warm air at the top. This modification is likely to induce a one-directional convective flow which is expected to be more effective than the convective cells occurring in a closed system. It is expected that the modified system is better adapted to a context where snow accumulated on the embankment slope is dense and crusty impeding heat extraction during winter. The construction of the test-section at Tasiujaq Airport is illustrated on figure 3 and 4.

Figure 3. Installation of the ventilation system in the air convection embankment (Doré et al., 2007)

Figure 4. Installation of geotextile in the upper part of the air convection embankment (Doré et al., 2007)

Heat drain (section D)

The heat drain is an innovative system developed at l'Université Laval in order to protect the side-slopes of road and airfield embankments. The heat drain method consists of a drainage geocomposite with high permeability, placed in the shoulder of an embankment. The geocomposite is composed of a corrugated plastic core covered by geotextile layers with a total thickness of 25 mm, allowing air to flow into the embankment. An air intake system is installed at the base in order to allow an upward movement of air in the membrane (Beaulac, 2006). This movement of air, also called the chimney effect, is a result of a lower density caused by the change in temperature. The drain is designed to facilitate heat extraction. The heat initially flows towards the heat drain by conduction and is then expelled of the embankment by convection (Figure 5). The purpose of the method is to extract heat from the ground and the embankment in order to rise or, at the minimum, to prevent a depression of the permafrost.

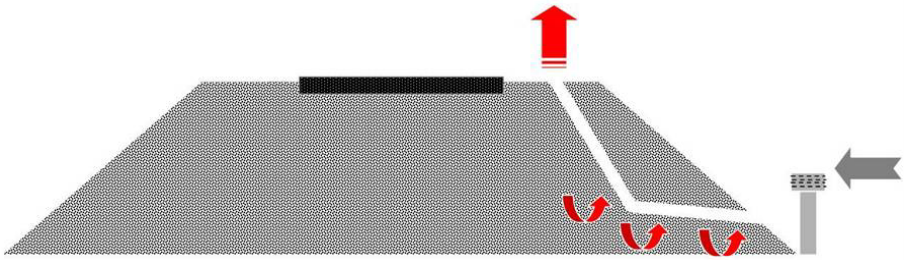

Figure 5. Heat drain placed in the shoulder of a road embankment (Beaulac, 2006)

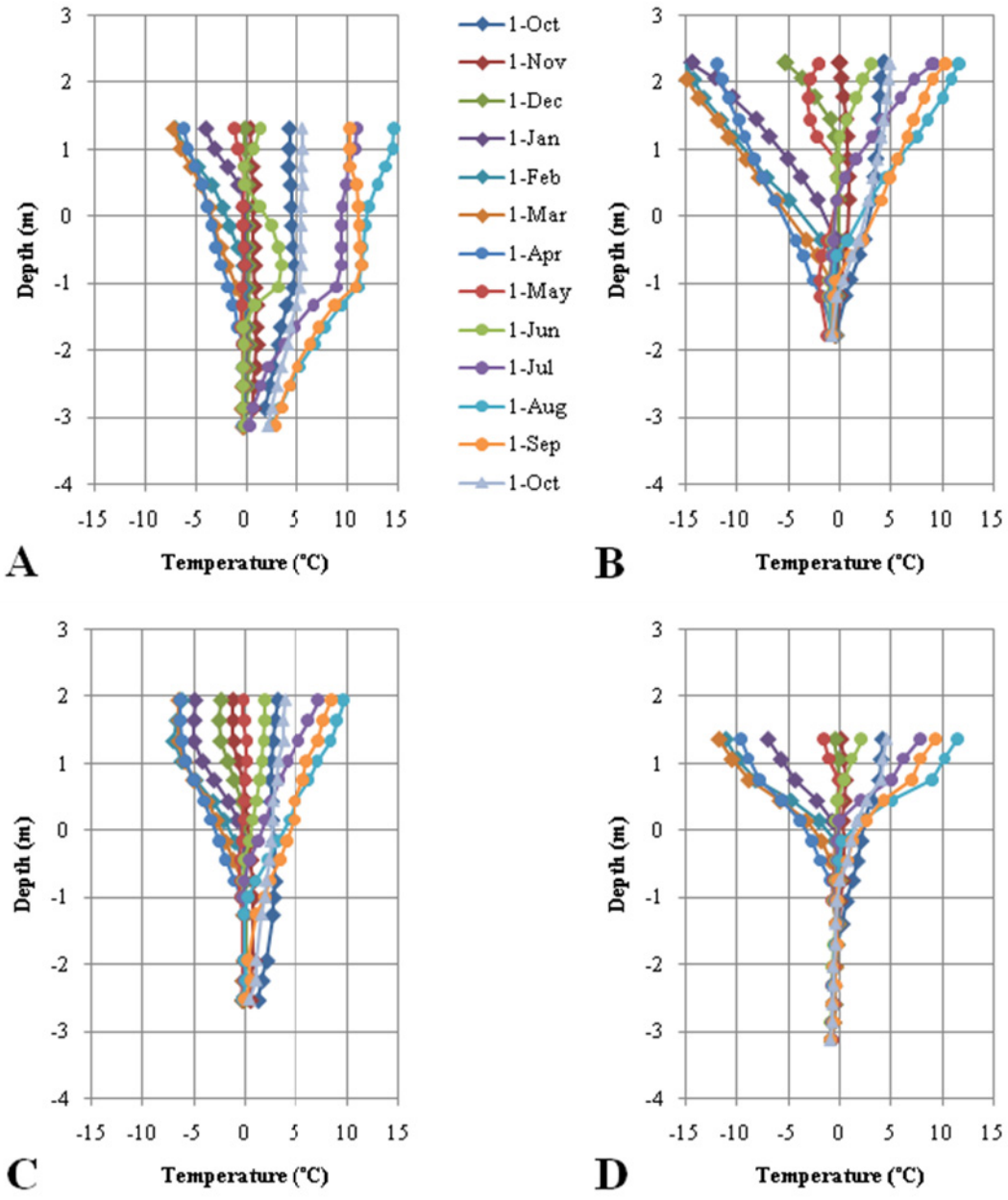

Figure 6. Trumpet diagrams of the thermal regime in each of the four embankment types from October 2007 until October 2008: reference embankment (A), gentle slope (B), air convection embankment (C) and heat drain (D)

RESULTS

Thermal regime of embankments

Figure 6 illustrates the temperature results from the first year of monitoring for each of the four embankment types: reference embankment (A), gentle slope (B), air convection embankment (C) and heat drain (D).

The measured temperatures for the first couple of months have been disturbed caused by the excavation required to place the protection systems in sections C and D and by the installation of the thermistors through an excavation pit in section A. Heat seems to be trapped in the embankments and in the upper part of the geological deposits (Figure 6). During the fall 2007 and the winter 2008, the temperatures seem to progressively cool down and return to a more natural temperature regime. The section with the gentle slope was almost undisturbed during the installation and does not show any significant temperature perturbation.

Looking at figure 6 it is seen that the three mitigation methods have a positive effect on reducing the annual temperature variations of the embankments compared to temperatures monitored in the reference embankment, and that the geological deposits underneath the three test-embankments is kept considerably colder than what have been monitored below the reference embankment.

From the period, where the daily average temperature drops below 0˚C, it is seen, that the three mitigation methods contribute to an increased cooling of the embankments. At level +1.3 m the effectiveness of the methods varies between 2˚C and 3˚C in comparison to the reference embankment. Figure 7 illustrates the differences in the thermal regime of the embankments on December 15.

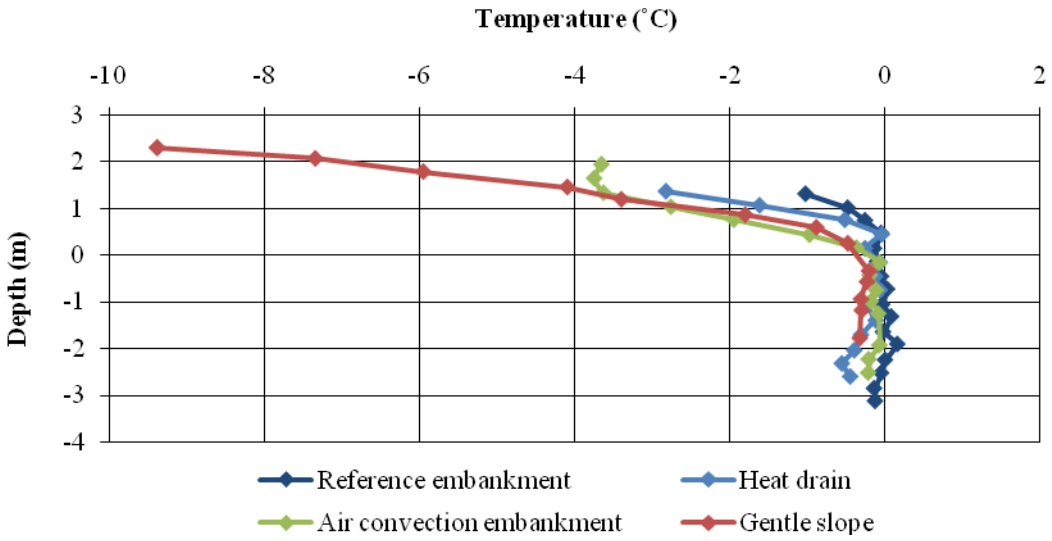

Figure 7. Temperature regime in the four sections on December 15, 2007

From this moment (December 15), the air convection embankment seems to become less effective and by the beginning of February the thermal regime in the air convection embankment and reference embankment is almost alike (Figure 8). It is also worth to note that an inversion of the temperatures seems to appear in the upper part of the air convection embankment at this time (Figure 8). This is probably caused by the ventilation pipes and their lack of potential to expel heat at the top of the embankment. A higher amount of drainage holes in the ventilation pipes would probably have increased the effectiveness of the system.

Figure 8 also illustrates the differences in the temperature gradient (temperature change per meter depth) of the four sections. It is seen that the gentle slope is the section with the highest temperature gradient, approximately twice the size the temperature gradient obtained in the reference embankment. Table 1 summarizes the variation of the temperature gradients for the four sections at three different dates during the winter 2008.

The observations from the first winter have shown that the sections with the gentle slope and the heat drain system have induced a cooling at approximately 4˚C at level +1.0 m compared to the reference embankment (Figure 8). The cooling did not result in an effective cooling of the permafrost underneath the embankments. This is expected to gradually change in the coming years.

A significant difference in the thermal regime of the test-sections compared with the reference embankment is seen during the summer period (Figure 9). The test-sections and the underlying geological deposits are kept significantly colder. The thaw depth underneath the reference embankment on August 1 is more than 3.0 m, whereas underneath the test-sections the thaw depth ranges between 0.5-1.0 m (Figure 9). The temperature difference between the test-sections and the reference embankment at level -1.0 m is approximately 10-12˚C in the late summer months.

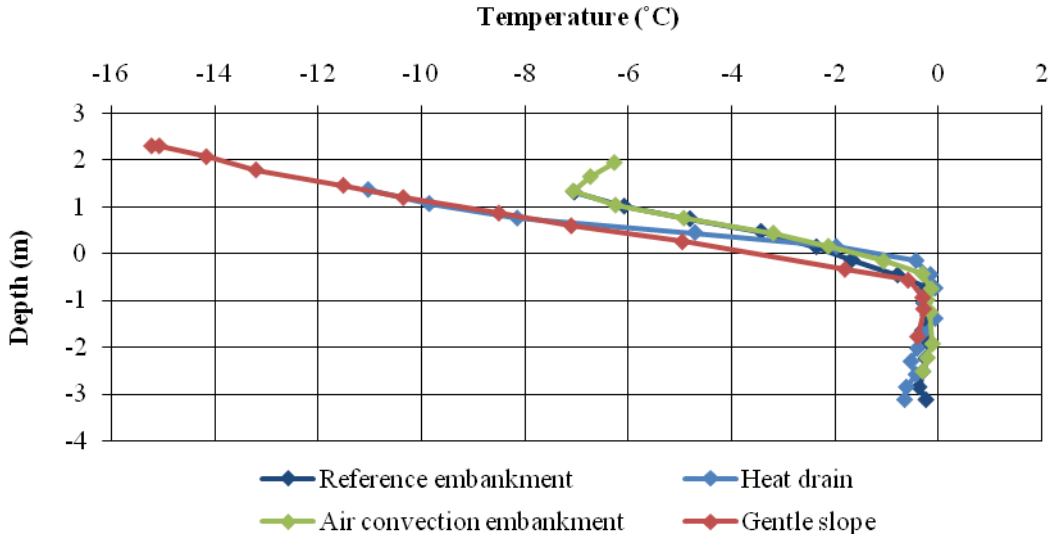

Figure 8. Temperature regime in the four sections on February 1, 2008

Table 1. Temperature gradient in the four embankments

	January 1, 2008	February 1, 2008	March 1, 2008
Reference embankment	3.0˚C	3.9˚C	2.8˚C
Gentle slope	5.6˚C	4.9˚C	4.9˚C
Air convection embankment	3.5˚C	4.4˚C	3.1˚C
Heat drain	4.9˚C	7.7˚C	6.6˚C

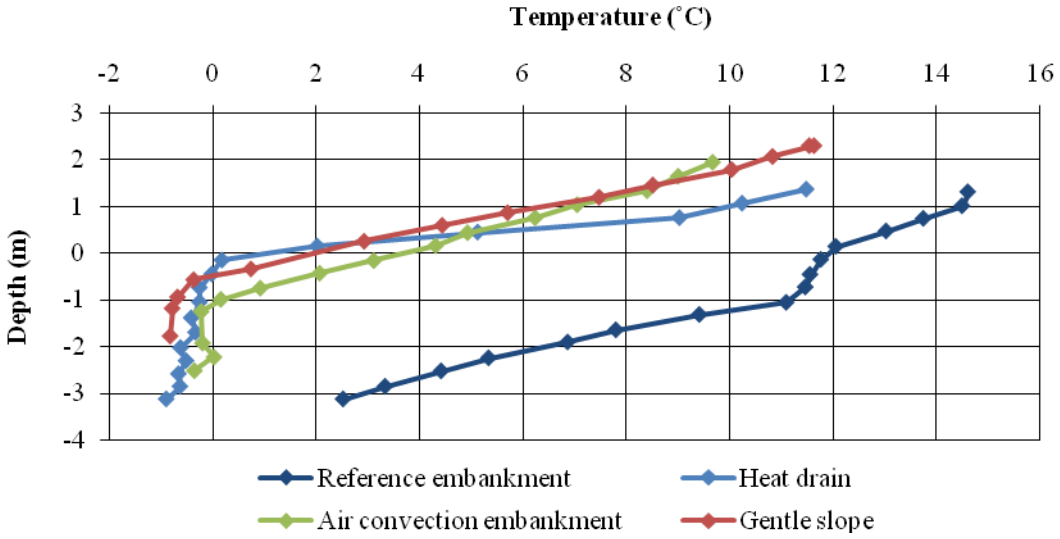

Figure 9. Temperature regime in the four sections on August 1, 2008

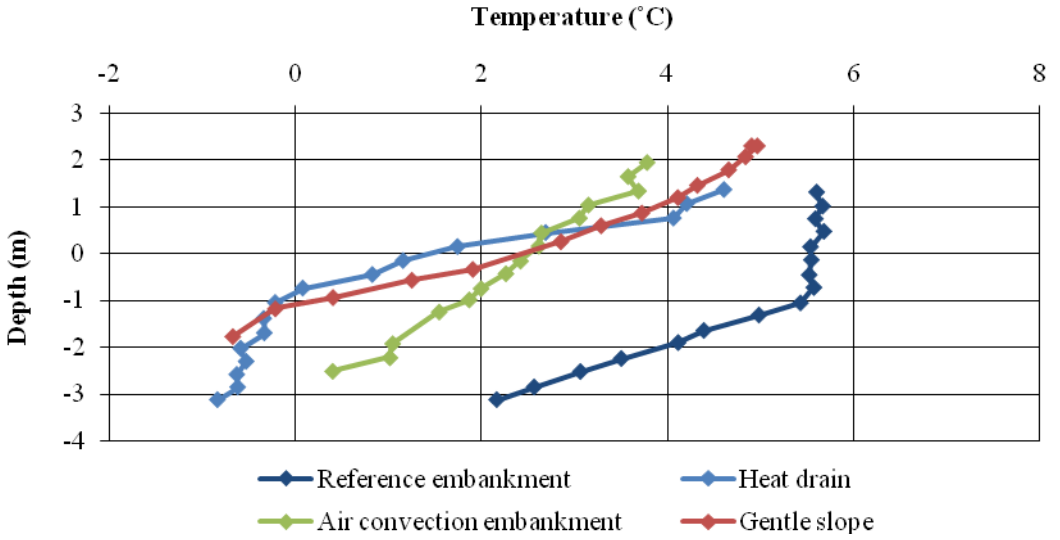

Figure 10. Temperature regime in the four sections on October 1, 2008

The thaw depth, underneath the gentle slope and heat drain sections, is measured to be approximately 1.5 m on October 1, whereas the thaw depth underneath the air convection embankment and the reference embankment is above 3.0 m (Figure 10). However, the thermal regime of the air convection embankment and the geological deposits is significantly colder than the thermal regime in the reference embankment (Figure 10).

Temperature at sub-grade level

The annual temperature variations at the sub-grade level are illustrated in figure 11. It is clearly seen that the three test-sections are kept significantly colder during the summer period compared to the reference embankment. During the winter period the section with the gentle slope is a couple of degrees colder than the rest of the embankments, which is caused by a reduced snow accumulation on this section and by the fact, that the section was not affected by thermal perturbation during construction. The mean annual sub-grade temperature is approximately 2.7˚C for the reference embankment, whereas it has been reduced to approximately -0.4˚C for the gentle slope, 1.0˚C for the air convection embankment and 0.1˚C for the heat drained embankment.

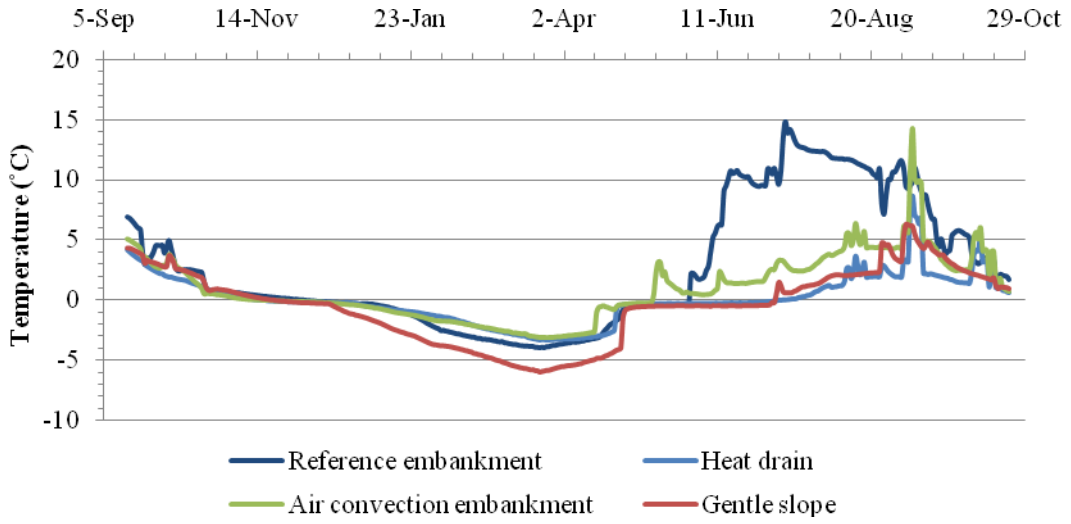

Figure 11. Annual temperature variations at sub-grade level for the four embankment types: reference embankment (A), gentle slope (B), air convection embankment (C) and heat drain (D)

CONCLUSION

The temperature data from the first year of monitoring at Tasiujaq Airport have shown some interesting cooling trends in the different test-sections. The three mitigation methods have a shown a positive effect on reducing the annual temperature variations of the test-embankments and the geological deposits is kept considerably colder during the summer period than underneath the reference embankment. A substantially reduced maximum annual thaw depth has been registered.

The results have also shown a noticeable reduction in the mean annual temperature at the sub-grade level. All three test-sections are kept significantly colder during the summer period compared to the reference embankment, whereas the gentle slope section is colder than the other test embankments during the winter period. This constitutes a large difference in the thermal regime of the test-sections compared to the reference embankment.

REFERENCES

Beaulac, I. (2006). Impacts de la fonte du pergélisol et adaptations des infrastructures de transport routier et aérien au Nunavik. Master thesis, Département de Génie Civil, Université Laval, Québec, Canada, 250 p.

Beaulac, I., Doré, G., Shur, Y., Allard, M. (2004). Road and airfields on permafrost, problem assessment and possible solutions. 12th International Conference on Cold Regions Engineering, Edmonton, Canada.

Beaulac, I., Doré, G. (2006). Airfields and access roads performance assessment in Nunavik, Québec, Canada. 13th International Conference on Cold Regions Engineering, Maine, USA.

Doré, G., Pierre, P., Juneau, S., Lemelin, J.-C. (2007). Experimentation de méthodes de mitigation des effets de la fonte du pergélisol sur les infrastructures du Nunavik – Aéroport de Tasiujaq, Rapport d'étape 1 – Compte rendu des travaux d'instrumentation et de supervision de construction des planches expérimentales de l'aéroport de Tasiujaq, description des planches construites et de l'instrumentation installée. Groupe de recherche en ingénierie des chaussées, Département de Génie Civil, Université Laval, Québec, Canada, 28 p.

Esch, D. C. (1996). Road and airfield design for permafrost conditions. Roads and Airfields in Cold Regions, Technical Council on Cold Regions Engineering Monograph, pp. 121-149.

Goering, D. J. (1996). Air convection embankments for roadway construction in permafrost zones. 8th International Conference on Cold Regions Engineering, Fairbanks, Alaska, pp. 1-12.

Goering, D. J., Kumar, P. (1996). Winter-time convection in open-graded embankments. Cold Regions Science and Technology, Vol. 24, pp. 57-74.

Jørgensen, A. S., Doré, G., Voyer, É., Chataigner, Y., Gosselin, L. (2008). Assessment of the effectiveness of two heat removal techniques for permafrost protection. Cold Regions Science and Technology, Vol. 53, pp. 179-192.

Lunardini, V. J. (1981). Heat Transfer in Cold Climates. Van Nostrand Reinhold, New York, 731 p.

Saboundjian, S., Goering, D. J. (2003). Air Convection Embankment for Roadways – Field Experimental Study in Alaska. Transportation Research Record, Issue 1821, pp. 20-28.

Wikimedia Commons (2008). Picture required through commons.wikimedia.org on November 11, 2008.

The construction of road and airfield embankments in the Arctic will change the thermal regime of the ground, and may lead to permafrost degradation and expose the embankments to thaw settlements. To minimize the damages caused by thaw settlements different mitigations techniques have been developed.

This thesis concerns laboratory tests and field studies of three mitigation techniques; air convection embankment, heat drain and reflective surfaces. The main objective has been to study the three above-mentioned techniques and evaluate their potential to avoid or at least minimize the problems with thaw settlements in permafrost areas.

DTU Civil Engineering
Department of Civil Engineering
Technical University of Denmark

Brovej, Building 118
2800 Kgs. Lyngby
Telephone 45 25 17 00

www.byg.dtu.dk